7th ISSP International Workshop and Symposium

Emergent Quantum Phases in Condensed Matter

-from topological to first principles approaches

Workshop June 3-21, 2013 , Symposium June 12-14, 2013

Kashiwa Chiba, Japan

Institute for Solid State Physics, University of Tokyo

Eliashberg Theory of Superconductivity

do we have it right?

F. Marsiglio

fm3@ualberta.ca

UNIVERSITY OF ALBERTA

What this seminar is about

1) An overview of Eliashberg Theory, as applied to conventional superconductors, and as I would teach in a graduate course, for example.

2) Some chinks in the armour as revealed by cuprates, for example.

3) Various aspects that I have been working on over the last 20 years or so
   (i) polarons --- how do electrons resist becoming polaronic?
   (ii) kinetic interactions --- is there more to Coulomb repulsions than μ^* ?

Please ask questions!!

Particle ‘zoo’

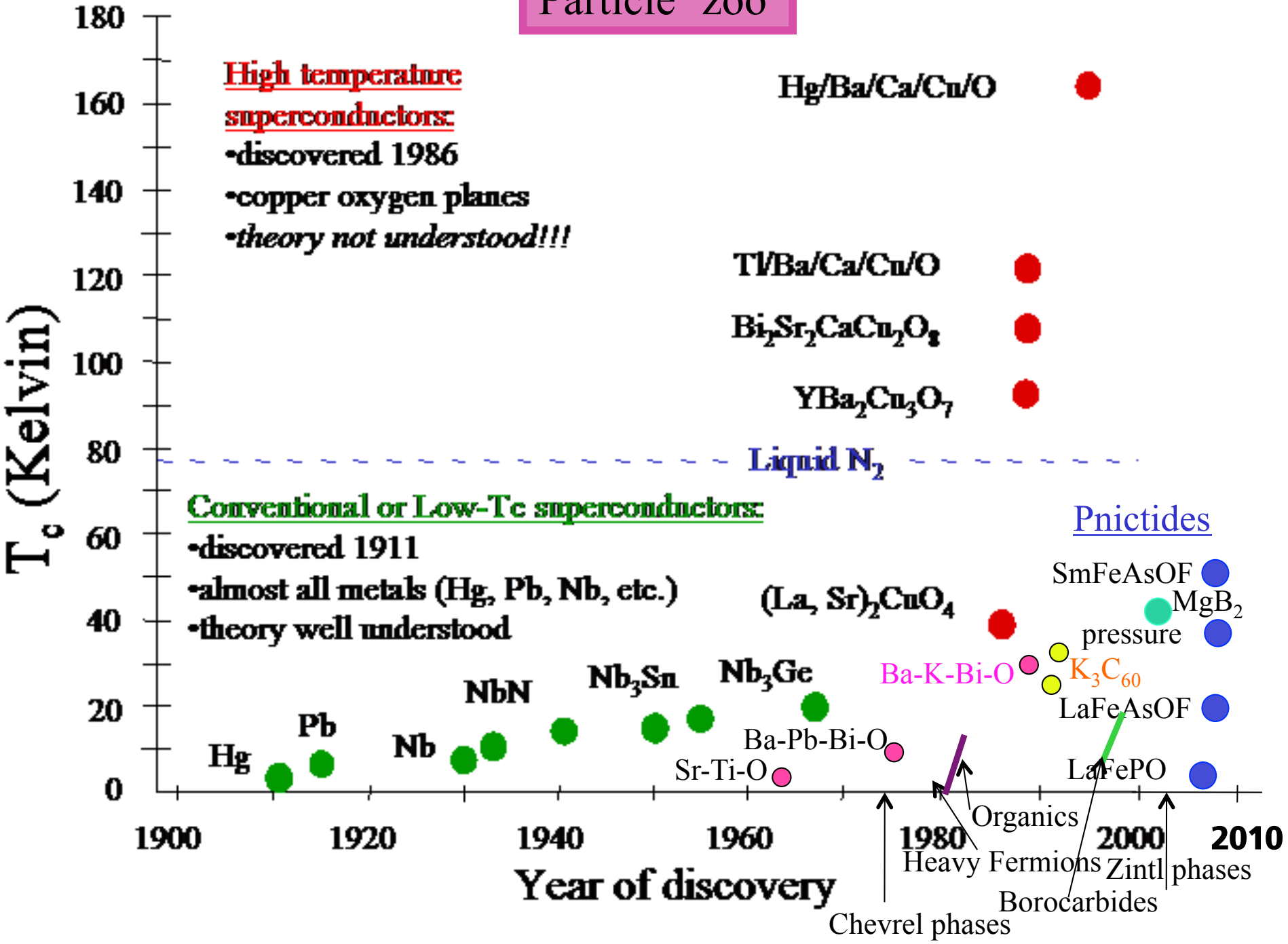

Particle ‘zoo’

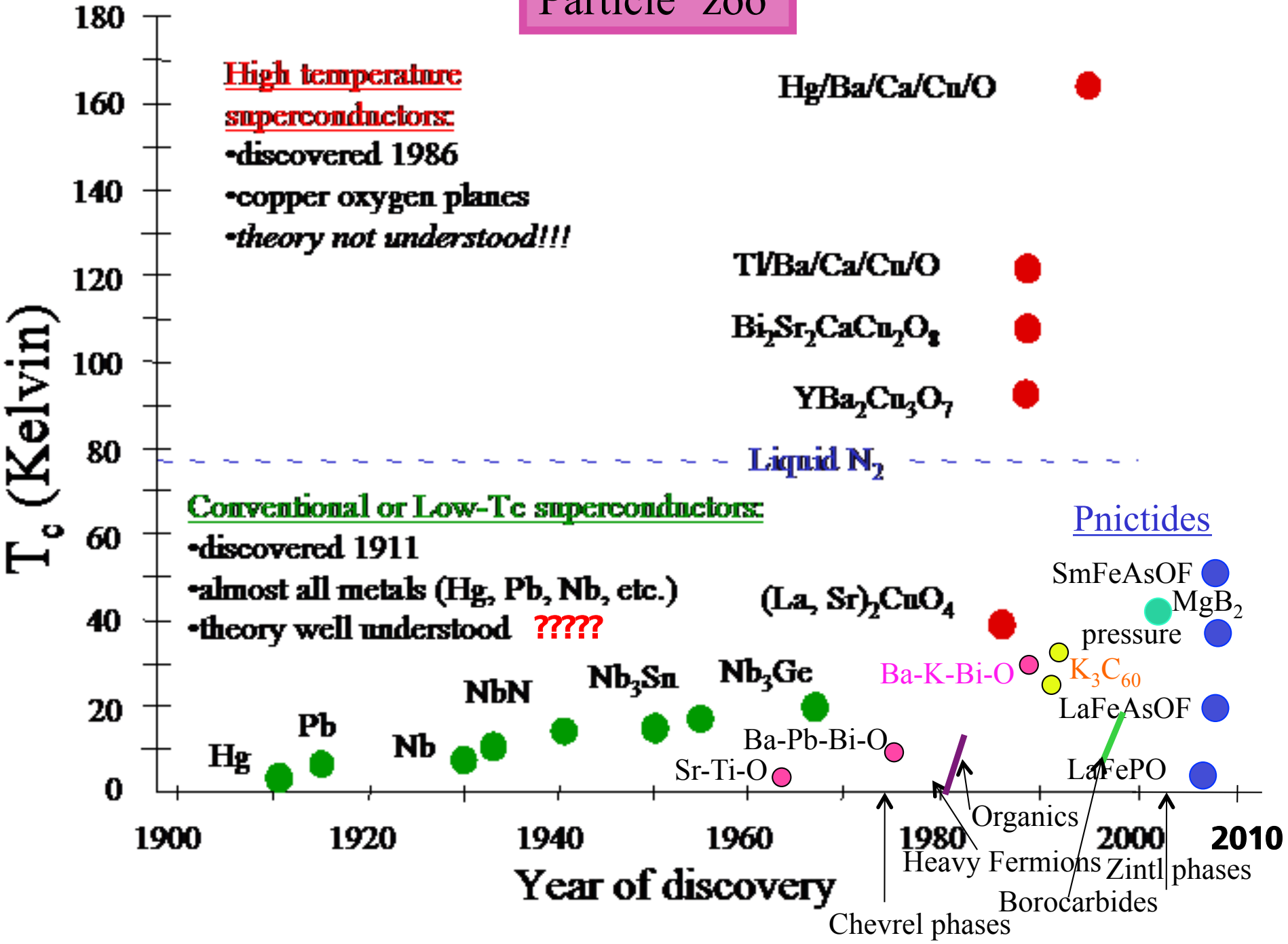

The Fermi Liquid—BCS Paradigm

A big “rug”: Fermi Liquid Theory

nothing very exceptional about the
normal state of electrons in a metal
(pretend they don’t interact)

… a premise for ‘conventional’ superconductivity

Electrons in solids

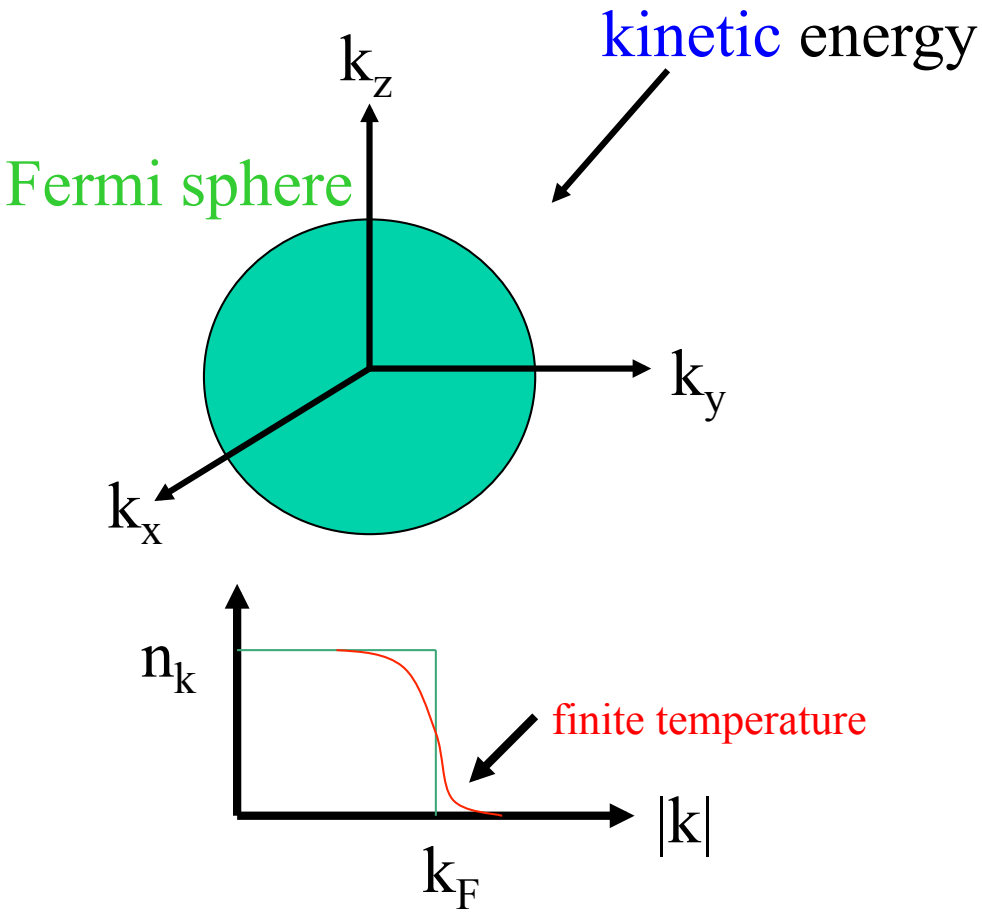

$$E_{kin} = 2 \Sigma \varepsilon_k n_k$$

Electrons in solids

kinetic vs. potential energy

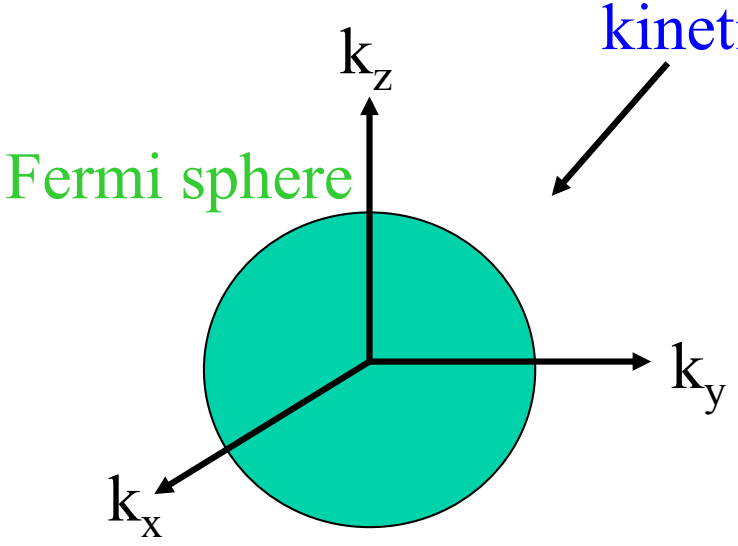

Mott insulator

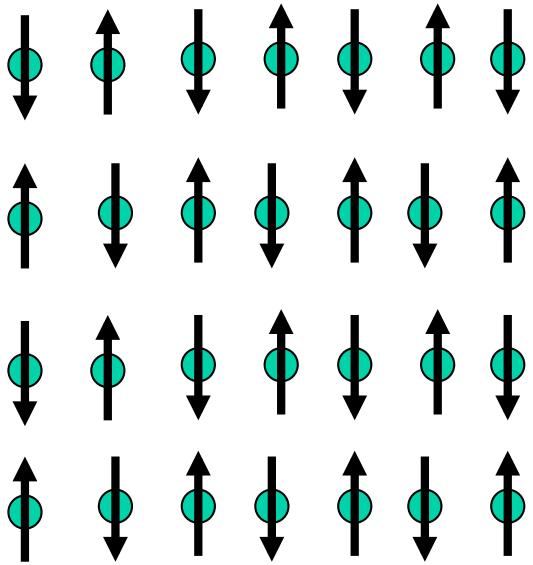

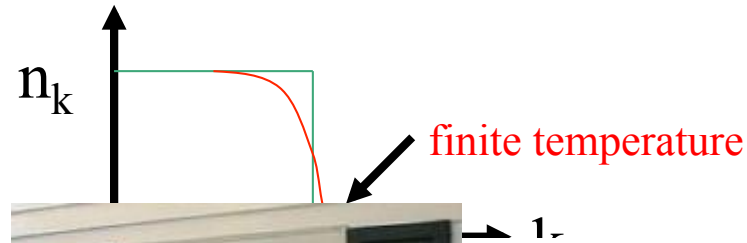

Introduce frustration, doping, and so on, and one can stabilize a spin liquid: maybe even a Resonating Valence Bond (RVB) state; lower the temperature, and one gets a high Tc superconductor! (P.W. Anderson)

The conventional scenario: BCS



J. Bardeen L.N. Cooper J.R. Schrieffer

$$\psi_{\mathrm{BCS}} = \prod_{k} (u_k + v_k c^{\dagger}_{k\uparrow} c^{\dagger}_{-k\downarrow})|0\rangle$$

Pairs!

It's all about pairs…

In Ogg's theory it was his intent
That the current keep flowing, once sent;
So to save himself trouble,
He put them in double,
And instead of stopping, it went.

George Gamow

Bose-Einstein Condensation of Trapped Electron Pairs. Phase Separation and Superconductivity of Metal-Ammonia Solutions

RICHARD A. OGG, JR.
Department of Chemistry, Stanford University, California
March 2, 1946

…Cooper pairs

The conventional scenario: BCS

J. Bardeen L.N. Cooper J.R. Schrieffer

$$\psi_{\mathrm{BCS}} = \prod_k (u_k + v_k c^\dagger_{k\uparrow} c^\dagger_{-k\downarrow})|0\rangle$$

$$\psi_{2\nu} = \int_0^{2\pi} \frac{d\theta}{2\pi} e^{-i\nu\theta} \prod_k (u_k + e^{i\theta} v_k c^\dagger_{k\uparrow} c^\dagger_{-k\downarrow})|0\rangle$$

Fixed number!

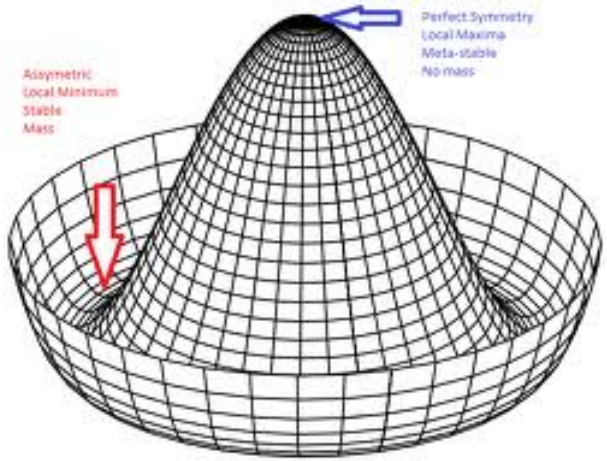

BCS formalism vs. Pairing Mechanism

$$\Delta = |V| \frac{1}{N} \sum_k \frac{\Delta}{2E_k}$$

Tc equation (useless)

$$\frac{2\Delta}{k_B T_c} = 3.53$$

Universality

$$\frac{\Delta C}{\gamma T_c} = 1.43$$

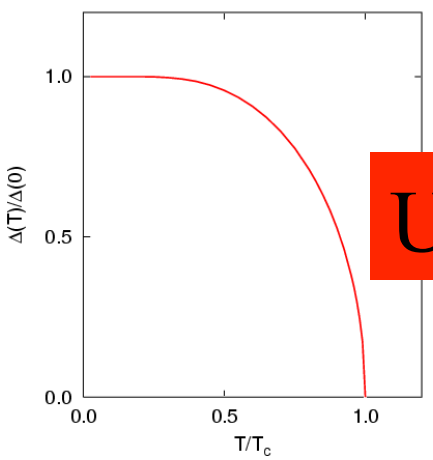

Universality is wonderful

Universality is a curse!

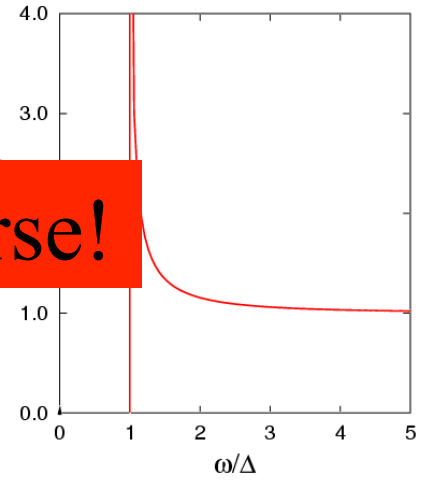

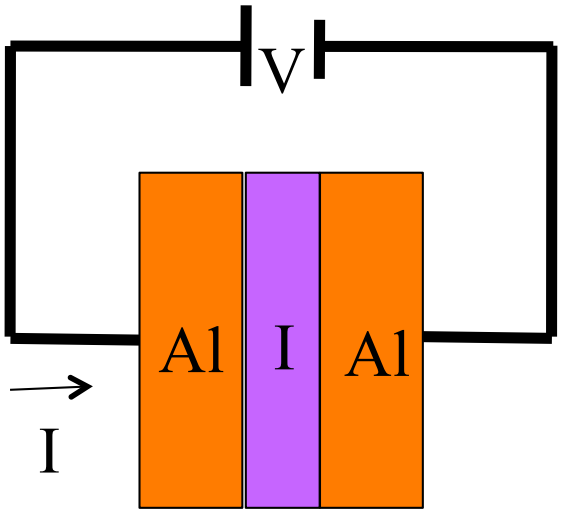

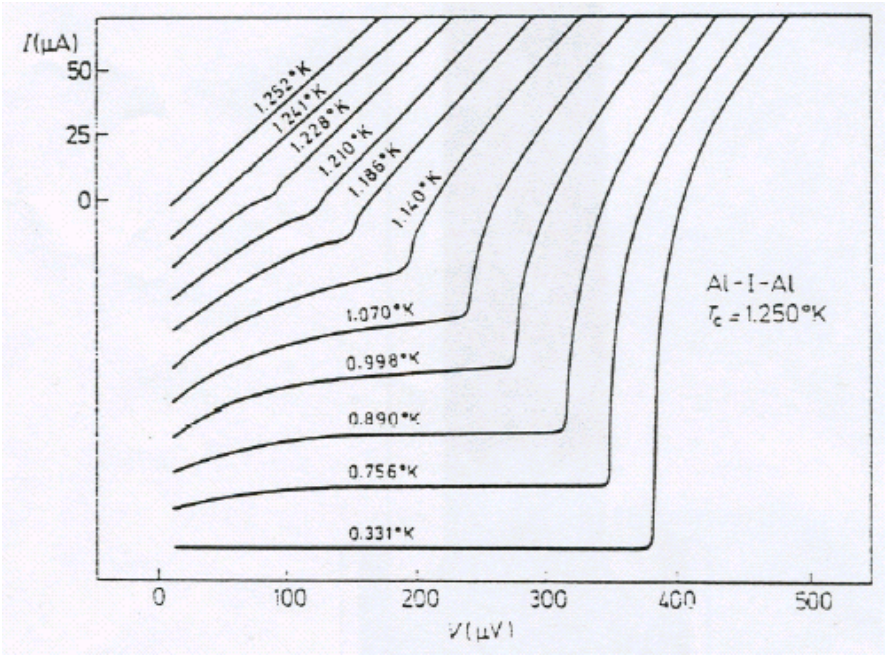

B.L. Blackford and R.H. March, Can. J. Phys. 46, 141 (1968)

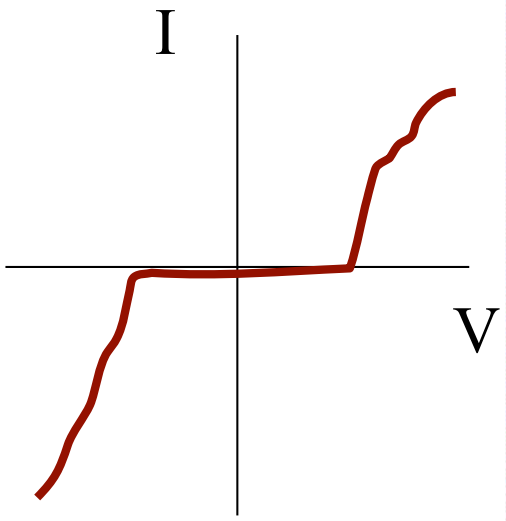

$$\frac{dI}{dV} \propto N(V)$$

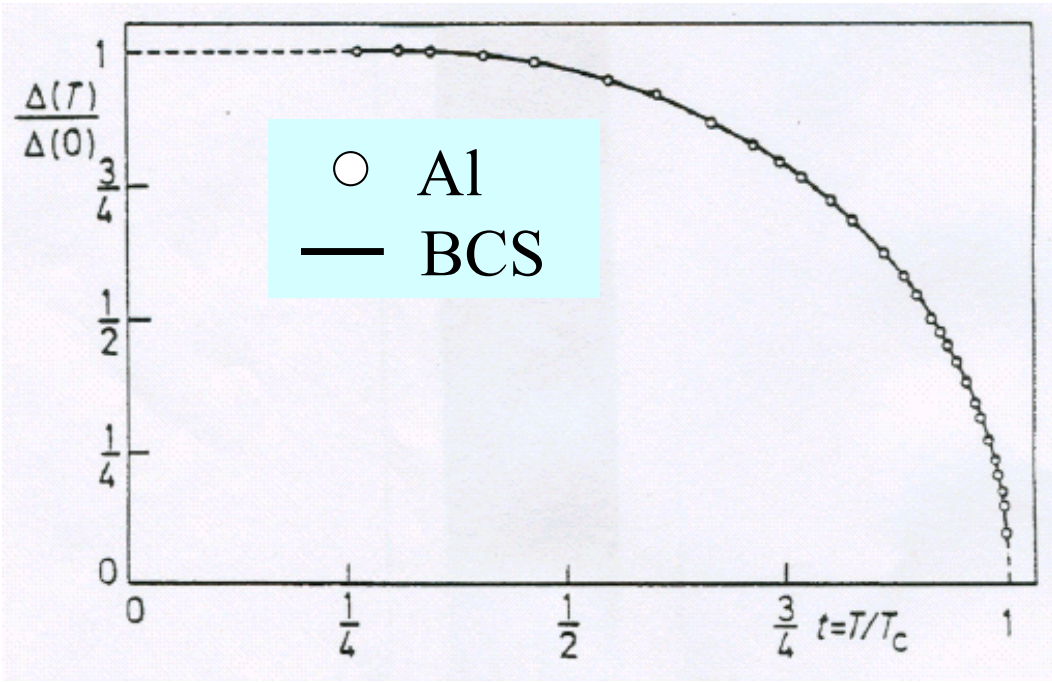

Eliashberg Theory

$$\Delta(k,\omega) = \mathcal{F}[V_{k,k'}(\omega,\omega')]$$

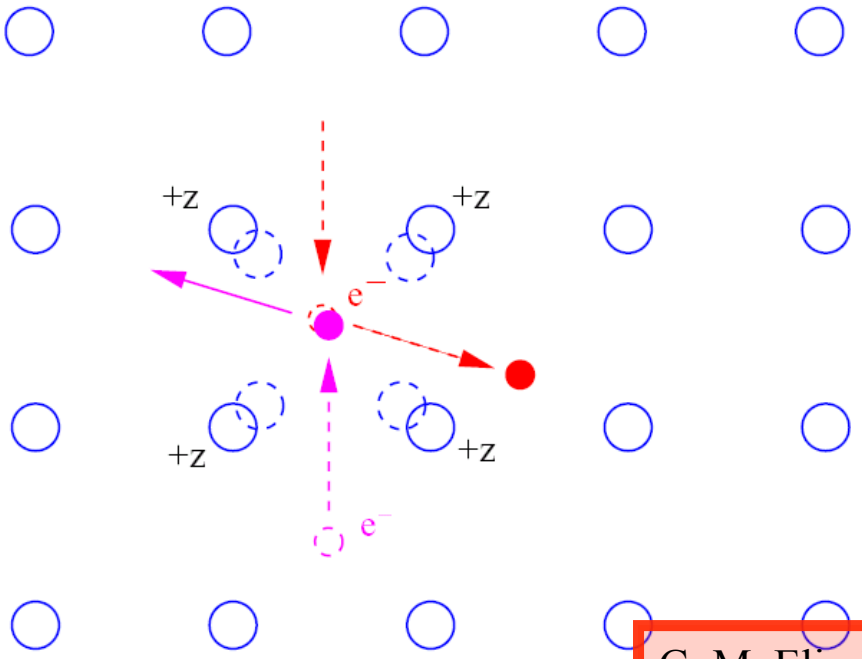

effective attraction

G. M. Eliashberg
Started graduate school in 1959
Wrote Eliashberg Theory paper in 1960
Graduated in 1963!

In the Superconducting State…
Eliashberg Theory

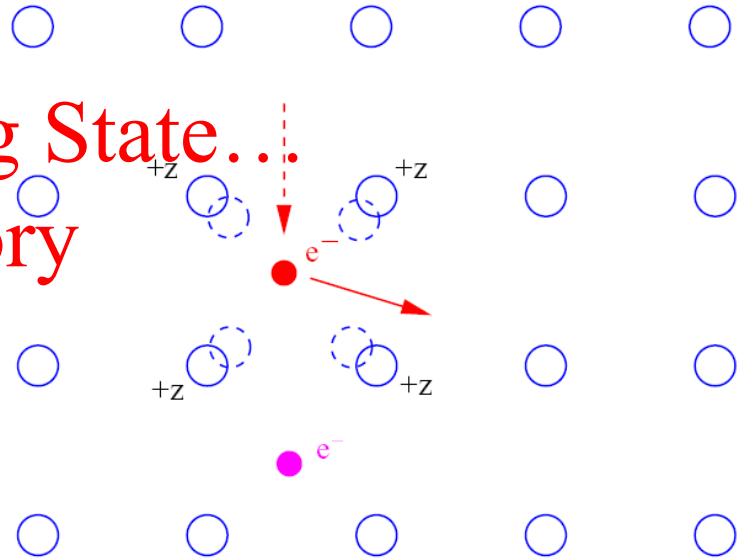

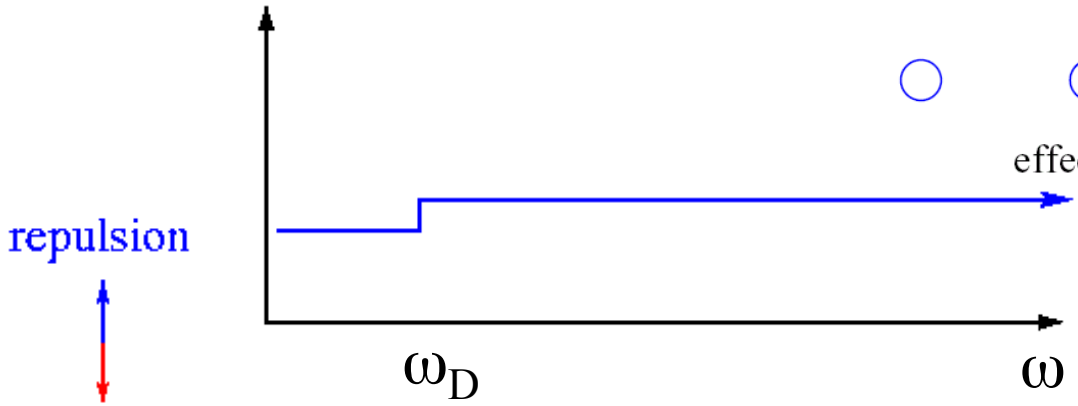

The "glue"

Poor man's Scaling (Tolmachev et al., Morel and Anderson)

The "achilles heel"

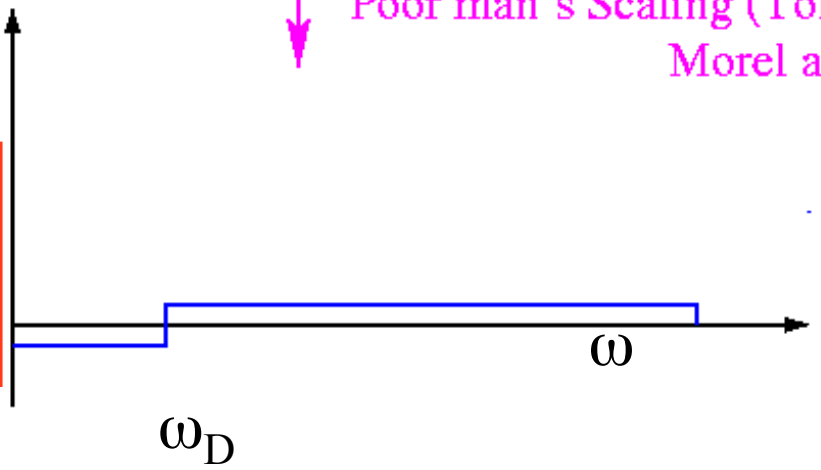

But…
Never seen in QMC simulations
Many other ways for U to be Reduced

In the Superconducting Eliashberg Theo

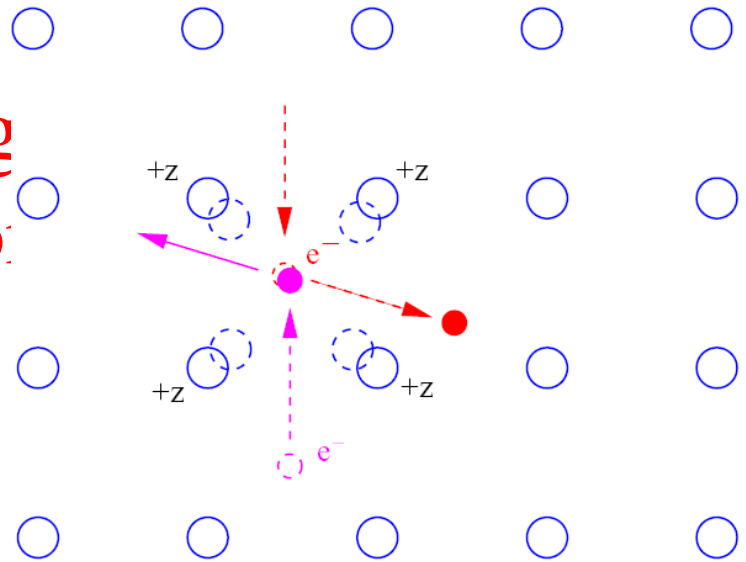

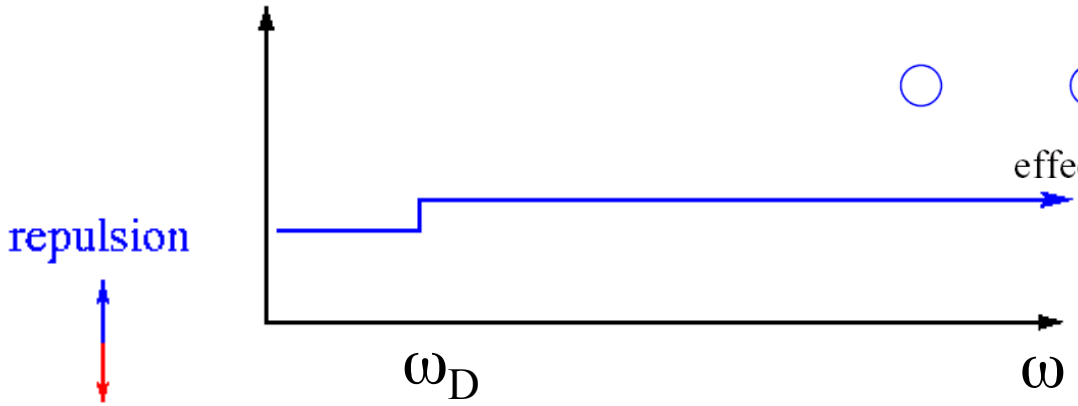

The "glue"

Poor man's Scaling (Tolmachev et al., Morel and Anderson)

The "achilles heel"

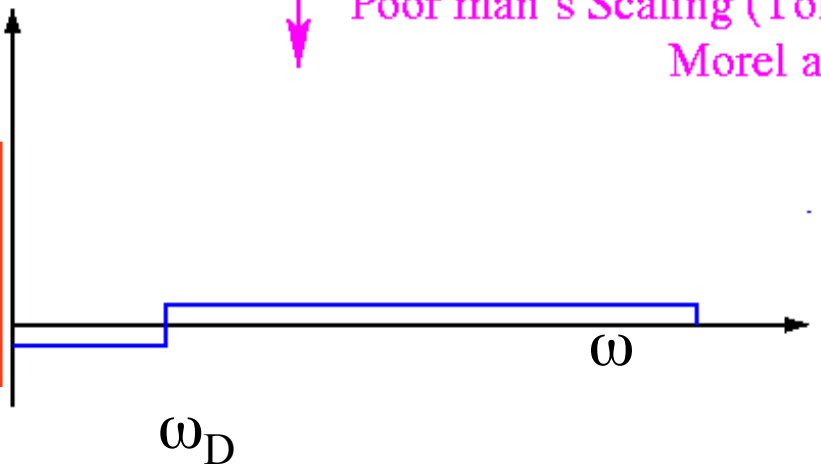

But…
Never seen in QMC simulations
Many other ways for U to be Reduced

Migdal approximation

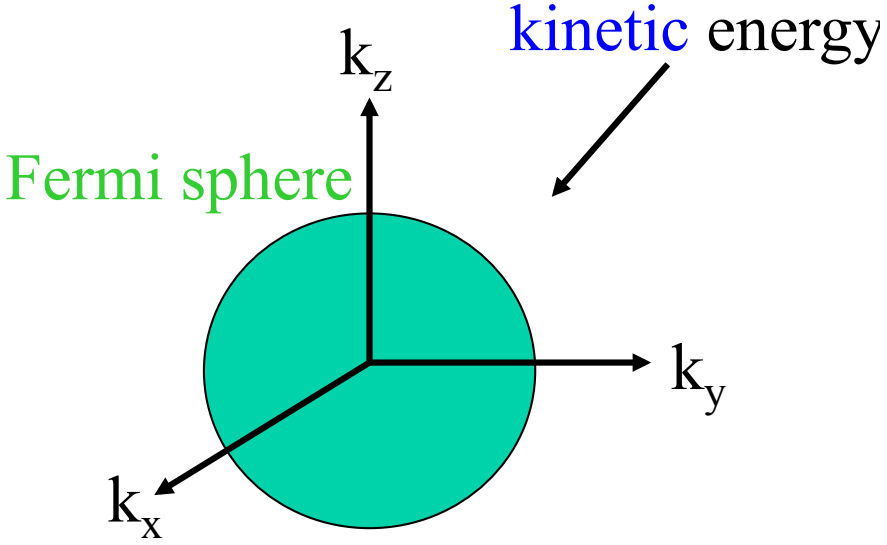

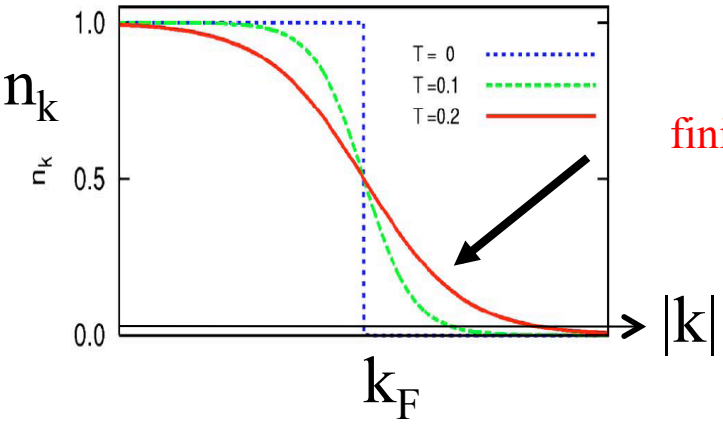

finite temperature

electron phonon coupling

$$\Sigma(\mathbf{k}, i\omega_m) = -\frac{1}{N\beta}\sum_{\mathbf{k}',m'} |g_{\mathbf{k},\mathbf{k}'}|^2 D(\mathbf{k}-\mathbf{k}', i\omega_m - i\omega_{m'}) G(\mathbf{k}', i\omega_{m'}). \quad (4.12)$$

$$\Sigma(\omega + i\delta) = \frac{\lambda\omega_E}{2}\left[\ln\left|\frac{\omega_E - \omega}{\omega_E + \omega}\right| - i\pi\theta(|\omega| - \omega_E)\right].$$

$$m^*/m = 1 + \lambda$$

where

$$\lambda \equiv 2\int_0^\infty d\omega \alpha^2 F(\omega)/\omega$$

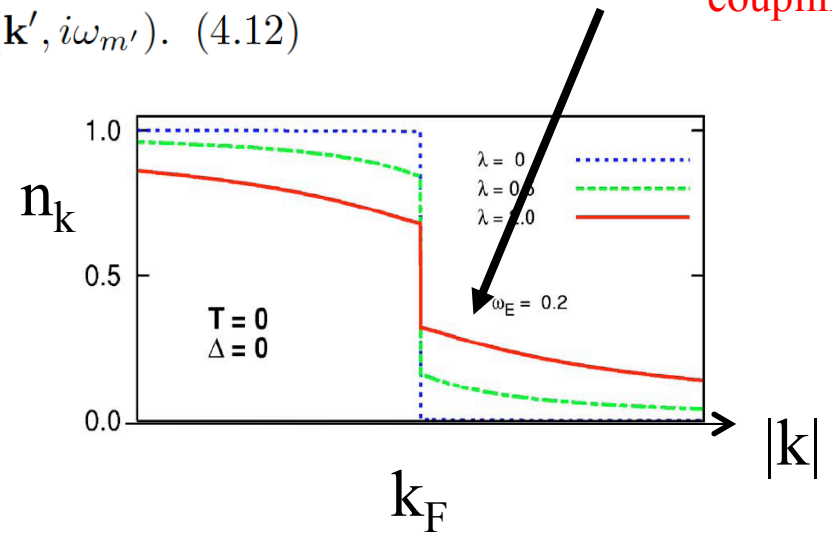

a somewhat renormalized mass

See **arXiv:cond-mat/0106143**

or Bennemann and Ketterson,
Superconductivity: Conventional and Unconventional Superconductors,
chapter 4, FM and J.P. Carbotte

$$\Sigma(\mathbf{k}, i\omega_m) \equiv \frac{1}{N\beta}\sum_{\mathbf{k}',m'} \frac{\lambda_{\mathbf{k}\mathbf{k}'}(i\omega_m - i\omega_{m'})}{N(\mu)} G(\mathbf{k}', i\omega_{m'}) \tag{42}$$

$$\phi(\mathbf{k}, i\omega_m) \equiv \frac{1}{N\beta}\sum_{\mathbf{k}',m'} \left[\frac{\lambda_{\mathbf{k}\mathbf{k}'}(i\omega_m - i\omega_{m'})}{N(\mu)} - V_{\mathbf{k}\mathbf{k}'}\right] F(\mathbf{k}', i\omega_{m'}), \tag{43}$$

$$G(\mathbf{k}, i\omega_m) = \frac{G_n^{-1}(\mathbf{k}, i\omega_m)}{G_n^{-1}(\mathbf{k}, i\omega_m)G_n^{-1}(-\mathbf{k}, -i\omega_m) + \phi(\mathbf{k}, i\omega_m)\bar{\phi}(\mathbf{k}, i\omega_m)} \tag{44}$$

$$F(\mathbf{k}, i\omega_m) = \frac{\phi(\mathbf{k}, i\omega_m)}{G_n^{-1}(\mathbf{k}, i\omega_m)G_n^{-1}(-\mathbf{k}, -i\omega_m) + \phi(-\mathbf{k}, -i\omega_m)\bar{\phi}(-\mathbf{k}, -i\omega_m)} \tag{45}$$

$$G_n^{-1}(\mathbf{k}, i\omega_m) = G_\circ^{-1}(\mathbf{k}, i\omega_m) - \Sigma(\mathbf{k}, i\omega_m). \tag{46}$$

where

$$\lambda_{\mathbf{k}\mathbf{k}'}(z) \equiv \int_0^\infty \frac{2\nu\alpha^2_{\mathbf{k}\mathbf{k}'}F(\nu)}{\nu^2 - z^2} d\nu$$

$$G_\circ(\mathbf{k}, i\omega_m) = [i\omega_m - (\epsilon_\mathbf{k} - \mu)]^{-1}$$

$$D_\circ(\mathbf{q}, i\nu_n) = [-M(\omega^2(\mathbf{q}) + \nu_n^2)]^{-1}$$

phonons

$$D(\mathbf{q}, i\nu_n) = \int_0^\infty d\nu B(\mathbf{q}, \nu) \frac{2\nu}{(i\nu_n)^2 - \nu^2}$$

phonon spectral function

$$B(\mathbf{q}, \nu) \equiv -\frac{1}{\pi} \mathrm{Im} D(\mathbf{q}, \nu + i\delta).$$

Normal state

$$\Sigma(\mathbf{k}, i\omega_m) = \frac{1}{N\beta} \sum_{\mathbf{k}', m'} \int_0^\infty d\nu |g_{\mathbf{k},\mathbf{k}'}|^2 B(\mathbf{k} - \mathbf{k}', \nu) \frac{2\nu}{(\omega_m - \omega_{m'})^2 + \nu^2} G_\circ(\mathbf{k}', i\omega_{m'}).$$

form of Eq. (15) allows one to introduce the electron-phonon spectral function,

$$\alpha^2 F(\mathbf{k}, \mathbf{k}', \nu) \equiv N(\mu) |g_{\mathbf{k},\mathbf{k}'}|^2 B(\mathbf{k} - \mathbf{k}', \nu),$$

$$\frac{1}{N}\sum_{\mathbf{k}} \rightarrow \int d\epsilon N(\epsilon) \tag{18}$$

along with a constant density of states approximation, extended over an infinite bandwidth, one obtains for the electron self energy

$$\Sigma(i\omega_m) = \lambda\omega_E^2 \int_{-\infty}^{\infty} d\epsilon \frac{1}{\beta}\sum_{m'} \frac{1}{\omega_E^2 + (\omega_{m'} - \omega_m)^2} \frac{1}{i\omega_{m'} - (\epsilon - \mu)}, \tag{19}$$

where we have used the standard definition for the electron-phonon mass enhancement parameter, λ:

$$\lambda \equiv 2\int_0^{\infty} d\nu \frac{\alpha^2 F(\nu)}{\nu}, \tag{20}$$

which, for the Einstein spectrum used here, reduces to

$$\lambda = 2N(\epsilon_F)g^2/\omega_E. \tag{21}$$

Performing the Matsubara sum yields

$$\Sigma(i\omega_m) = \frac{\lambda\omega_E}{2}\int_{-\infty}^{\infty} d\epsilon \Big(\frac{n(\omega_E) + 1 - f(\epsilon - \mu)}{i\omega_m - \omega_E - (\epsilon - \mu)} + \frac{n(\omega_E) + f(\epsilon - \mu)}{i\omega_m + \omega_E - (\epsilon - \mu)} \Big) \tag{22}$$

where $f(\epsilon - \mu)$ is the Fermi function and $n(\omega_E)$ is the Bose distribution function. The remaining integral can also be performed [13]

$$\Sigma(z) = \frac{\lambda\omega_E}{2}\Big[-2\pi i(n(\omega_E) + 1/2) + \psi(\frac{1}{2} + i\frac{\omega_E - z}{2\pi T}) - \psi(\frac{1}{2} - i\frac{\omega_E + z}{2\pi T}) \Big] \tag{23}$$

where $\psi(x)$ is the digamma function [92, 13] and the entire expression has been analytically continued to a general complex frequency z. Because we performed the Matsubara sum first, before replacing $i\omega_m$ with z, this is the physically correct analytic continuation [93].

is the Heaviside step function), the self energy at $T = 0$ is

$$\Sigma(z) = \frac{\lambda\omega_E}{2} \ln\left(\frac{\omega_E - z}{\omega_E + z}\right). \tag{24}$$

Spectroscopic measurements yield properties as a function of real frequency; because of the analytic properties of the Green function, this corresponds to a frequency either slightly above or below the real axis. We will use frequencies slightly above, and designate the infinitesmal positive imaginary part by '$i\delta$'. Thus,

$$\Sigma(\omega + i\delta) = \frac{\lambda\omega_E}{2}\left[\ln \mid \frac{\omega_E - \omega}{\omega_E + \omega} \mid -i\pi\theta(\mid \omega \mid -\omega_E)\right]. \tag{25}$$

The real and imaginary parts of this self energy are shown in Fig. 3, along with the non-interacting inverse Green function $(\omega - (\epsilon_{\mathbf{k}} - \mu))$ to determine the poles of the electron Green function (see Eq. (6)) graphically. A quantity often measured in single particle spectroscopies is the spectral function, $A(\mathbf{k}, \omega)$ defined by

$$A(\mathbf{k}, \omega) \equiv -\frac{1}{\pi}\mathrm{Im}G(\mathbf{k}, \omega + i\delta). \tag{26}$$

With this definition, we obtain, through Eq. (6) and (25),

$$\begin{aligned} A(\mathbf{k}, \omega) &= \delta\left(\omega - (\epsilon_{\mathbf{k}} - \mu) - \frac{\lambda\omega_E}{2} \ln \mid \frac{\omega_E - \omega}{\omega_E + \omega} \mid\right) && \text{if } \mid \omega \mid < \omega_E, \\ &= \frac{\lambda\omega_E/2}{\left(\omega - (\epsilon_{\mathbf{k}} - \mu) - \frac{\lambda\omega_E}{2} \ln \mid \frac{\omega_E - \omega}{\omega_E + \omega} \mid\right)^2 + \left(\frac{\pi\lambda\omega_E}{2}\right)^2} && \text{if } \mid \omega \mid > \omega_E. \end{aligned} \tag{27}$$

Plots are shown in Fig. 4. Each spectral function displays a quasiparticle peak, whose strength $a_{\mathbf{k}}$ and frequency $\omega_{\mathbf{k}}$ is implicitly dependent on wavevector

$$a_{\mathbf{k}} = \left(1 + \frac{\lambda}{1 - (\omega_{\mathbf{k}}/\omega_E)^2}\right)^{-1}, \tag{28}$$

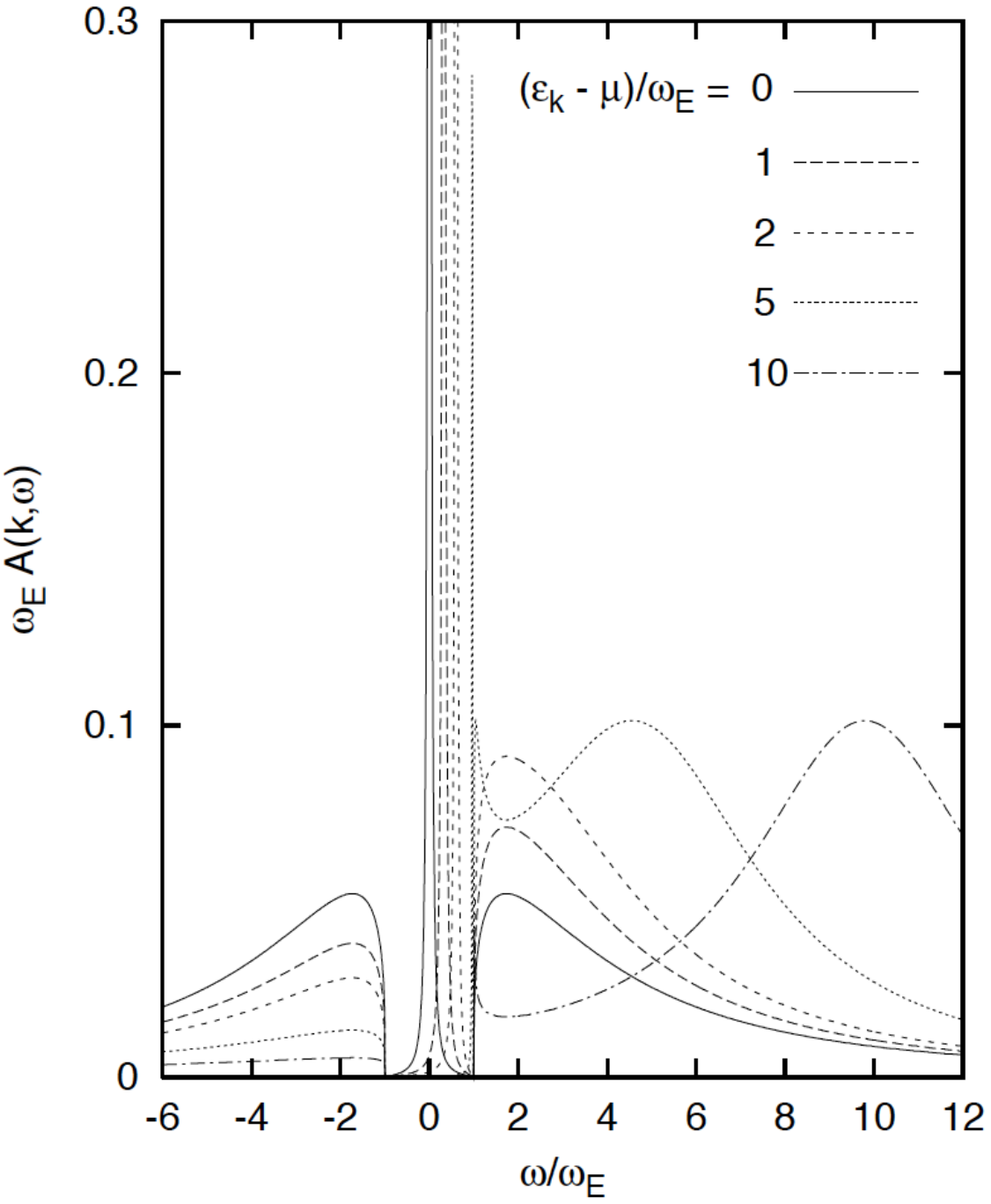
0.3
0.2
0.1
0
-6
-4
-2
0
2
4
6
8
10
12
$\omega_E A(k,\omega)$
ω/ω_E
$(\varepsilon_k - \mu)/\omega_E =$ 0
1
2
5
10

phonons

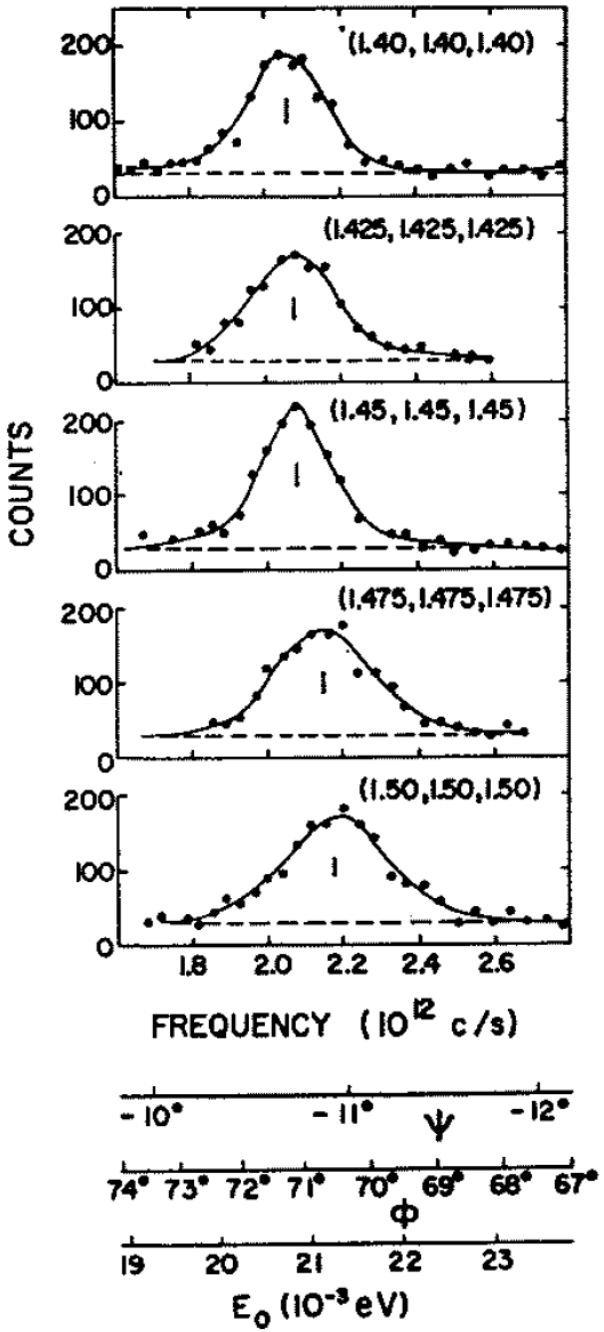
(1.40, 1.40, 1.40)
(1.425, 1.425, 1.425)
(1.45, 1.45, 1.45)
(1.475, 1.475, 1.475)
(1.50, 1.50, 1.50)
COUNTS
FREQUENCY (10^12 c/s)
Ψ
Φ
E0 (10^-3 eV)

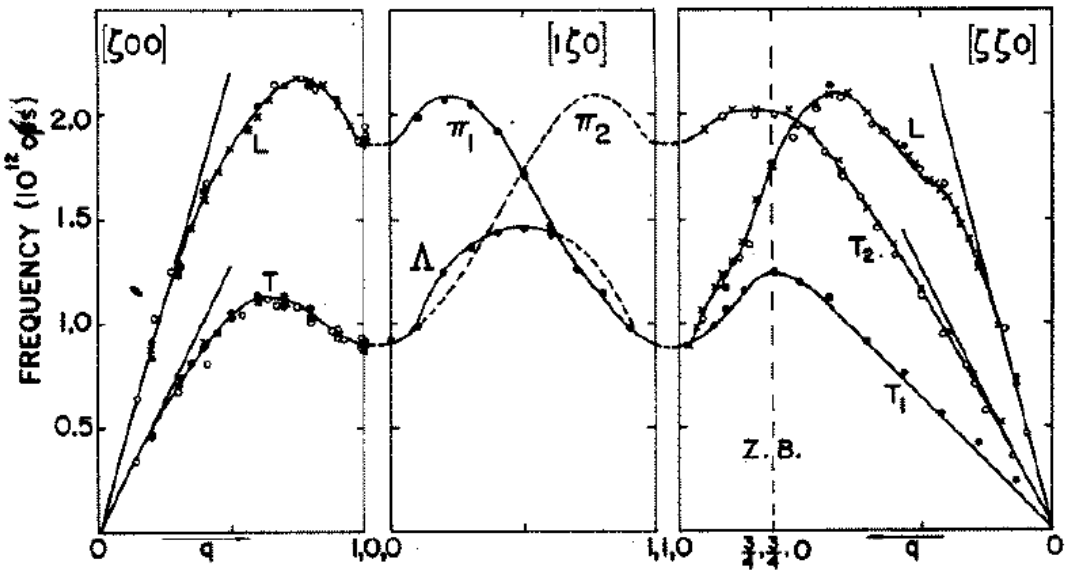
[ζ00]
[1ζ0]
[ζζ0]
FREQUENCY (10^12 cps)
L
T
Λ
Z. B.

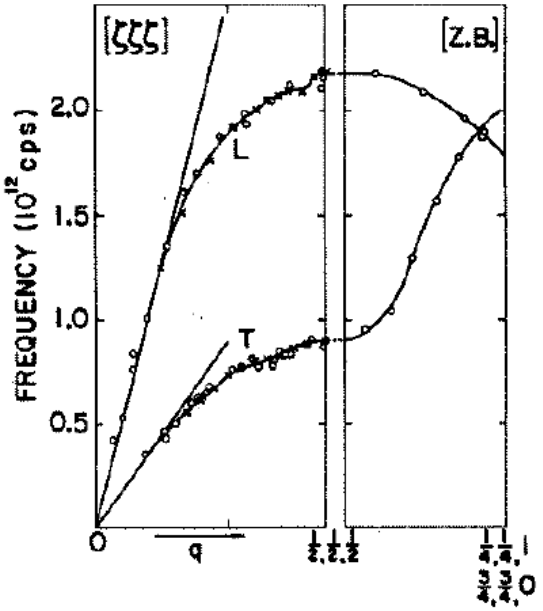
[ζζζ]
[Z.B.]
FREQUENCY (10^12 cps)
L
T

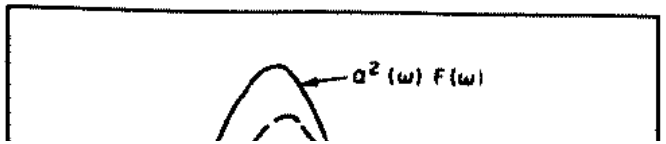

Recall:

$$\Sigma(\mathbf{k}, i\omega_m) = \frac{1}{N\beta} \sum_{\mathbf{k}',m'} \int_0^\infty d\nu |g_{\mathbf{k},\mathbf{k}'}|^2 B(\mathbf{k}-\mathbf{k}', \nu) \frac{2\nu}{(\omega_m - \omega_{m'})^2 + \nu^2} G_\circ(\mathbf{k}', i\omega_{m'}).$$

form of Eq. (15) allows one to introduce the electron-phonon spectral function,

$$\alpha^2 F(\mathbf{k}, \mathbf{k}', \nu) \equiv N(\mu) |g_{\mathbf{k},\mathbf{k}'}|^2 B(\mathbf{k}-\mathbf{k}', \nu),$$

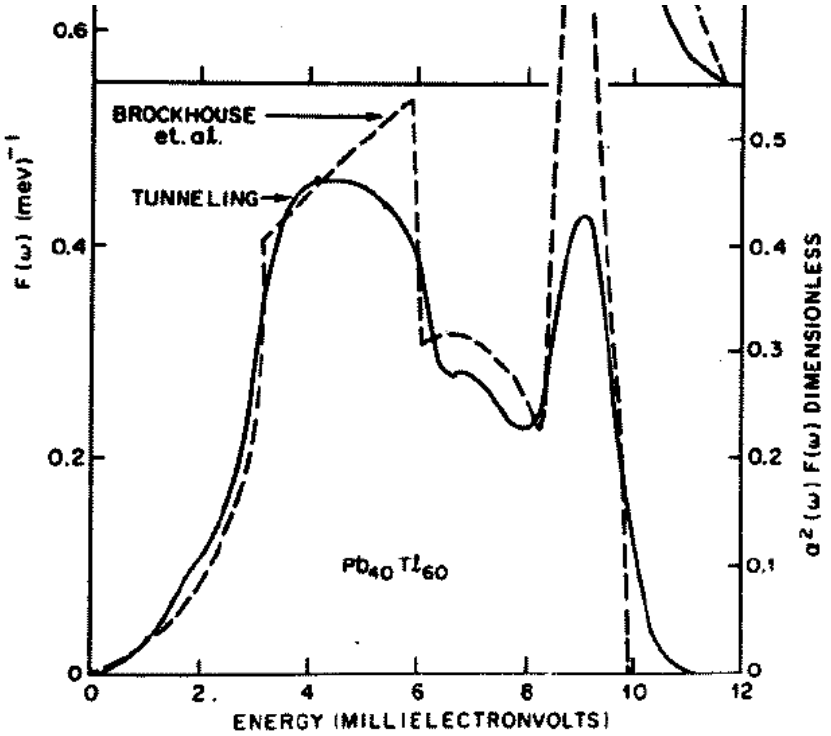

Recall:

$$\Sigma(\mathbf{k}, i\omega_m) \equiv \frac{1}{N\beta}\sum_{\mathbf{k}',m'} \frac{\lambda_{\mathbf{k}\mathbf{k}'}(i\omega_m - i\omega_{m'})}{N(\mu)} G(\mathbf{k}', i\omega_{m'}) \tag{42}$$

$$\phi(\mathbf{k}, i\omega_m) \equiv \frac{1}{N\beta}\sum_{\mathbf{k}',m'} \left[\frac{\lambda_{\mathbf{k}\mathbf{k}'}(i\omega_m - i\omega_{m'})}{N(\mu)} - V_{\mathbf{k}\mathbf{k}'}\right] F(\mathbf{k}', i\omega_{m'}), \tag{43}$$

$$G(\mathbf{k}, i\omega_m) = \frac{G_n^{-1}(\mathbf{k}, i\omega_m)}{G_n^{-1}(\mathbf{k}, i\omega_m)G_n^{-1}(-\mathbf{k}, -i\omega_m) + \phi(\mathbf{k}, i\omega_m)\bar{\phi}(\mathbf{k}, i\omega_m)} \tag{44}$$

$$F(\mathbf{k}, i\omega_m) = \frac{\phi(\mathbf{k}, i\omega_m)}{G_n^{-1}(\mathbf{k}, i\omega_m)G_n^{-1}(-\mathbf{k}, -i\omega_m) + \phi(-\mathbf{k}, -i\omega_m)\bar{\phi}(-\mathbf{k}, -i\omega_m)} \tag{45}$$

$$G_n^{-1}(\mathbf{k}, i\omega_m) = G_\circ^{-1}(\mathbf{k}, i\omega_m) - \Sigma(\mathbf{k}, i\omega_m). \tag{46}$$

Use:

$$i\omega_m[1 - Z(\mathbf{k}, i\omega_m)] \equiv \frac{1}{2}[\Sigma(\mathbf{k}, i\omega_m) - \Sigma(\mathbf{k}, -i\omega_m)]$$

$$\chi(\mathbf{k}, i\omega_m) \equiv \frac{1}{2}[\Sigma(\mathbf{k}, i\omega_m) + \Sigma(\mathbf{k}, -i\omega_m)]$$

$$Z(\mathbf{k}, i\omega_m) = 1 + \frac{1}{N\beta}\sum_{\mathbf{k}',m'} \frac{\lambda_{\mathbf{k}\mathbf{k}'}(i\omega_m - i\omega_{m'})}{N(\mu)} \frac{(\omega_{m'}/\omega_m) Z(\mathbf{k}', i\omega_{m'})}{\omega_{m'}^2 Z^2(\mathbf{k}', i\omega_{m'}) + \left(\epsilon_{\mathbf{k}'} - \mu + \chi(\mathbf{k}', i\omega_{m'})\right)^2 + \phi^2(\mathbf{k}', i\omega_{m'})} \quad (49)$$

$$\chi(\mathbf{k}, i\omega_m) = -\frac{1}{N\beta}\sum_{\mathbf{k}',m'} \frac{\lambda_{\mathbf{k}\mathbf{k}'}(i\omega_m - i\omega_{m'})}{N(\mu)} \frac{\epsilon_{\mathbf{k}'} - \mu + \chi(\mathbf{k}', i\omega_{m'})}{\omega_{m'}^2 Z^2(\mathbf{k}', i\omega_{m'}) + \left(\epsilon_{\mathbf{k}'} - \mu + \chi(\mathbf{k}', i\omega_{m'})\right)^2 + \phi^2(\mathbf{k}', i\omega_{m'})} \quad (50)$$

along with the gap equation (Eq. (43)):

$$\phi(\mathbf{k}, i\omega_m) = \frac{1}{N\beta}\sum_{\mathbf{k}',m'} \left(\frac{\lambda_{\mathbf{k}\mathbf{k}'}(i\omega_m - i\omega_{m'})}{N(\mu)} - V_{\mathbf{k}\mathbf{k}'} \right) \frac{\phi(\mathbf{k}', i\omega_{m'})}{\omega_{m'}^2 Z^2(\mathbf{k}', i\omega_{m'}) + \left(\epsilon_{\mathbf{k}'} - \mu + \chi(\mathbf{k}', i\omega_{m'})\right)^2 + \phi^2(\mathbf{k}', i\omega_{m'})}. \quad (51)$$

Simplifications (ignore momentum dependence) give rise to:

along with :

See FM JLTP 87, 659 (1992), and F. Dogan and FM PRB 78, 165102 (2003)

$$Z_m = 1 + \pi T \sum_{m'} \lambda(i\omega_m - i\omega_{m'}) \frac{(\omega_{m'}/\omega_m) Z_{m'}}{\sqrt{\omega_{m'}^2 Z_{m'}^2 + \phi_{m'}^2}} A_0(m') \quad (54)$$

$$\chi_m = -\pi T \sum_{m'} \lambda(i\omega_m - i\omega_{m'}) A_1(m') \quad (55)$$

$$\phi_m = \pi T \sum_{m'} \left(\lambda(i\omega_m - i\omega_{m'}) - N(\mu) V_{\text{coul}} \right) \frac{\phi_{m'}}{\sqrt{\omega_{m'}^2 Z_{m'}^2 + \phi_{m'}^2}} A_0(m') \quad (56)$$

$$n = 1 - 2\pi T N(\mu) \sum A_1(m') \quad (57)$$

then, with the additional approximation of infinite bandwidth, $A_0(m') \equiv 1$ (actually a cutoff, $\theta(\omega_c - |\,\omega_{m'}\,|)$, is required in Eq. (56)), and $A_1(m') \equiv 0$. This last result effectively removes χ_m (and Eqs. (55,57)) from further consideration. An earlier review by one of us [11]

3.3 Extraction from Experiment

of the function $\alpha^2 F(\nu)$

$$G(\mathbf{k}, i\omega_m) = \int_{-\infty}^{\infty} d\omega \, \frac{A(\mathbf{k}, \omega)}{i\omega_m - \omega}$$

$$F(\mathbf{k}, i\omega_m) = \int_{-\infty}^{\infty} d\omega \, \frac{C(\mathbf{k}, \omega)}{i\omega_m - \omega},$$

Eq. (26) and $C(\mathbf{k}, \omega)$ is given by a simil

$$C(\mathbf{k}, \omega) \equiv -\frac{1}{\pi} \mathrm{Im} F(\mathbf{k}, \omega + i\delta).$$

$$I_S(V) \propto \int d\omega \mathrm{Re}\left[\frac{|\omega|}{\sqrt{\omega^2 - \Delta^2(\omega)}}\right] [f(\omega) - f(\omega + V)],$$

used the gap function, $\Delta(\omega)$, defined as

$$\Delta(\omega) \equiv \phi(\omega + i\delta)/Z(\omega + i\delta).$$

ality constant contains information about the density of state
eptor), and the tunneling matrix element. These are usuall
e takes the zero temperature limit, then the derivative of t
oltage is simply proportional to the superconducting densit

$$\left(\frac{dI}{dV}\right)_S \Big/ \left(\frac{dI}{dV}\right)_N = \mathrm{Re}\left(\frac{|V|}{\sqrt{V^2 - \Delta^2(V)}}\right),$$

T= 0 AND $\omega < \nu_E$

A naïve analytic continuation is correct!

$$Z(\omega + i\delta) = 1 + \frac{i\pi T}{\omega} \sum_{m=-\infty}^{\infty} \lambda(\omega - i\omega_m) \frac{\omega_m Z(i\omega_m)}{\sqrt{\omega_m^2 Z^2(i\omega_m) + \phi^2(i\omega_m)}}.$$

$$\phi(\omega + i\delta) =$$

$$\pi T \sum_{m=-\infty}^{\infty} [\lambda(\omega - i\omega_m) - \mu^*(\omega_c)\theta(\omega_c - |\omega_m|)] \frac{\phi(i\omega_m)}{\sqrt{\omega_m^2 Z^2(i\omega_m) + \phi^2(i\omega_m)}}$$

$\omega > \nu_E$: no iteration necessary !

I. Giaever, H.R. Hart, Jr., and K. Megerle, PRB 126, 941 (1962)

$$\frac{dI}{dV} \sim N(\varepsilon)$$

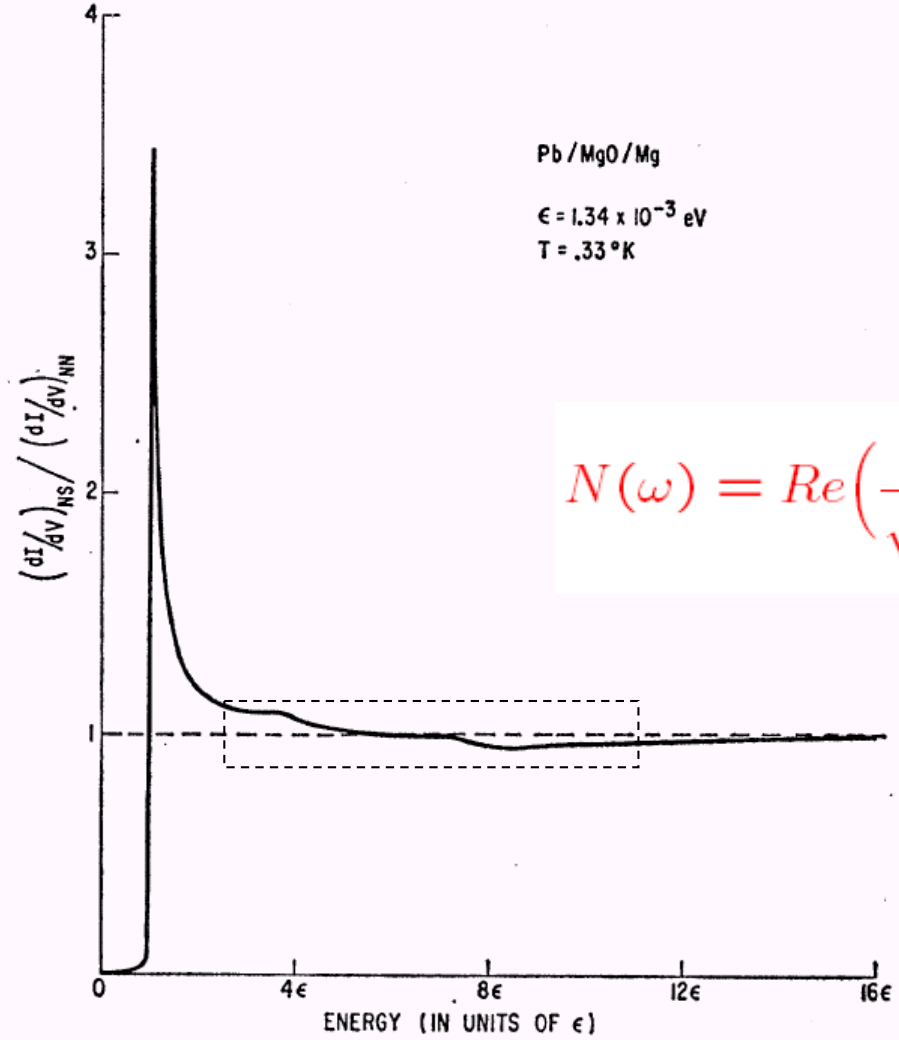

$$N(\omega) = Re\left(\frac{\omega}{\sqrt{\omega^2 - \Delta^2(\omega)}}\right)$$

FIG. 10. The relative conductance of a Pb-MgO-Mg sandwich plotted against energy. At higher energies there are definite divergences from the BCS density of states as can be seen from the bumps in the experimental curve. Note that the crossover point corresponds in energy to the Debye temperature.

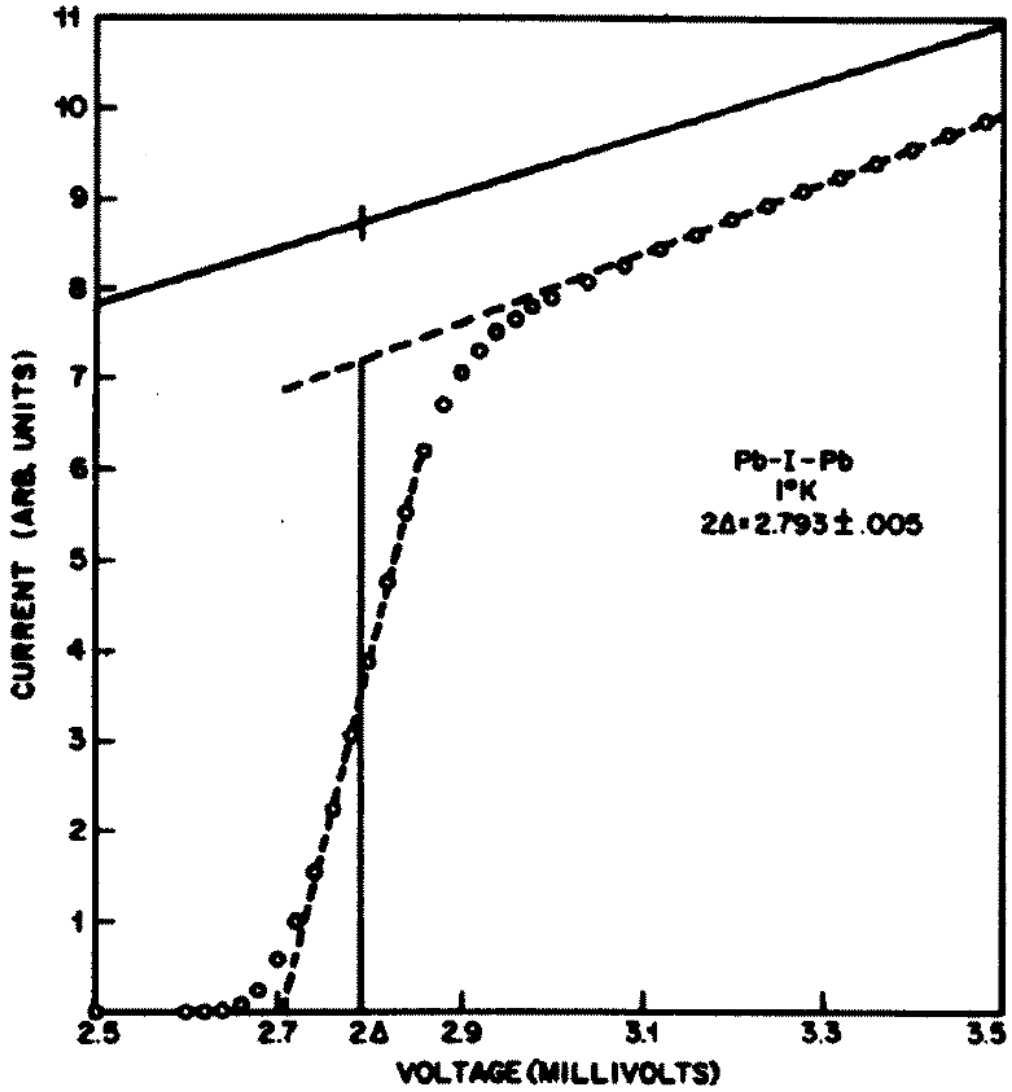

Figure 12: I-V characteristic of a Pb-I-Pb junction showing the construction used to find the energy gap. The solid line and open circles are the current in the normal and superconducting states, respectively. Reproduced from Ref. [52].

I. Giaever, H.R. Hart, Jr., and K. Megerle, PRB 126, 941 (1962)

$$\frac{dI}{dV} \sim N(\varepsilon)$$

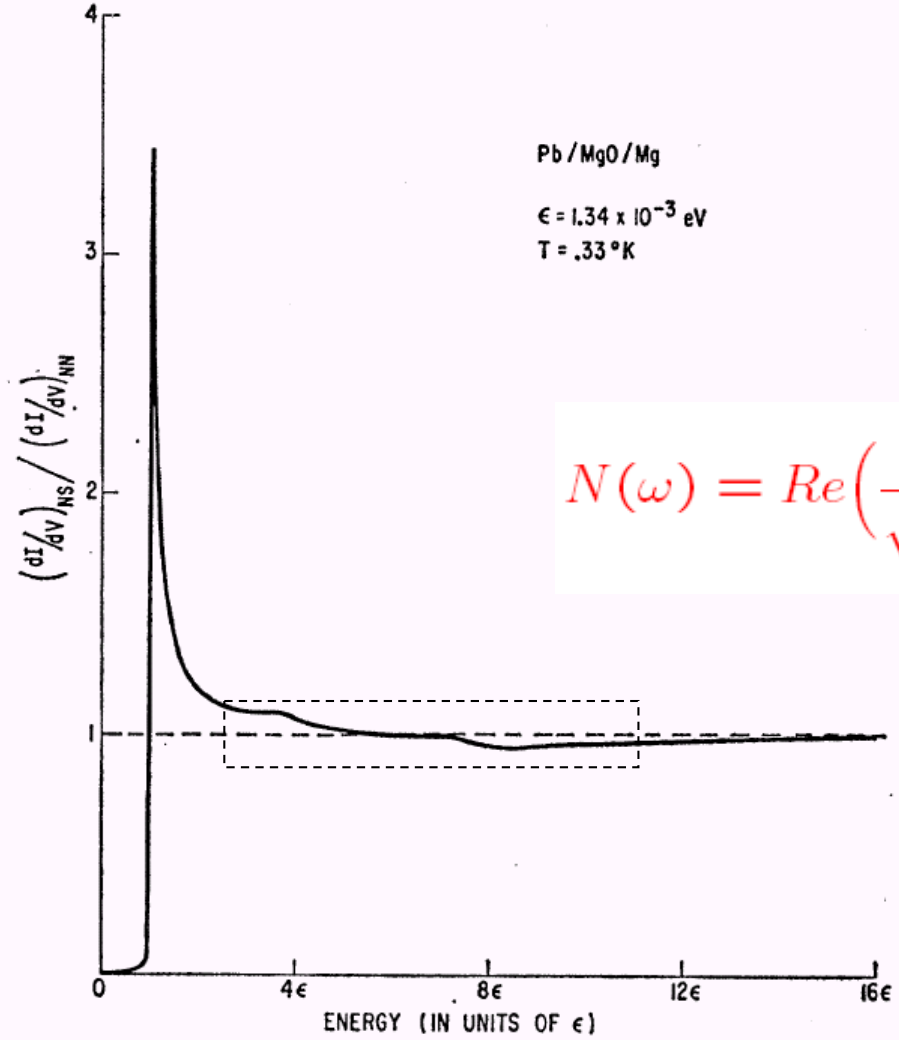

$$N(\omega) = Re\left(\frac{\omega}{\sqrt{\omega^2 - \Delta^2(\omega)}}\right)$$

FIG. 10. The relative conductance of a Pb-MgO-Mg sandwich plotted against energy. At higher energies there are definite divergences from the BCS density of states as can be seen from the bumps in the experimental curve. Note that the crossover point corresponds in energy to the Debye temperature.

Eliashberg Theory

$$\Delta(k,\omega) = \mathcal{F}[V_{k,k'}(\omega,\omega')]$$

$$\downarrow$$

A functional of the interaction

Question: Can we invert the theory to extract the potential uniquely from a knowledge of $\Delta(k,\omega)$?

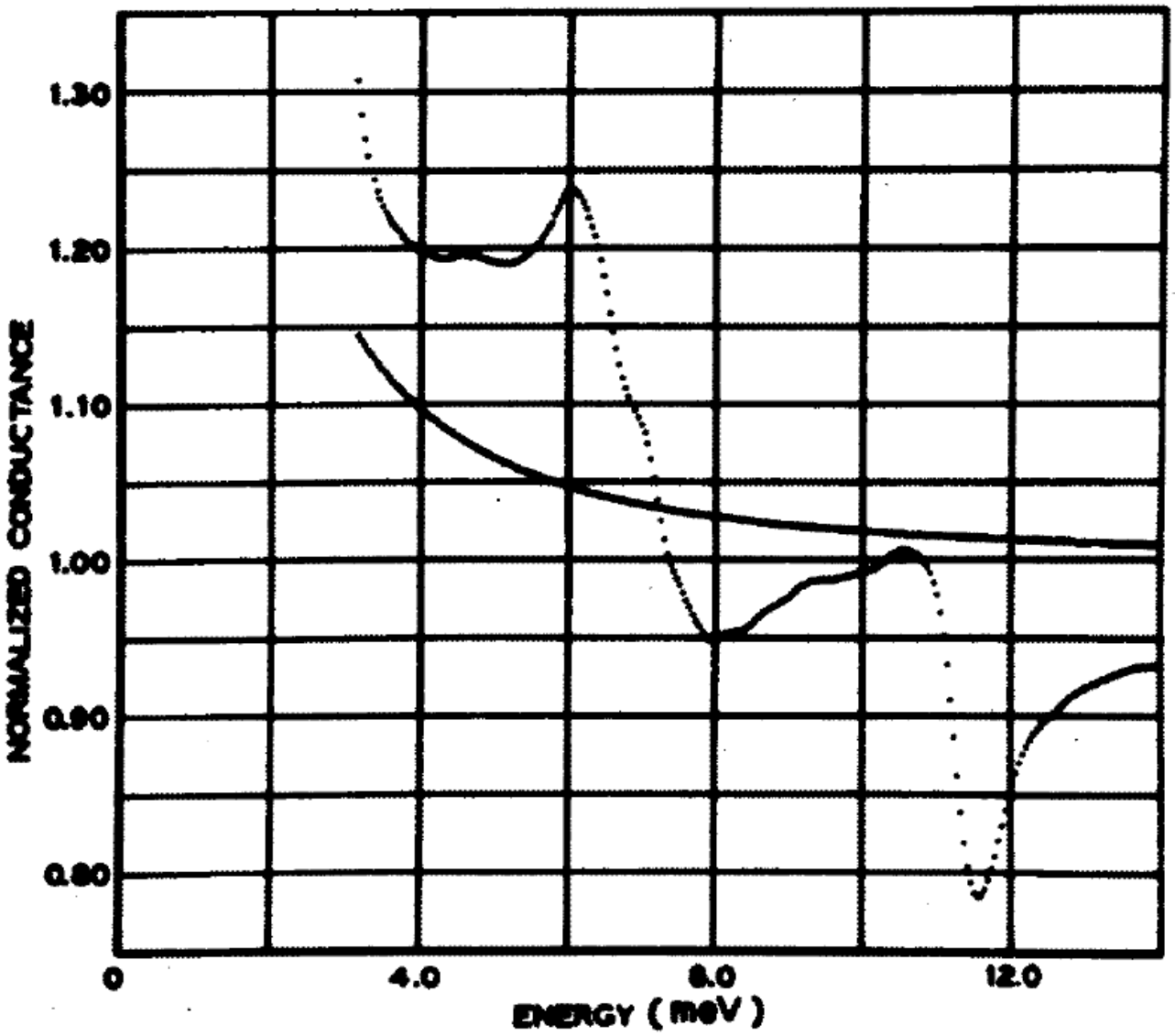

Figure 13: Conductance dI/dV of a Pb-I-Pb junction in the superconducting state normalized by the conductance in the normal state vs. voltage. Also shown is the two-superconductor conductance calculated from the BCS density of states which contains no phonon structure. Reproduced from Ref. [52].

McMillan and Rowell, Superconductivity, ed. By R.D. Parks (1969)

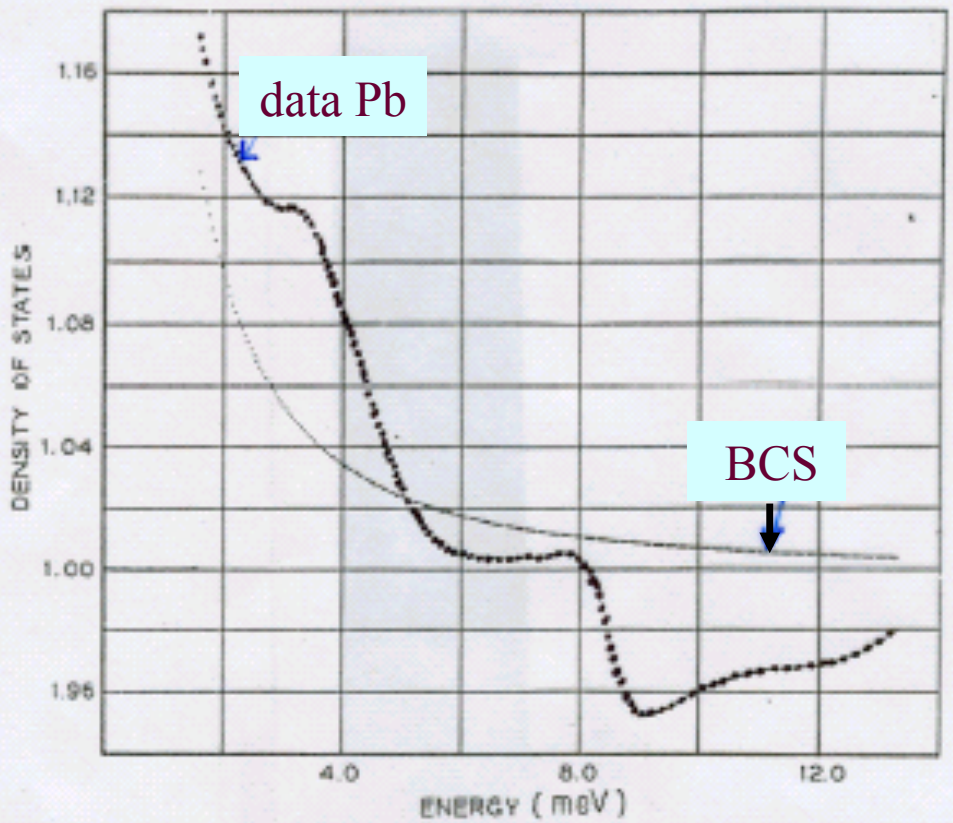

Fig. 23. Electronic density of states $N(E)$ for lead vs. $E-\Delta_0$ obtained from the data of Fig. 19. The smooth curve is the BCS density of states.

requires Eliashberg theory:

- phonon dynamics (retardation) taken into account $[\alpha^2 F(\Omega)]$
  - gap is a function of frequency $\Delta(\omega) = \mathcal{F}[\{\alpha^2 F(\Omega)\}, \mu^*]$
  - density of states is modified: $\frac{dI}{dV} \propto N(\omega) = N(\epsilon_F)\mathrm{Re}\{\frac{\omega}{\sqrt{\omega^2 - \Delta^2(\omega)}}\}$

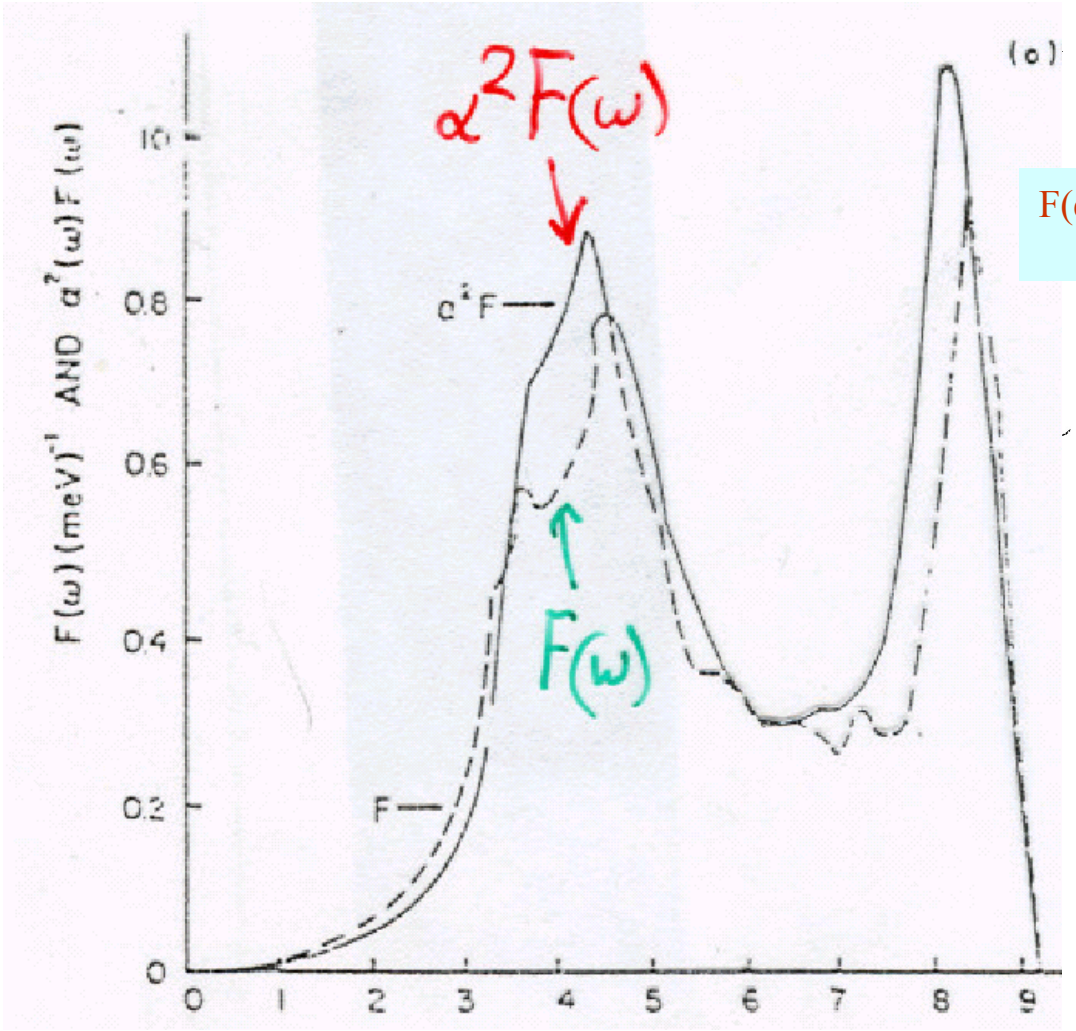

F(ω): density of phonon states from neutron scattering

$$\alpha^2(\omega) \equiv \frac{\alpha^2 F(\omega)}{F(\omega)} \sim \text{constant}$$

McMillan and Rowell, in Superconductivity, ed. By R.D. Parks (1969)

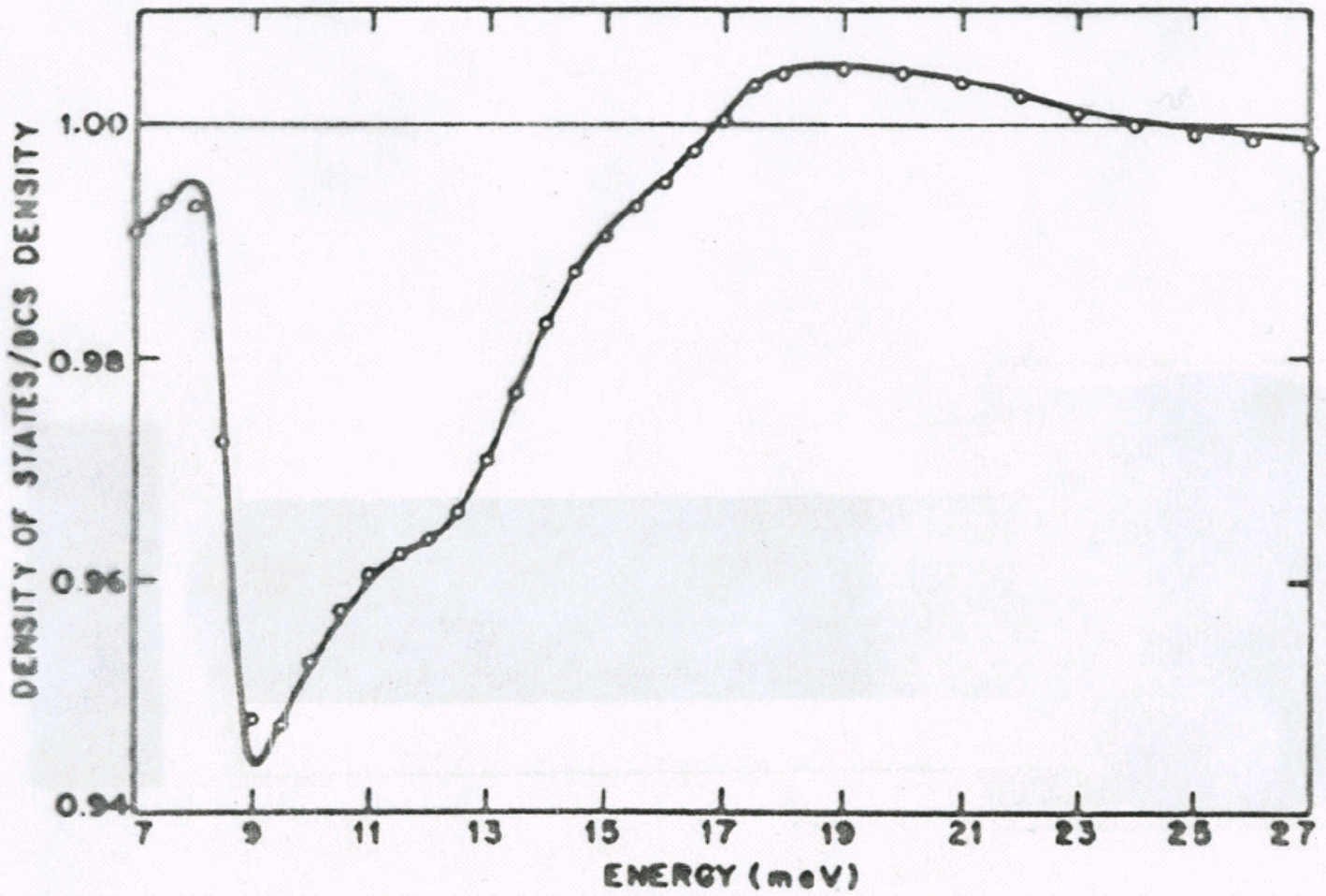

Fig. 32. Calculated (——) and measured (○○○) electronic density of states $N(E)$ for Pb normalized by the BCS density of states vs. $E-\Delta_0$. The measured density of states for $E-\Delta_0 > 11$ meV was not used in the fitting procedure and a comparison of theory and experiment in this "multiple-phonon-emission" region is a valied tst of the theory. In the experiment the sharp drop near 9 meV is affected by thermal smearing.

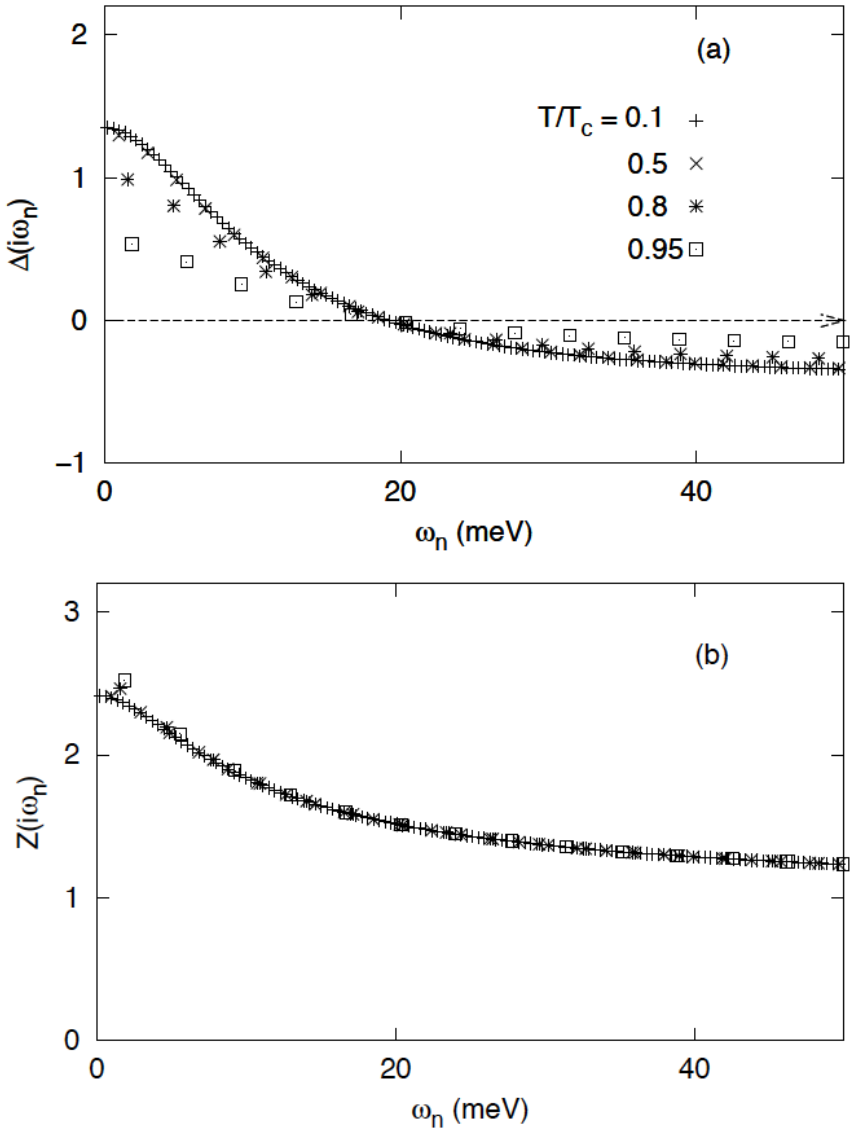

Eliashberg

Figure 22: (a) $\Delta(i\omega_n)$ and $Z(i\omega_n)$ vs ω_n, the fermion Matsubara frequency, for various temperatures, as indicated. Note that the curves are relatively smooth and featureless, and at low temperatures little change occurs, except that more Matsubara frequencies are present. In (a) the units of Δ are meV. These were produced for Pb.

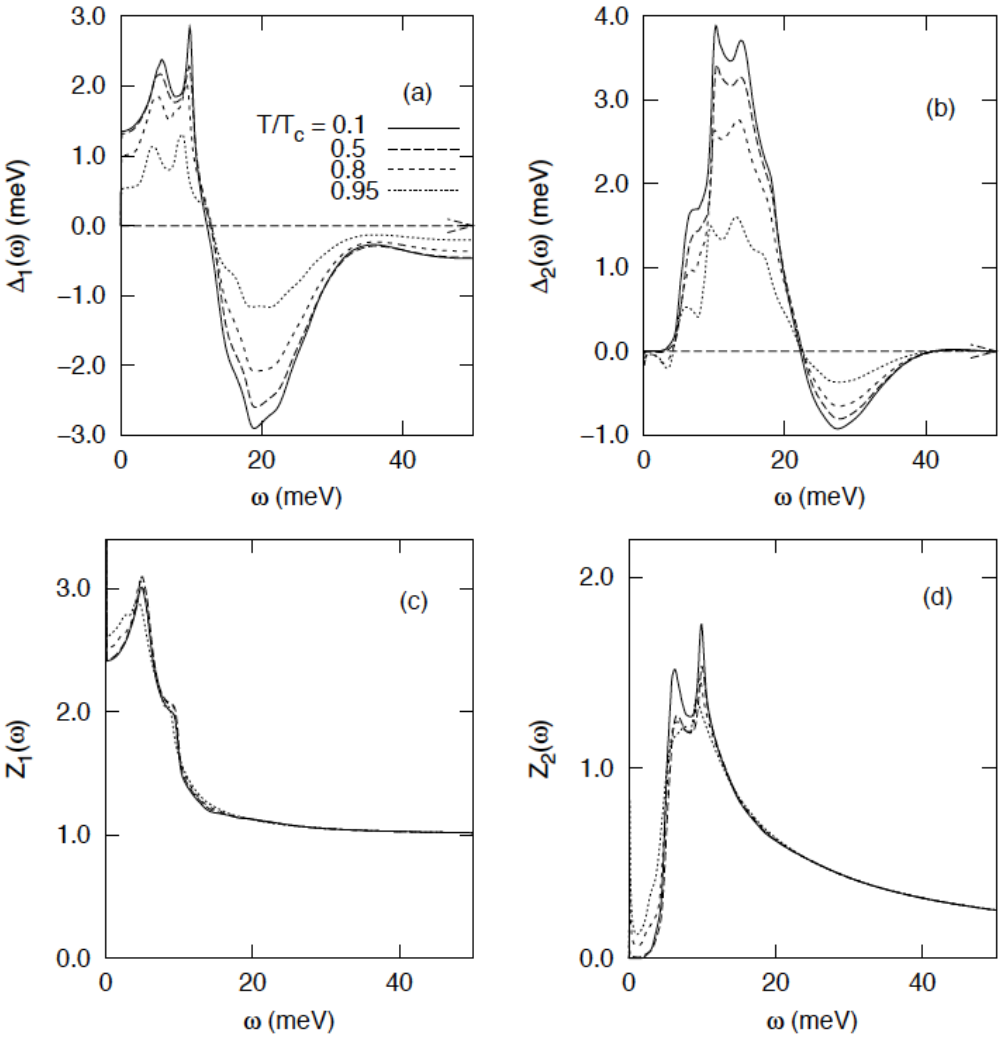

Eliashberg
(real frequency axis)

Figure 23: The (a) real and (b) imaginary parts of the gap function (in meV) on the real frequency axis, for Pb, for various temperatures, as in the previous figure. Note the considerable structure present on the real axis. Also shown is the (c) real and (d) imaginary part of the renormalization function, $Z(\omega)$ vs ω.

Eliashberg Theory

Density of states at finite temperature

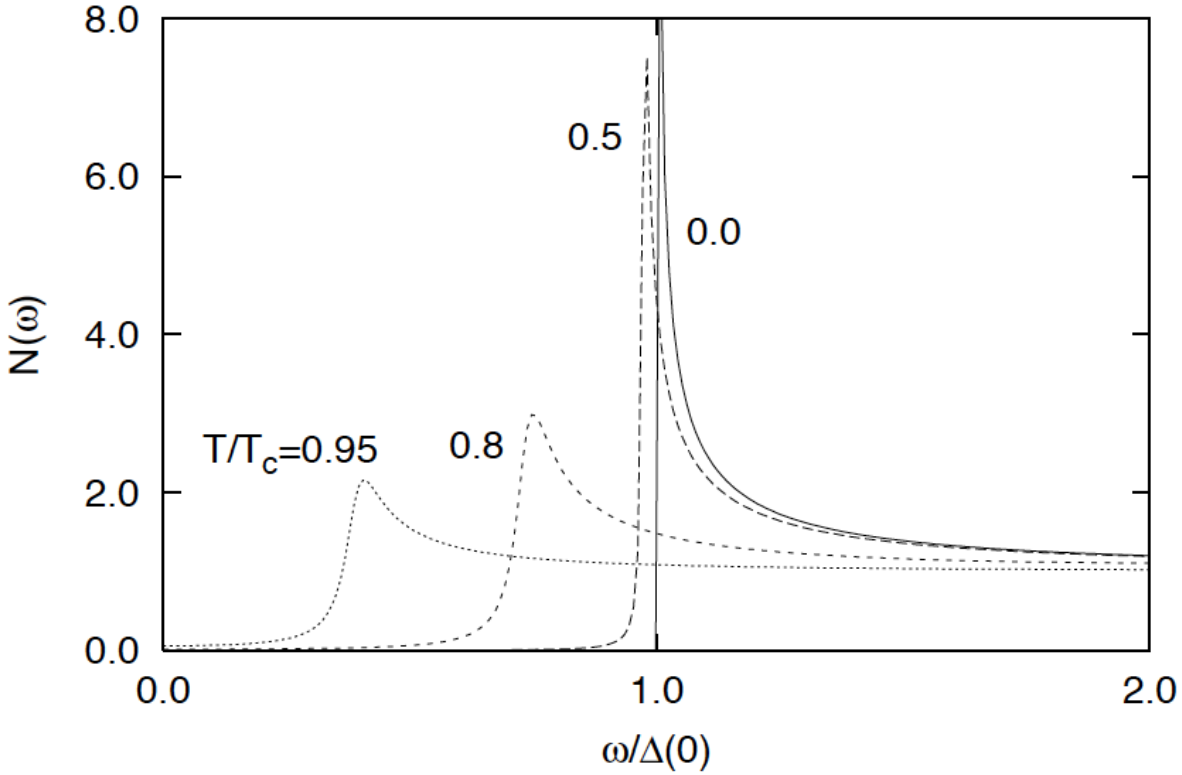

Figure 24: Calculated densities of states of Pb for various temperatures. In contrast to the BCS case (Fig. (21b), at high temperatures there is considerable smearing.

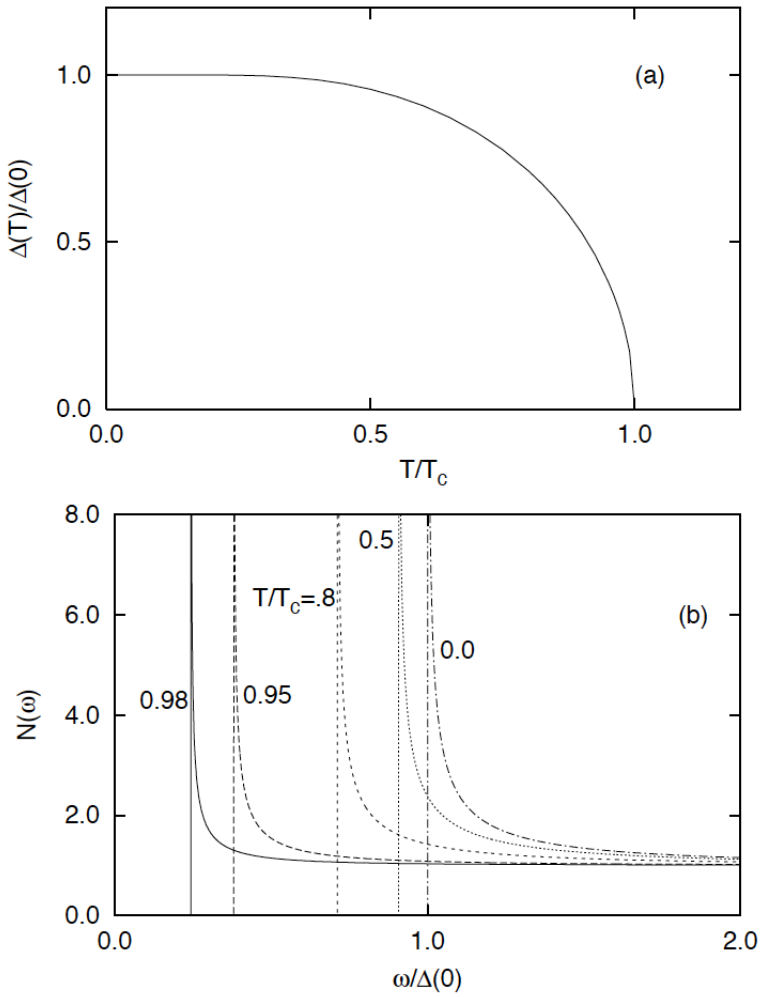

BCS
(at finite temperature)

Figure 21: (a) The temperature dependence of the BCS order parameter, and (b) the resulting densities of states at various temperatures below T_c. The only effect of finite temperatures on these latter curves is a reduced gap.

$$2\Delta_0/k_BT_c = 3.53[1 + 12.5(T_c/\omega_{\ell n})^2 \ell n(\omega_{\ell n}/2T_c)]$$

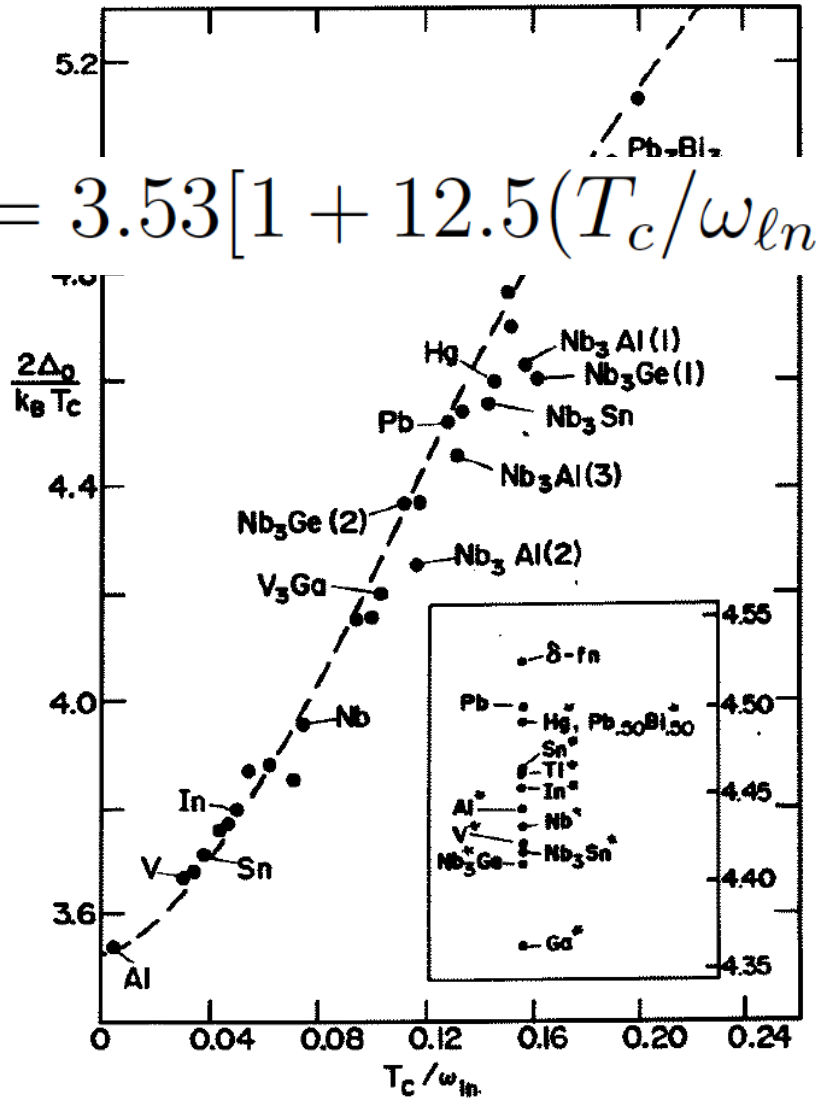

The gap ratio

$$\omega_{\ln} \equiv \exp\left[\frac{2}{\lambda}\int_0^\infty d\nu\, \ln(\nu)\frac{\alpha^2F(\nu)}{\nu}\right].$$

Figure 25: The ratio $2\Delta_0/k_BT_c$ vs $T_c/\omega_{\ell n}$. The solid dots represent results from the full numerical solutions of the Eliashberg equations. Experiment tends to agree to within 10%. In increasing order of $T_c/\omega_{\ell n}$, the dots correspond to the following systems: $A\ell$, V, Ta, Sn, $T\ell$, $T\ell_{0.9}Bi_{0.1}$, In, Nb (Butler), Nb (Arnold), $V_3Si(1)$, V_3Si (Kihl.), Nb (Rowell), Mo, $Pb_{0.4}T\ell_{0.6}$, La, V_3Ga, $Nb_3A\ell(2)$, $Nb_3Ge(2)$, $Pb_{0.6}T\ell_{0.4}$, Pb, $Nb_3A\ell(3)$, $Pb_{0.8}T\ell_{0.2}$, Hg, Nb_3Sn, $Pb_{0.9}Bi_{0.1}$, $Nb_3A\ell(1)$, $Nb_3Ge(1)$, $Pb_{0.8}Bi_{0.2}$, $Pb_{0.7}Bi_{0.3}$, and $Pb_{0.65}Bi_{0.35}$. The drawn curve corresponds to $2\Delta_0/k_BT_c = 3.53[1 + 12.5(T_c/\omega_{\ell n})^2\ell n(\omega_{\ell n}/2T_c)]$. The insert shows results for different scaled $\alpha^2F(\omega)$ spectra. They all correspond to the same value of T_c and of $\omega_{\ell n}$ as Pb. They serve to show that some deviation from the general trend is possible. Reproduced from Ref. [11].

The Specific Heat Jump at Tc

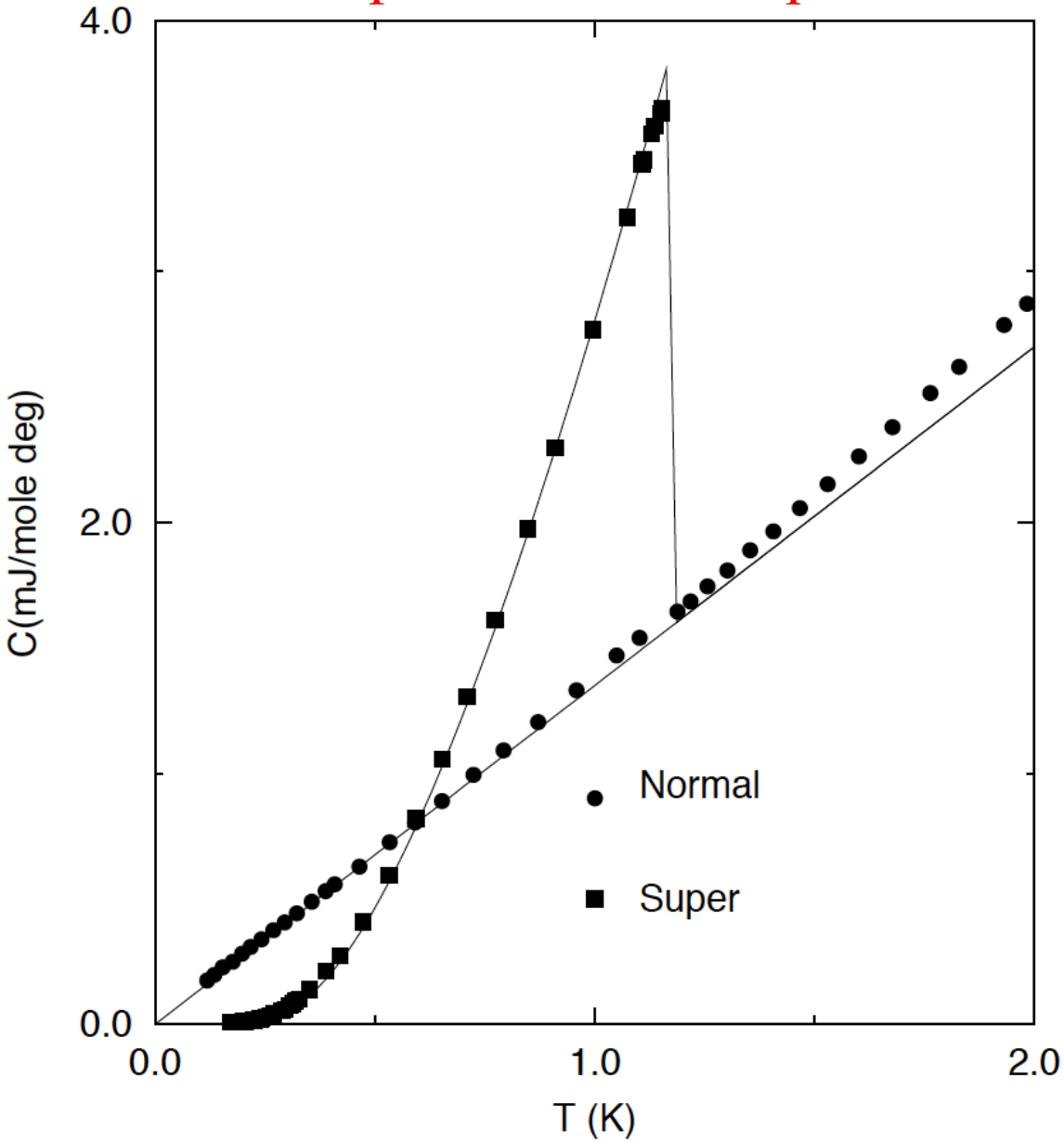

Figure 26: Specific heat of aluminium as a function of temperature in the superconducting state and the normal state (applied field of 300 Gauss). Data taken from Ref. [237]. The BCS prediction, given the normal state data, is given by the solid curve.

Figure 27: The specific heat ratio, $\Delta C(T_c)/(\gamma T_c)$ vs $T_c/\omega_{\ell n}$. The dots represent results from the full numerical solutions of the Eliashberg equations. Experiment tends to agree to within 10%. In increasing order of $T_c/\omega_{\ell n}$, the dots correspond to the following systems: $A\ell$, V, Ta, Sn, $T\ell$, $T\ell_{0.9}Bi_{0.1}$, In, Nb (Butler), Nb (Arnold), V_3Si 1, V_3Si (Kihl.), Nb (Rowell), Mo, $Pb_{0.4}T\ell_{0.6}$, La, V_3Ga, $Nb_3A\ell(2)$, $Nb_3Ge(2)$, $Pb_{0.6}T\ell_{0.4}$, Pb, $Nb_3A\ell(3)$, $Pb_{0.8}T\ell_{0.2}$, Hg, Nb_3Sn, $Pb_{0.9}Bi_{0.1}$, $Nb_3A\ell(1)$, $Nb_3Ge(1)$, $Pb_{0.8}Bi_{0.2}$, $Pb_{0.7}Bi_{0.3}$, and $Pb_{0.65}Bi_{0.35}$. The drawn curve corresponds to $\Delta C(T_c)/\gamma T_c = 1.43(1 + 53(T_c/\omega_{\ell n})^2 \ell n(\omega_{\ell n}/3T_c))$. Adapted from Ref. [221].

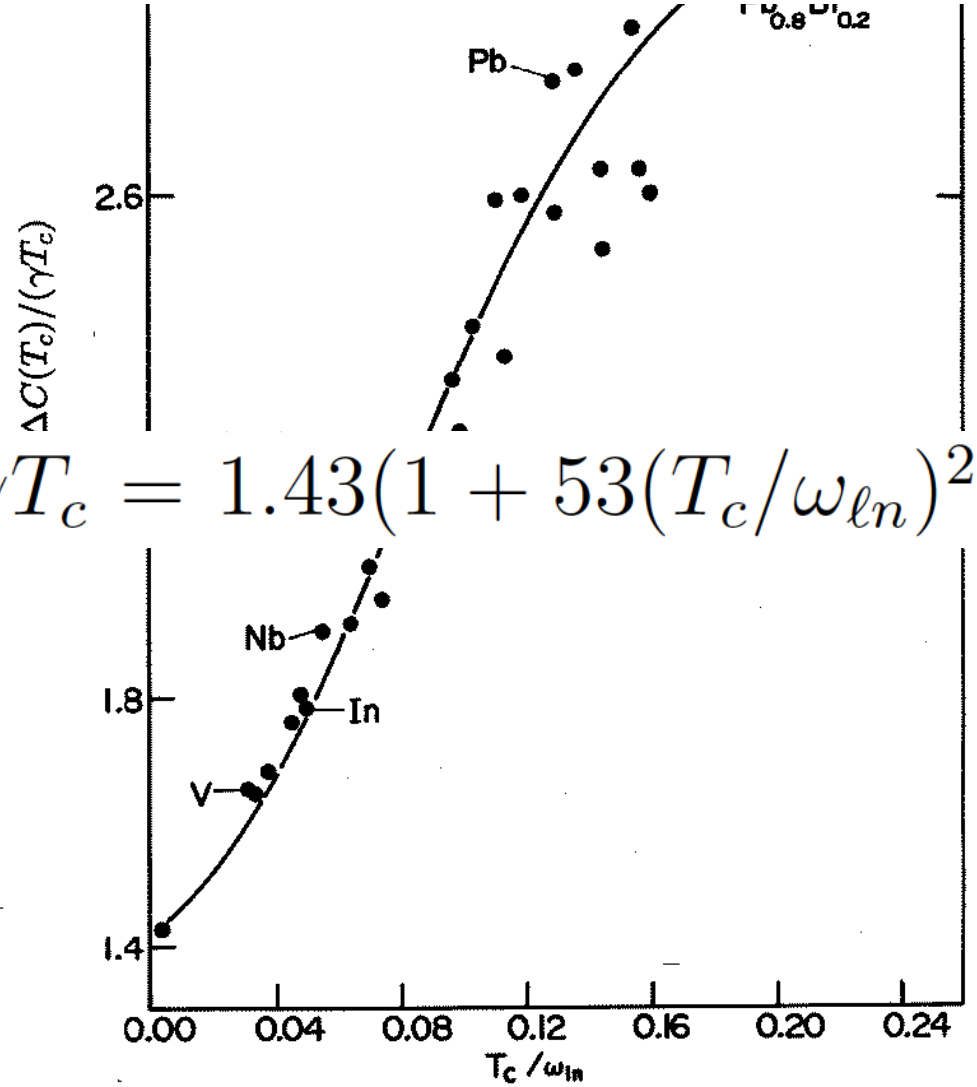

$$\Delta C(T_c)/\gamma T_c = 1.43(1 + 53(T_c/\omega_{\ell n})^2 \ell n(\omega_{\ell n}/3T_c))$$

Optical Conductivity

BCS Theory

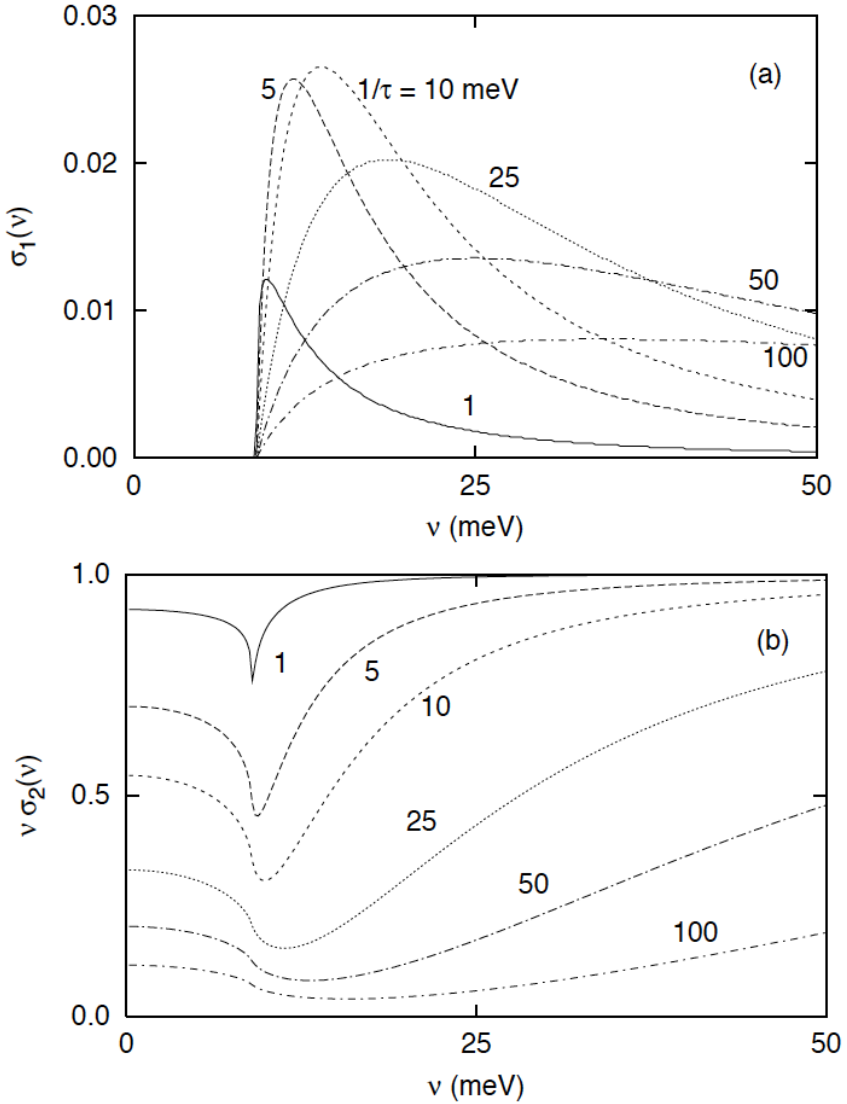

Figure 28: (a) $\sigma_1(\nu)$ vs. ν in the zero temperature BCS superconducting state for the various impurity scattering rates indicated. The absorption onset at $2\Delta(0)$ remains sharp independent of the scattering rate. A delta-function contribution (not shown) is also present at the origin. (b) Same as in (a) except for the frequency times the imaginary part of the conductivity. The optical gap is a little less evident in the dirty limit. The conductivity is given in units of $ne^2/m \equiv \omega_P^2/4\pi$). Taken from Ref. [181].

Optical Conductivity

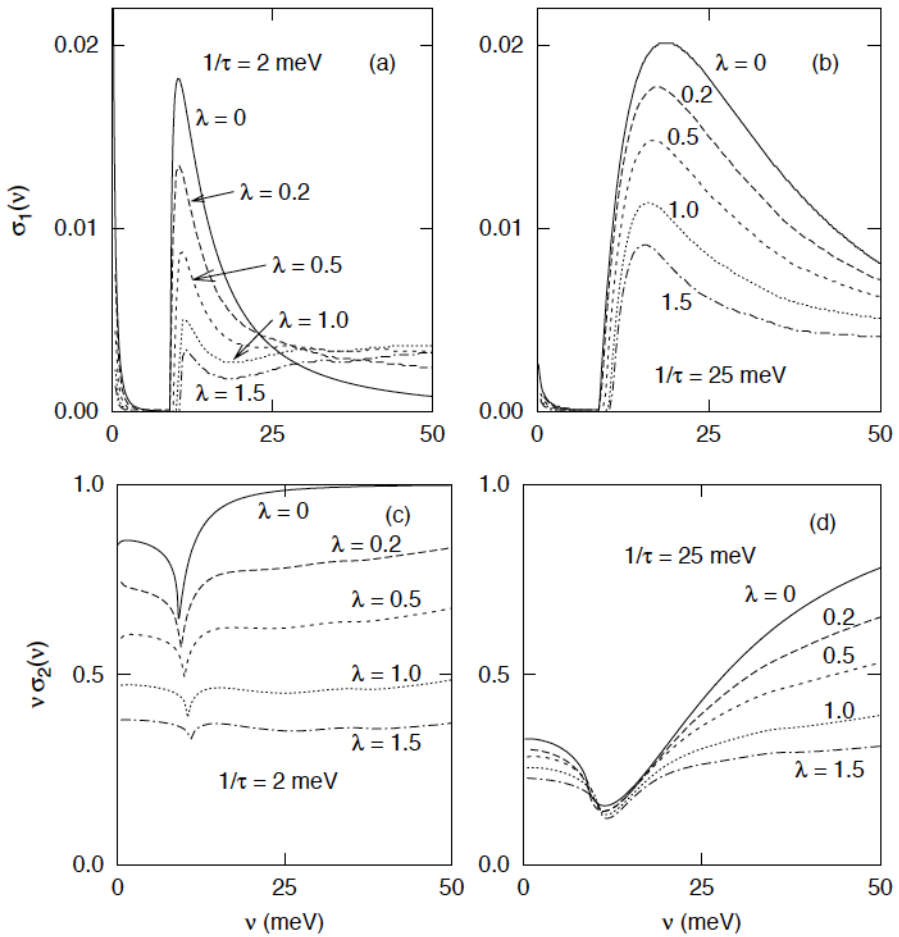

Eliashberg Theory

Figure 34: The real part (a,b) and the imaginary part (c,d) of the conductivity at essentially zero temperature ($T/T_c = 0.3$) with $1/\tau = 2$ meV (a,c) and $1/\tau = 25$ meV (b,d). In all cases we have used the BKBO spectrum scaled to give the designated value of, λ, while T_c is held fixed at 29 K by adjusting μ^*. Increased coupling strength suppresses both $\sigma_1(\nu)$ and $\nu\sigma_2(\nu)$ and broadens the minimum in the latter at 2Δ. Note that 2Δ increases slightly as the coupling strength is increased. The conductivity is given in units of $ne^2/m \equiv \omega_P^2/4\pi$).

Far-Infrared Absorption in Thin Superconducting Lead Films*

LEIGH HUNT PALMER†
Department of Physics, University of California, Berkeley, California
AND
M. TINKHAM‡

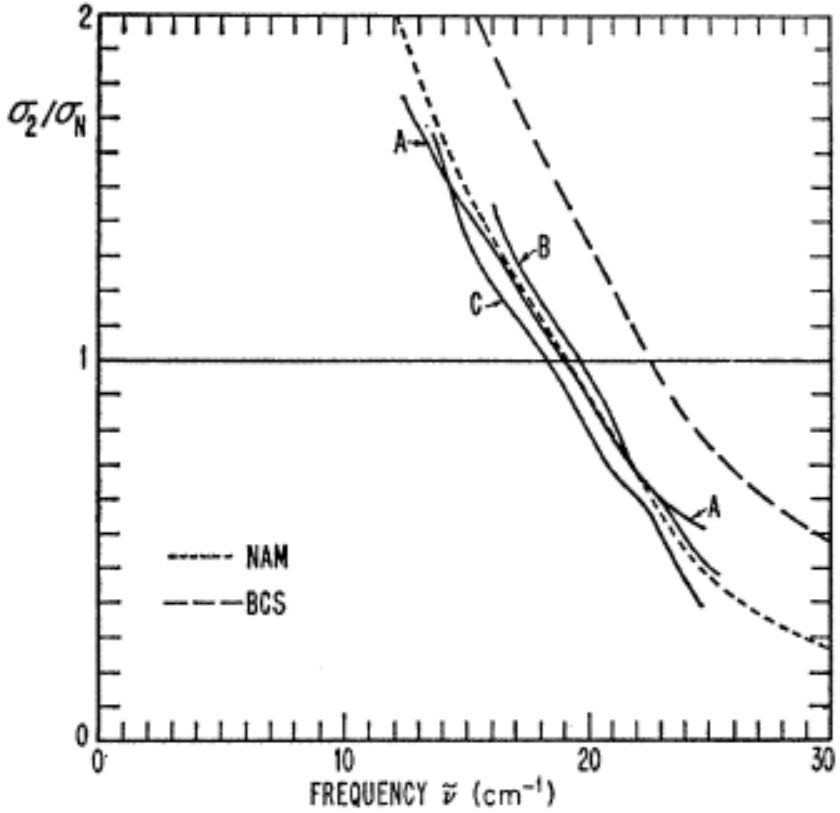

FIG. 6. Smoothed results of measurements of the imaginary part of the normalized conductivity of three lead films (A, B, and C) at 2°K. Curve labeled BCS is the weak-coupling result of Mattis and Bardeen, while that labeled Nam presents a revised version of a curve shown in Ref. 5. In both cases, the gap frequency was taken to be 22.5 cm^{-1}.

Model of the Electron-Phonon Interaction and Optical Conductivity of $Ba_{1-x}K_xBiO_3$ Superconductors

R. Nourafkan,[1] F. Marsiglio,[2] and G. Kotliar[1]

PRL 109, 017001 (2012) PHYSICAL RE

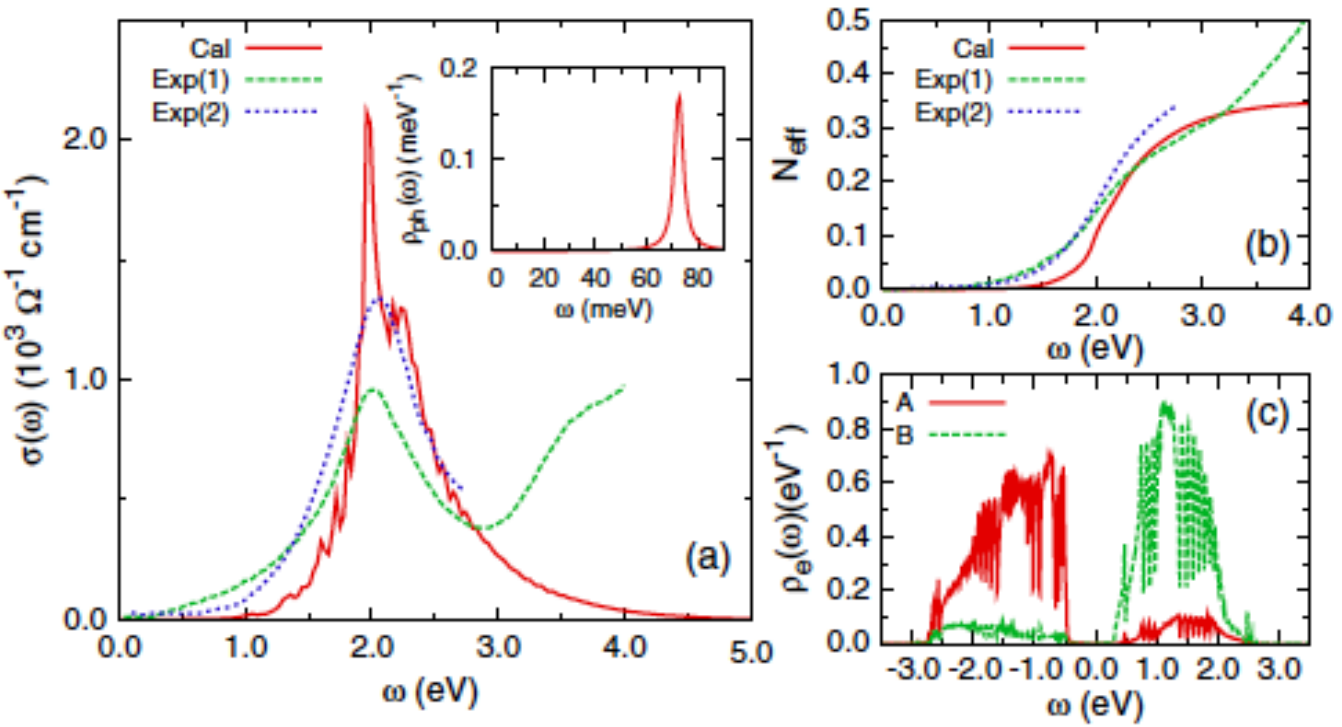

So what's wrong?

1) The building block is the polaron !

How do 'polaron' effects become 'undone'?

Sasha Alexandrov

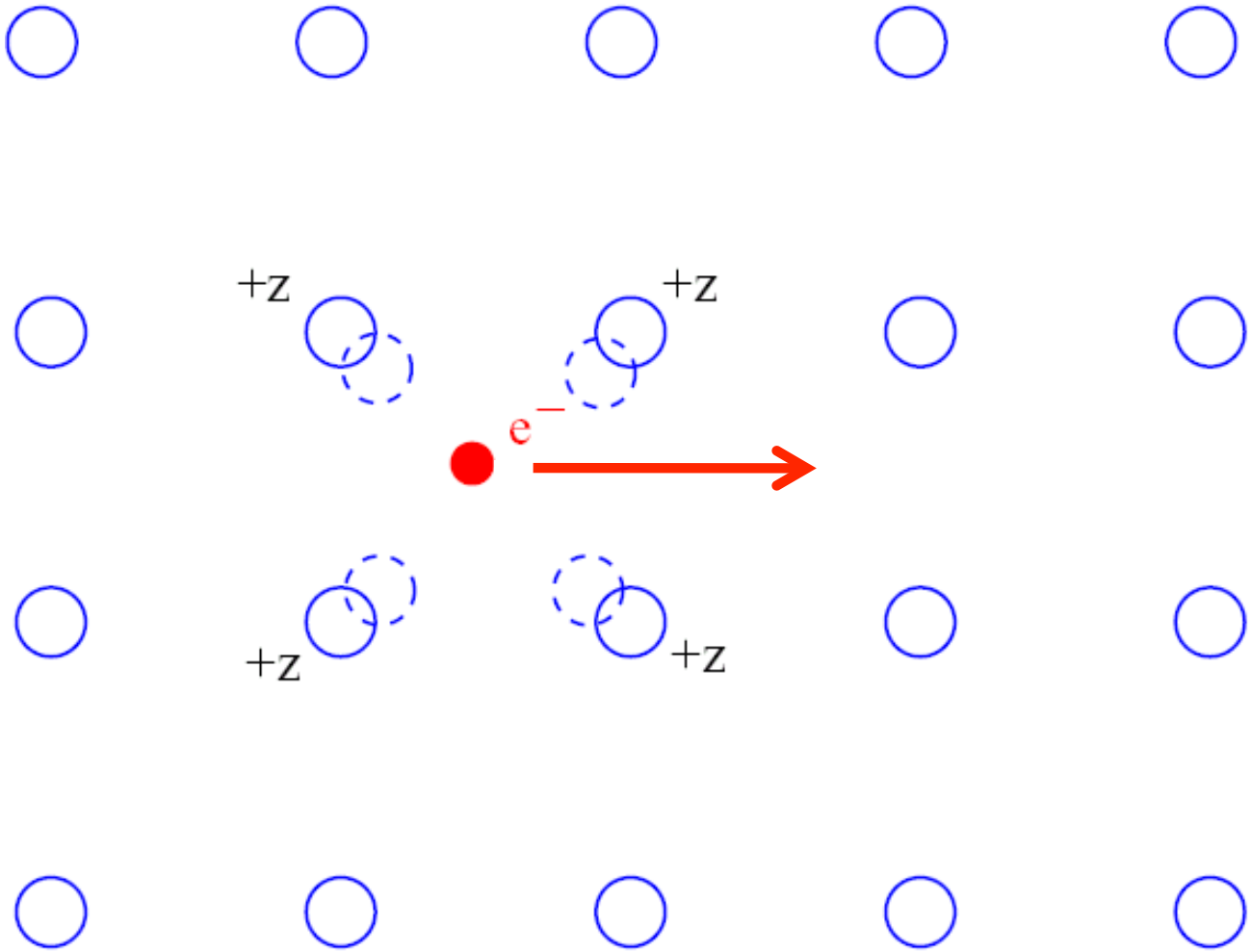
+z
+z
e−
+z
+z

The "High-T_c" experience

VOLUME 60, NUMBER 26 PHYSICAL REVIEW LETTERS 27 JUNE 1988

Spectral Function of Holes in a Quantum Antiferromagnet

S. Schmitt-Rink and C. M. Varma
AT&T Bell Laboratories, Murray Hill, New Jersey 07974
and
A. E. Ruckenstein

PHYSICAL REVIEW B VOLUME 43, NUMBER 13 1 MAY 1991

Spectral function of a single hole in a two-dimensional quantum antiferromagnet

Frank Marsiglio*
Department of Physics, University of California at San Diego, La Jolla, California 92093
Andrei E. Ruckenstein
Serin Physics Laboratory, Rutgers University, Piscataway, New Jersey 08855
Stefan Schmitt-Rink and Chandra M. Varma
AT&T Bell Laboratories, Murray Hill, New Jersey 07974

The message:

First question is,
what is the basic building block?

PHYSICAL REVIEW B VOLUME [illegible] 1 APRIL 1989

Motion of a single hole in a quantum antiferromagnet

[illegible] and P. [illegible]
Department of Physics, Massachusetts Institute of Technology, Cambridge, Massachusetts 02139
N. Read
Department of Applied Physics, Yale University, New Haven, Connecticut 06520

PHYSICAL REVIEW B VOLUME 57, NUMBER 9 1 MARCH 1998-I

Dispersion of a single hole in an antiferromagnet

Andrey V. Chubukov and Dirk K. Morr
Department of Physics, University of Wisconsin-Madison, 1150 University Avenue, Madison, Wisconsin 53706

POLARONS AND EXCITONS

Scottish Universities' Summer School

1962

Edited by

C. G. KUPER B.SC., M.A., PH.D.

and

G. D. WHITFIELD M.A., PH.D.

Two paradigms for electron-phonon coupling:

1) Holstein (the `Hubbard' model for electron-phonon interactions)
2) BLF-SSH (`off-diagonal' coupling)

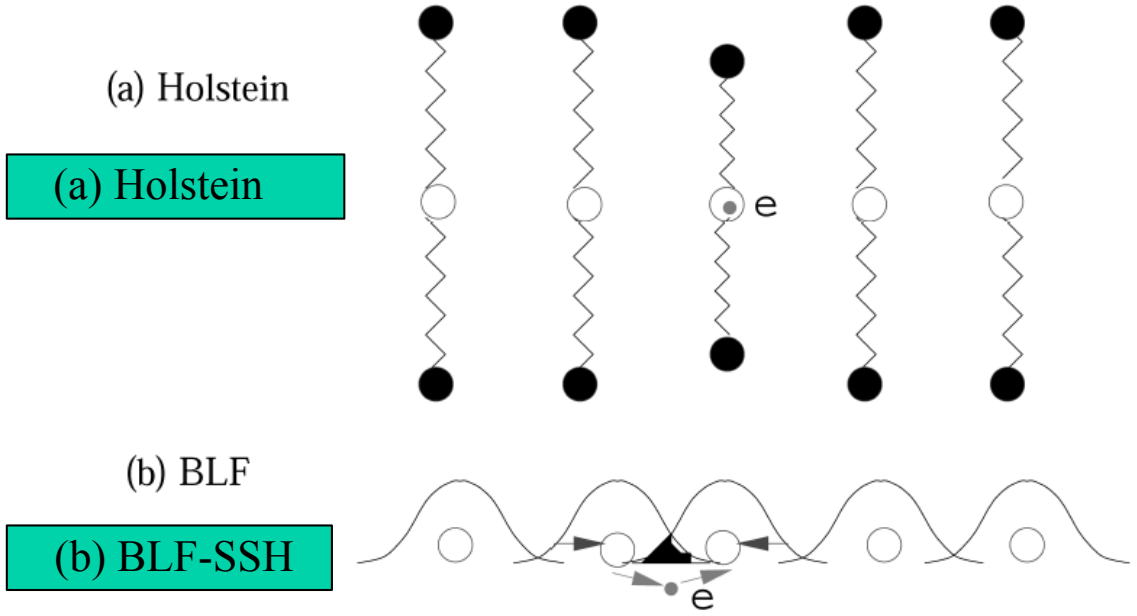

"SSH" (polyacetylene)

71. W.-P. Su, J.R. Schrieffer, and A.J. Heeger, Phys. Rev. Lett. **42** 1698 (1979); Phys. Rev. B **22**, 2099 (1980).

75. A.J. Heeger, S. Kivelson, J.R. Schrieffer, and W.–P. Su, Rev. Mod. Phys. **60** 781 (1988).

"BLF"

[10]S. Barisić, J. Labbé, and J. Friedel, Phys. Rev. Lett. **25**, 919 (1970); S. Barisić, Phys. Rev. B **5**, 932 (1972); **5**, 941 (1972).

TIGHT BINDING AND TRANSITION-METAL SUPERCONDUCTIVITY*

S. Barišić,† J. Labbé, and J. Friedel

$$H = \sum_{j,\alpha,\delta_\alpha,\sigma} J_{j,\delta_\alpha} a_{j,\sigma}^{\dagger} a_{j+\delta_\alpha,\sigma} + U \sum_j n_{j\uparrow} n_{j\downarrow}.$$

where

$$J_{j\delta_\alpha} = J(\vec{a}_\alpha) + \left.\frac{\partial J(\vec{R})}{\partial \vec{R}}\right|_{\vec{R}=\vec{a}_{\delta_\alpha}} (\vec{u}_{j+\delta_\alpha} - \vec{u}_j).$$

Methods of Solution

- Variational
- Perturbation Theory: weak coupling
- Perturbation Theory: strong coupling
- Quantum Monte Carlo
- Exact Diagonalization on small systems
- Variational Lanczos Method (Trugman, Bonca)

Exact results for the single polaron in the thermodynamic limit!

[5] S. A. Trugman, in *Applications of Statistical and Field Theory Methods to Condensed Matter*, edited by D. Baeriswyl, A. R. Bishop, and J. Carmelo (Plenum Press, New York, 1990).

[6] J. Bonča, S. A. Trugman, and I. Batistíc, Phys. Rev. B **60**, 1633 (1999).

1) Let the Hamiltonian generate new states;
2) Orthogonalize to previous states;
3) Incorporate Bloch's Theorem analytically

1) Results are numerically exact;
2) Thermodynamic limit, i.e. no finite size effects;
3) Arbitrary wave vector

Use Lanczos diagonalization of Bloch States.
The computer keeps track of states like:

$$c_0^\dagger$$

$$\frac{(a_0^\dagger)^4}{\sqrt{4!}} c_0^\dagger$$

$$\frac{(a_0^\dagger)^3}{\sqrt{3!}} \frac{(a_{-1}^\dagger)^2}{\sqrt{2!}} \frac{(a_{+1}^\dagger)^1}{\sqrt{1!}} c_0^\dagger$$

To us these states really mean:

$$\frac{1}{\sqrt{N}} \sum_i e^{ikR_i} c_i^\dagger$$

$$\frac{1}{\sqrt{N}} \sum_i e^{ikR_i} \frac{(a_i^\dagger)^4}{\sqrt{4!}} c_i^\dagger$$

$$\frac{1}{\sqrt{N}} \sum_i e^{ikR_i} \frac{(a_i^\dagger)^3}{\sqrt{3!}} \frac{(a_{i-1}^\dagger)^2}{\sqrt{2!}} \frac{(a_{i+1}^\dagger)^1}{\sqrt{1!}} c_i^\dagger$$

Trugman Method uses Lanczos diagonalization of Bloch States.

To us these states really mean:

$$\frac{1}{\sqrt{N}}\sum_i e^{ikR_i}c_i^\dagger$$

$$\frac{1}{\sqrt{N}}\sum_i e^{ikR_i}\frac{(a_i^\dagger)^4}{\sqrt{4!}}c_i^\dagger$$

$$\frac{1}{\sqrt{N}}\sum_i e^{ikR_i}\frac{(a_i^\dagger)^3}{\sqrt{3!}}\frac{(a_{i-1}^\dagger)^2}{\sqrt{2!}}\frac{(a_{i+1}^\dagger)^1}{\sqrt{1!}}c_i^\dagger$$

$$H = -t \sum_{\langle i,j\rangle,\alpha=\uparrow\downarrow} (c_{i,\alpha}^\dagger c_{j,\alpha} + c_{j,\alpha}^\dagger c_{i,\alpha})$$

$$- g\omega_E \sum_{i,s=\uparrow\downarrow} c_{i,s}^\dagger c_{i,s}(a_i + a_i^\dagger) + \omega_E \sum_i a_i^\dagger a_i ,$$

$$H = -t\sum_{i,\delta}(c_i^\dagger c_{i+\delta} + c_{i+\delta}^\dagger c_i) + \sum_i \left[\frac{p_i^2}{2M} + \frac{1}{2}M\omega_E^2 x_i^2\right] - \alpha\sum_i n_i x_i,$$

PHYSICAL REVIEW B **81**, 115114 (2010)

Ground-state properties of the Holstein model near the adiabatic limit

Zhou Li, D. Baillie,* C. Blois,† and F. Marsiglio

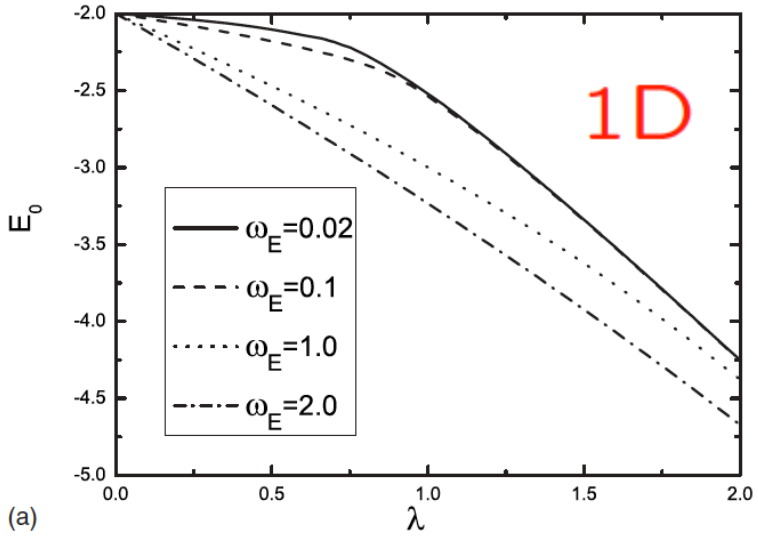

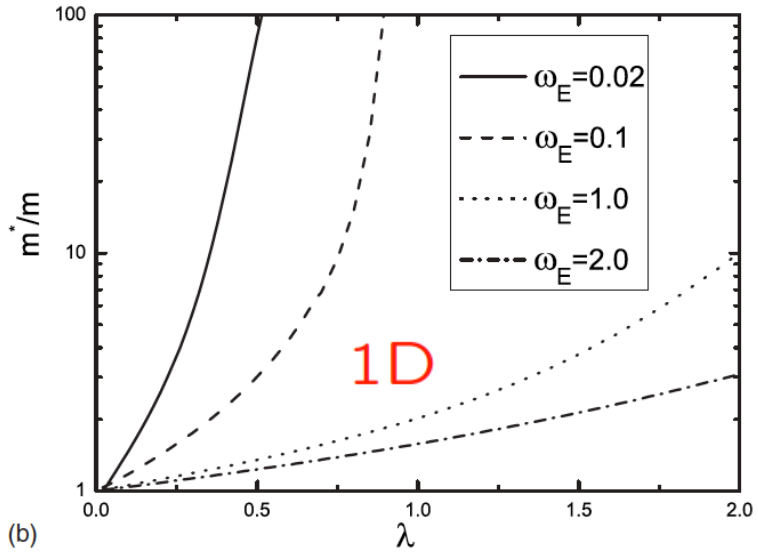

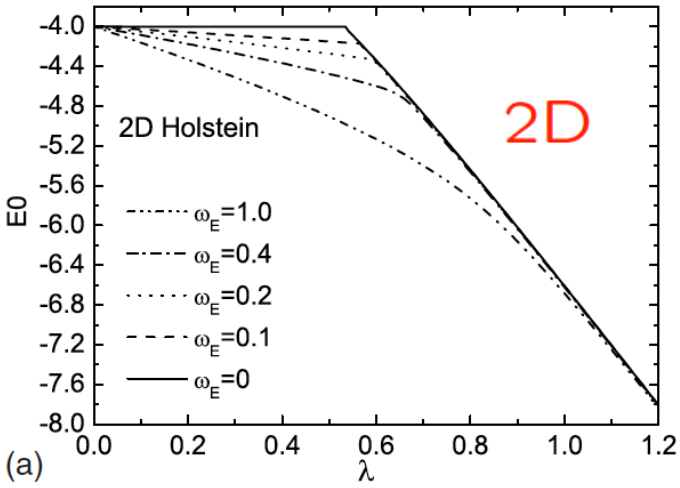

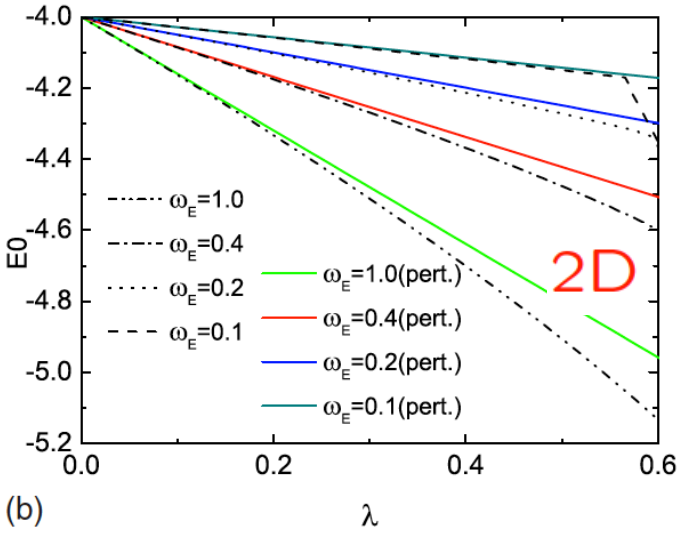

In the strong coupling limit, start with
the so-called coherent state:

$$|\psi\rangle = e^{-g^2/2} \sum_{\ell} e^{ikR_\ell} e^{-g\hat{a}_\ell^\dagger \hat{c}_\ell^\dagger} |0\rangle$$

J Supercond Nov Magn
DOI 10.1007/s10948-012-1601-6

ORIGINAL PAPER

The Polaron-Like Nature of an Electron Coupled to Phonons

Zhou Li · F. Marsiglio

ground state energy

effective mass enhancement

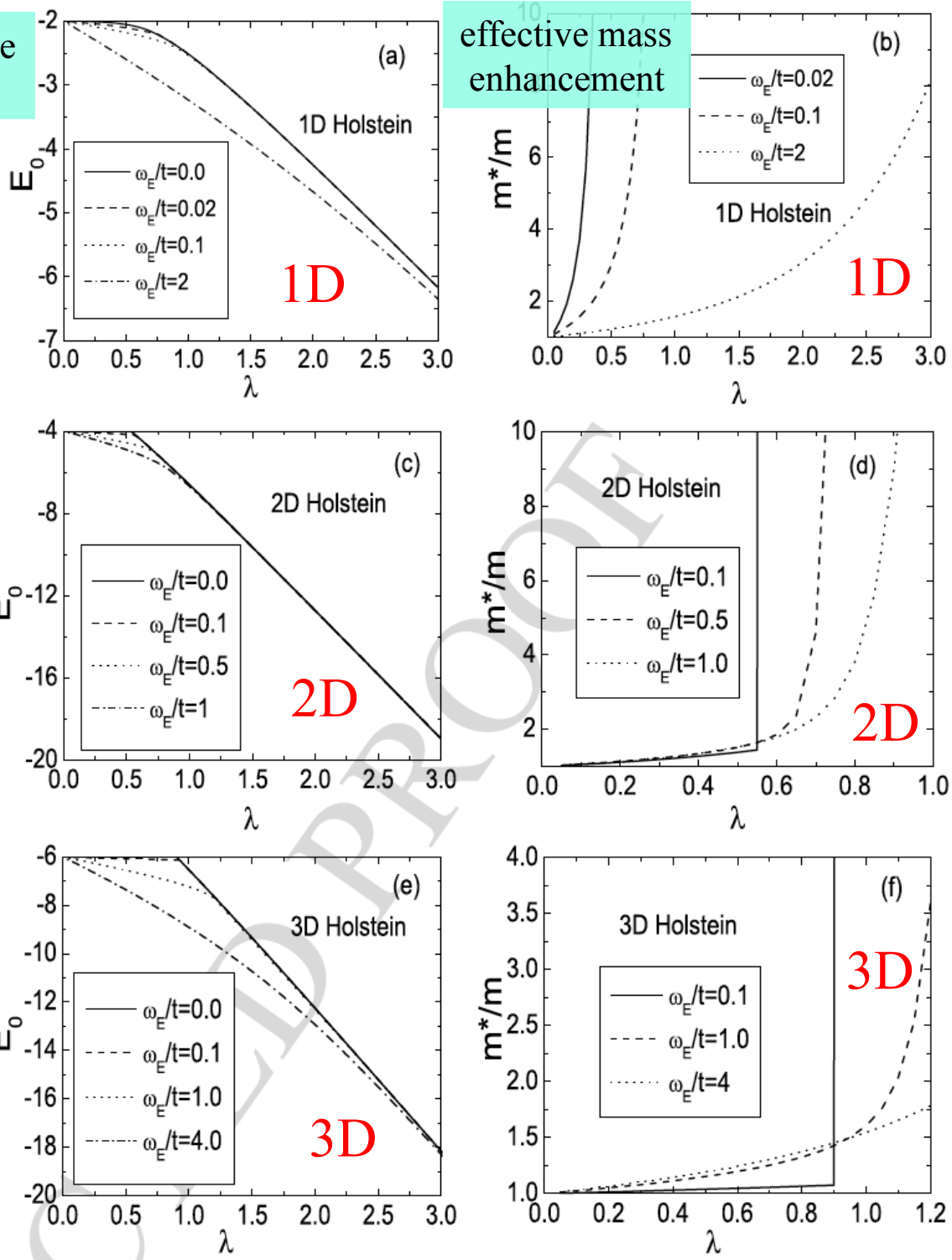

For the Holstein model,

1) In 1D the electron is always "polaronic' (Kabanov and Mashtakov, 1993)

2) In 2D (and 3D) there is a sharp increase in the effective mass as a function of electron-phonon coupling. This increase becomes sharper for lower phonon frequency, but it is always a crossover.

3) Perturbation fails for intermediate coupling strength.

How do you reconcile this with Eliashberg phenomenology of Pb, Hg, A15's etc?

Answer:

No real answer, yet.

1) Maybe the construction of a Fermi sea reduces (via Pauli blocking) polaronic effects

2) Maybe the `bare' coupling strength is fairly weak, and as the Fermi sea arises, the phonons soften with an increase in the `effective' coupling strength (requires a kind of fine tuning).

cond-mat 1105.2833 Phys. Rev. B 84 (2011), 184531

Quantitative reliability of Migdal-Eliashberg theory for strong electron-phonon coupling

Johannes Bauer[1], Jong E. Han[1,2], and Olle Gunnarsson[1]

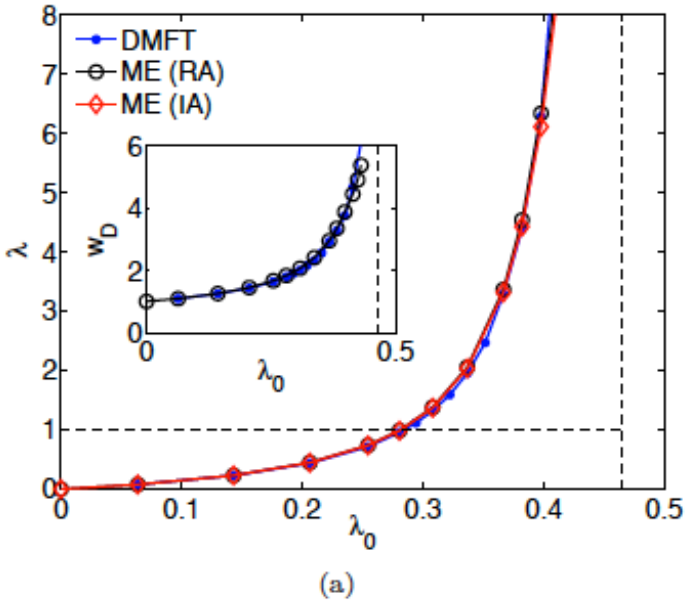

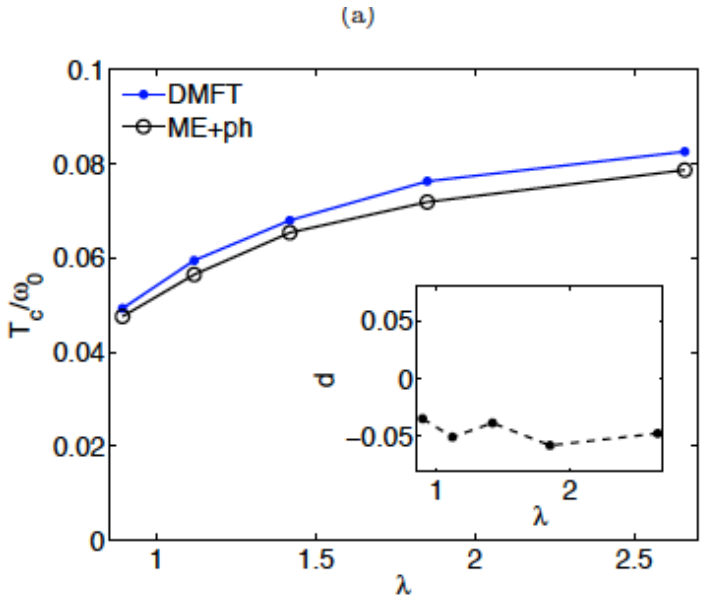

but…

PHYSICAL REVIEW B VOLUME 42, NUMBER 4 1 AUGUST 1990

Pairing and charge-density-wave correlations in the Holstein model at half-filling

F. Marsiglio
Department of Physics, University of California at San Diego, La Jolla, California 92093

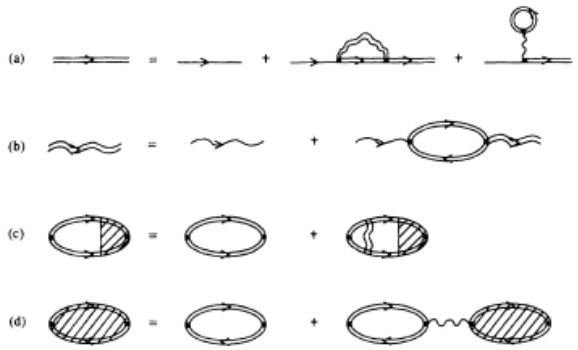

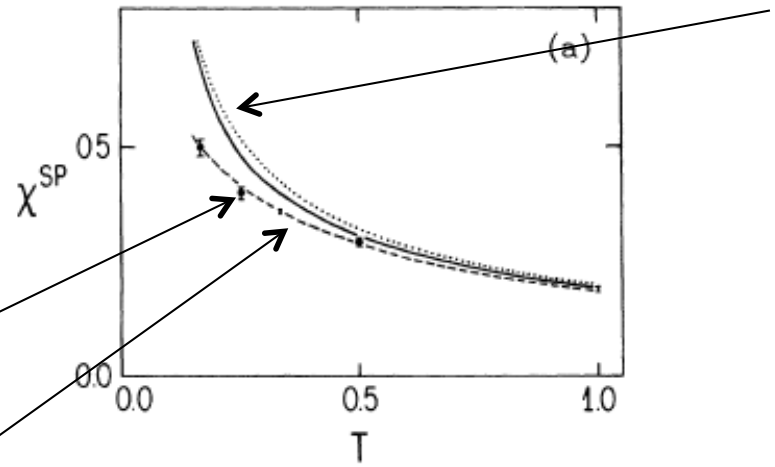

Non-self-consistent
Migdal approximation

QMC

Self-consistent
Migdal approximation, i.e. with phonon renormalization

J Supercond Nov Magn (2012) 25:1313–1317
DOI 10.1007/s10948-012-1601-6

ORIGINAL PAPER

The Polaron-Like Nature of an Electron Coupled to Phonons

Zhou Li · F. Marsiglio

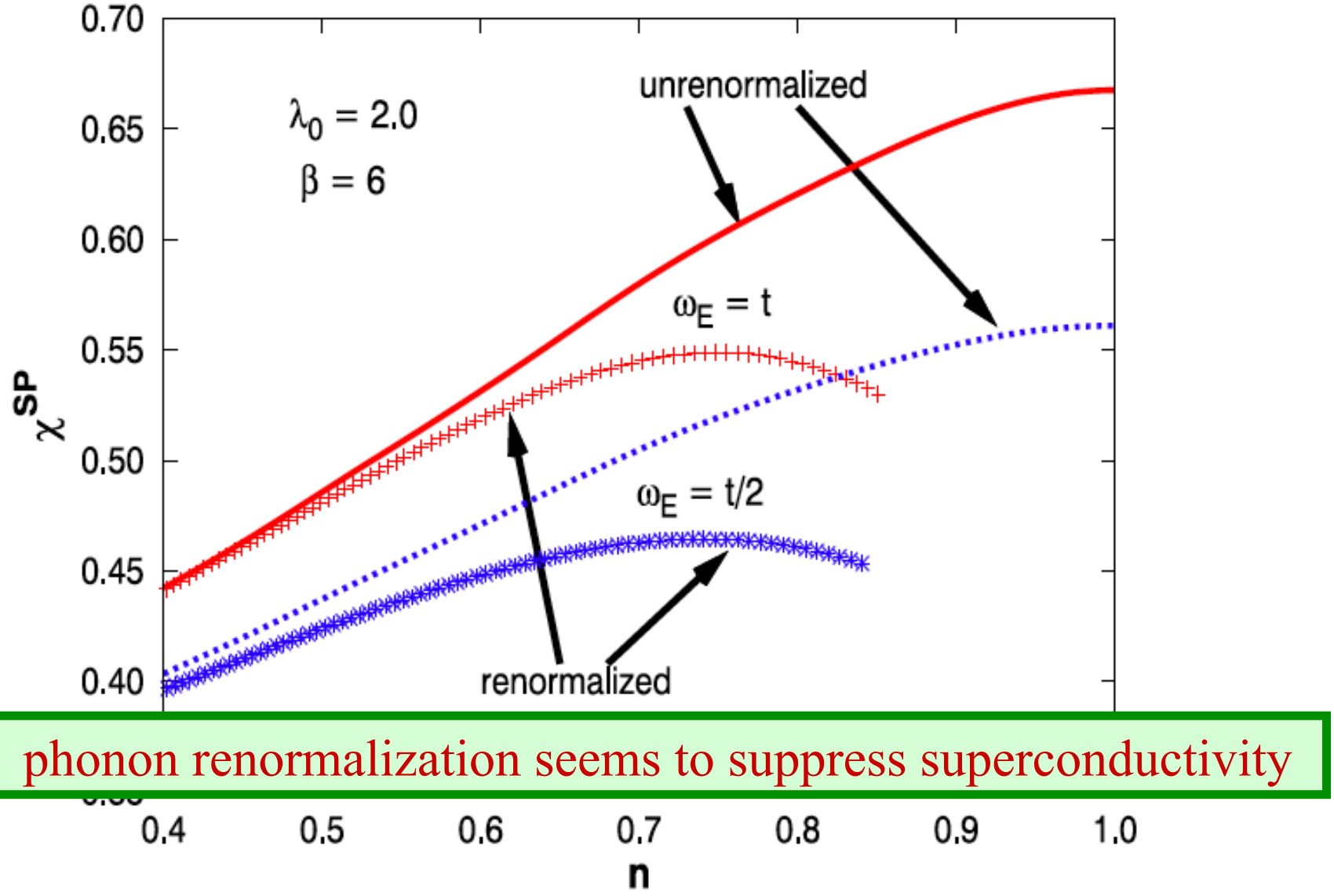

phonon renormalization seems to suppress superconductivity

Open questions:

1) What happens with many electrons?

2) What about the conventional theory and all the evidence that favours it (that I, amongst others, have promoted for the last several decades)??

So what's wrong?

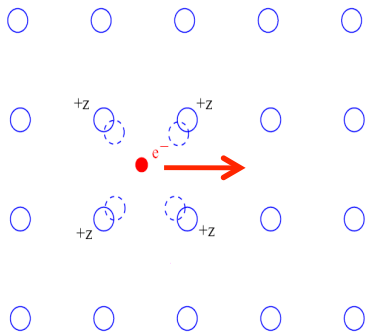

1) The building block is the polaron !
How do 'polaron' effects become 'undone'?

Can't seem to couple without very strong polaron effects!

See Zhou Li, D. Baillie, C. Blois, FM, **PRB 81, 115114 2010**
Zhou Li, C. Chandler, FM, **PRB 83, 045104 2011**
Zhou Li and FM, **J Supercond Nov Mat PRB 83, 045104 2011**

So what's wrong (part 2)?

1) How did $\mu = UN(E_F)$ get reduced to μ^*?

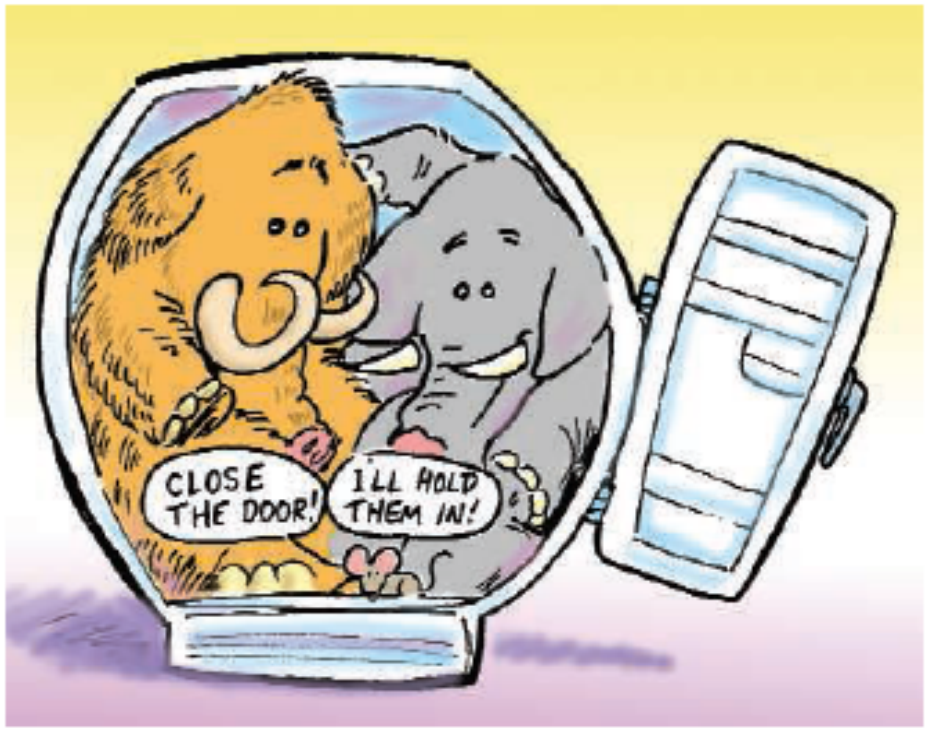

"We have a mammoth and an elephant in our refrigerator—do we care much if there is also a mouse?"

Is There Glue in Cuprate Superconductors?
Philip W. Anderson
Science **316**, 1705 (2007);

Eliashberg Theory

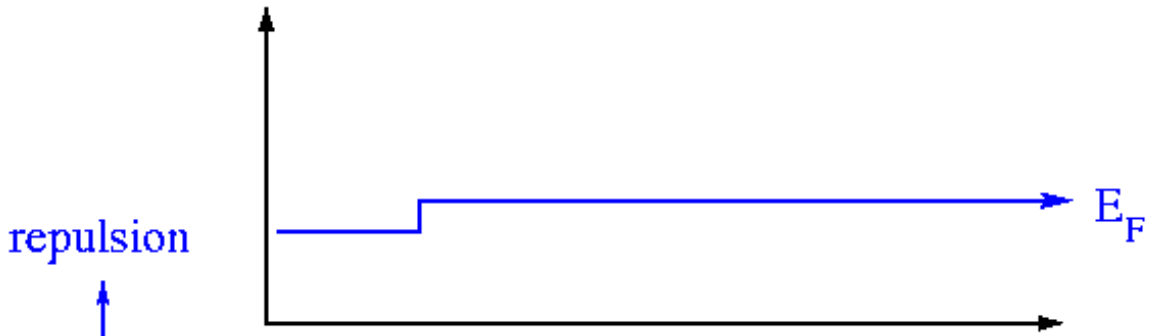

Poor man's Scaling (Tolmachev et al., Morel and Anderson)

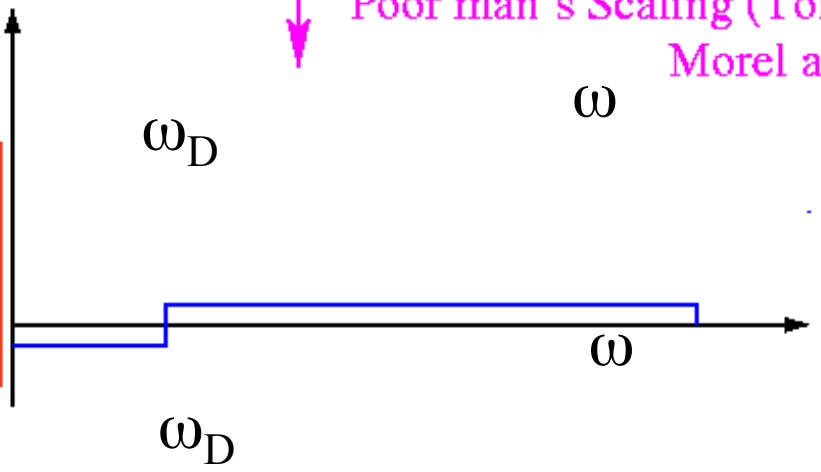

But…
Never seen in QMC simulations
Many other ways for U to be reduced

IOP FTC
IOP PUBLISHING
JOURNAL OF PHYSICS: CONDENSED MATTER
J. Phys.: Condens. Matter **24** (2012) 492202 (5pp)
doi:10.1088/0953-8984/24/49/492202

FAST TRACK COMMUNICATION

The theory of electron–phonon superconductivity: does retardation really lead to a small Coulomb pseudopotential?

Johannes Bau

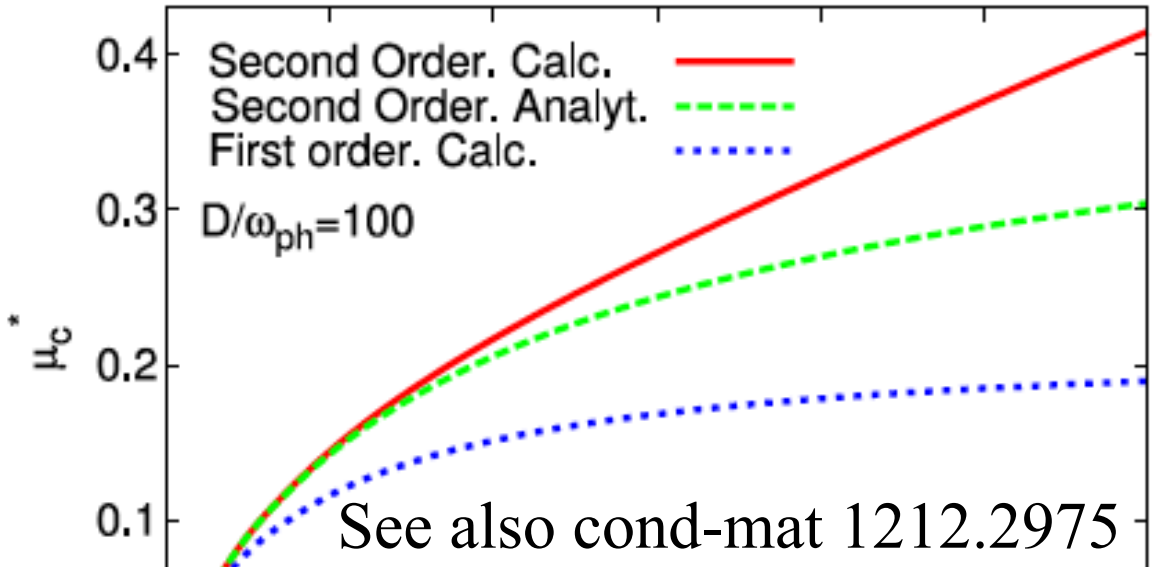

See also cond-mat 1212.2975

Retardation effects and the Coulomb pseudopotential in the theory of superconductivity

Phys. Rev. B **87, 054507 (2013)**

Johannes Bauer,[1,2] Jong E. Han,[1,3] and Olle Gunnarsson[1]

What is important, what can we 'throw out' ?

Copper-Oxygen Planes

http://www.cnms.ornl.gov/images/gordon-bell-1.gif

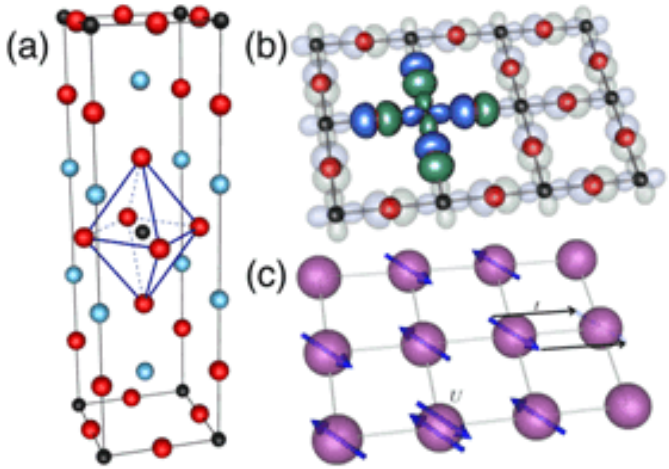

Fig. 1: (a) The crystal structure of La2CuO4, a typical cuprate, where black, red, and blue sphere represent Cu, O, and La, respectively. (b) The CuO2 plane with outlines of the Cu dx2-y2 and O px and py orbitals. Also shown in full color is the Zhang-Rice singlet state that forms from hybridization of the Cu orbitals with the neighboring O orbitals. (c) Pictorial representation of the single band 2D Hubbard model with on-site Coulomb repulsion U and inter-site hopping t.

High T_c Cuprates: a Case Study

The (single band) Hubbard model

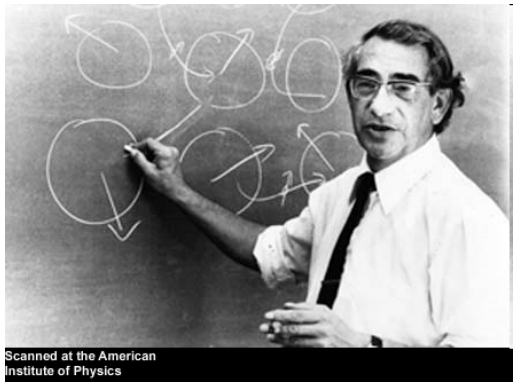

J. Hubbard

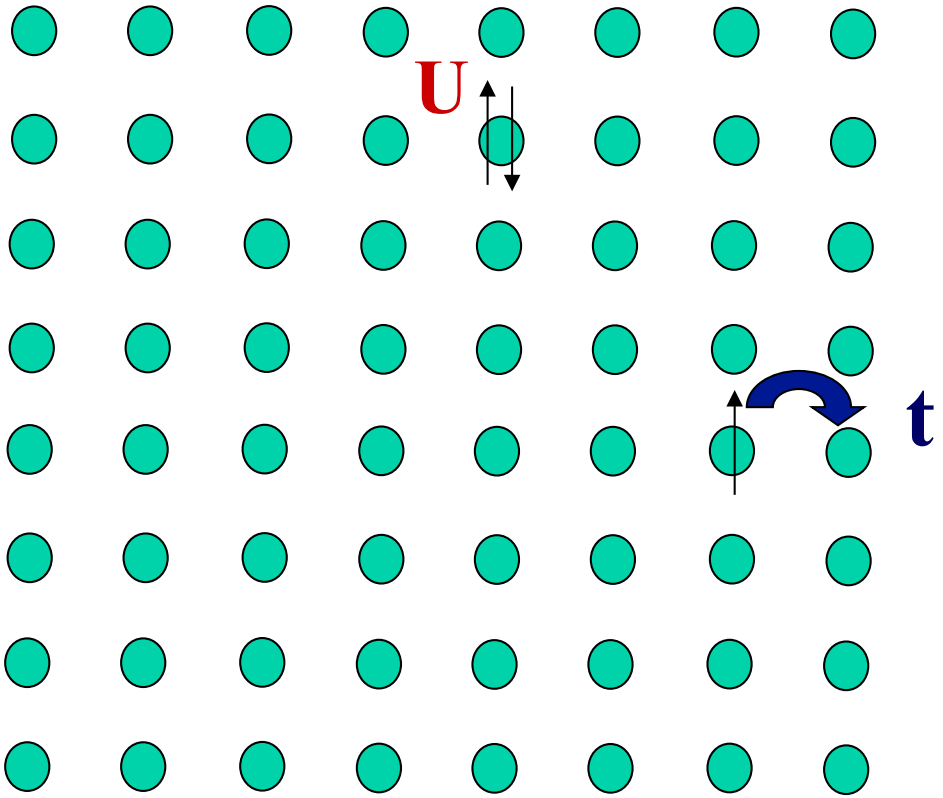

$$H = -t \sum_{\langle ij \rangle, \sigma} (\hat{c}^{\dagger}_{i\sigma} \hat{c}_{j\sigma} + \hat{c}^{\dagger}_{j\sigma} \hat{c}_{i\sigma}) + U \sum_{i} \hat{n}_{i\uparrow} \hat{n}_{i\downarrow}$$

Does it have the 'right stuff' (Doug Scalapino)?

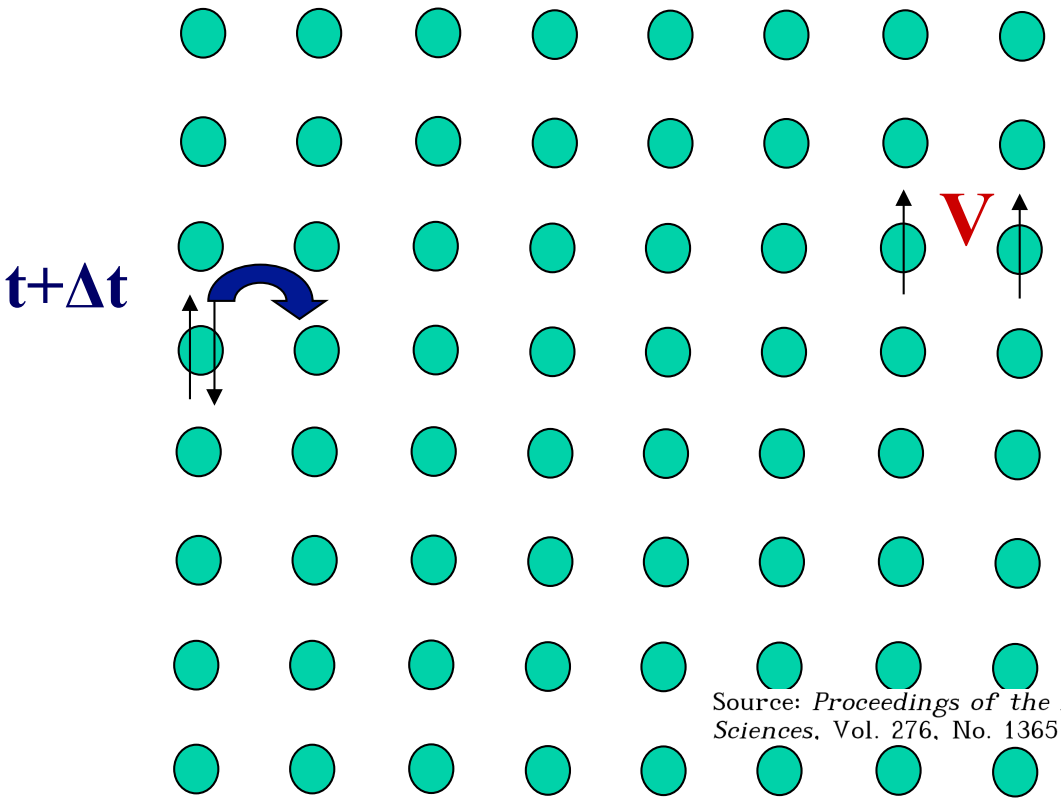

Nearest neighbour interactions

$$(ij|\ 1/r\ |ij) \sim \frac{2e^{-\kappa|\mathbf{R}_i-\mathbf{R}_j|}}{|\mathbf{R}_i-\mathbf{R}_j|}\ \mathrm{Ry}\ (6\ \mathrm{eV})$$

Electron correlations in narrow energy bands

By J. Hubbard

Theoretical Physics Division, A.E.R.E., Harwell, Didcot, Berks

(*Communicated by B. H. Flowers, F.R.S.—Received* 23 *April* 1963)

Source: *Proceedings of the Royal Society of London. Series A, Mathematical and Physical Sciences*, Vol. 276, No. 1365 (Nov. 26, 1963), pp. 238-257

$$(ii|\ 1/r\ |ij) \sim q\,\mathrm{Ry} \sim \tfrac{1}{2}\mathrm{eV},$$
$$(ij|\ 1/r\ |ik) \sim \tfrac{1}{4}q\,\mathrm{Ry} \sim \tfrac{1}{10}\mathrm{eV},$$
$$(ii|\ 1/r\ |jj) \sim (ij|\ 1/r\ |ji) \sim q^2\,\mathrm{Ry} \sim \tfrac{1}{40}\mathrm{eV},$$

Modulated hopping Δt
3-site hopping (t-J model)
Exchange term J

phonons, oxygen (or other) orbitals, longer range hopping, polarons, lunar effects, etc.

Or have we missed a key ingredient all along?

VOLUME 87, NUMBER 20 PHYSICAL REVIEW LETTERS 12 NOVEMBER 2001

Dynamic Hubbard Model

J. E. Hirsch
Department of Physics, University of California–San Diego, La Jolla, California 92093-0319
(Received 24 July 2001; published 26 October 2001)

…a parable involving the lowly Helium atom…

atoms

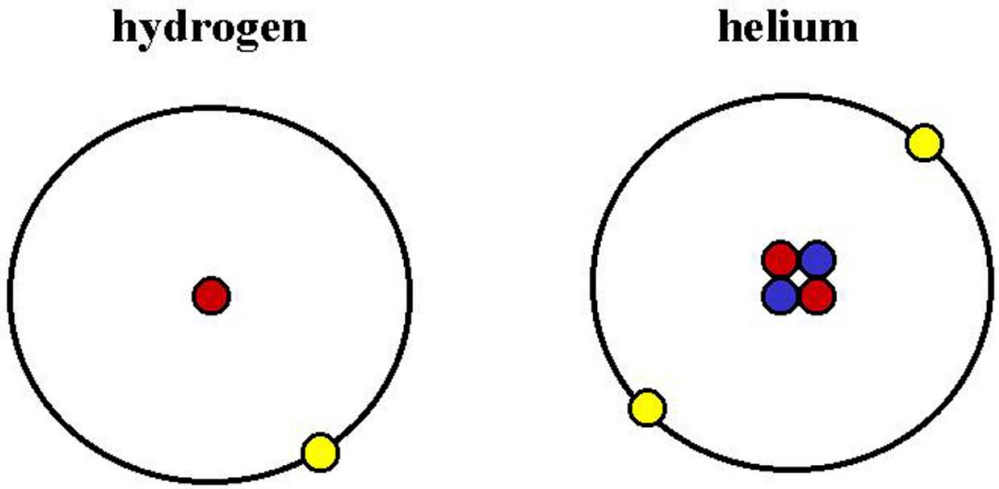

Neutrons and protons are held together in the nucleus by the "strong" force, which has to overcome the electrical repulsion of the two positively charged protons in helium (and in more complex atoms too). Electrons are held around the atom by the electrical attraction between their negative charge and the positive charge of the protons in the nucleus.

Ashcroft and Mermin, inside front cover

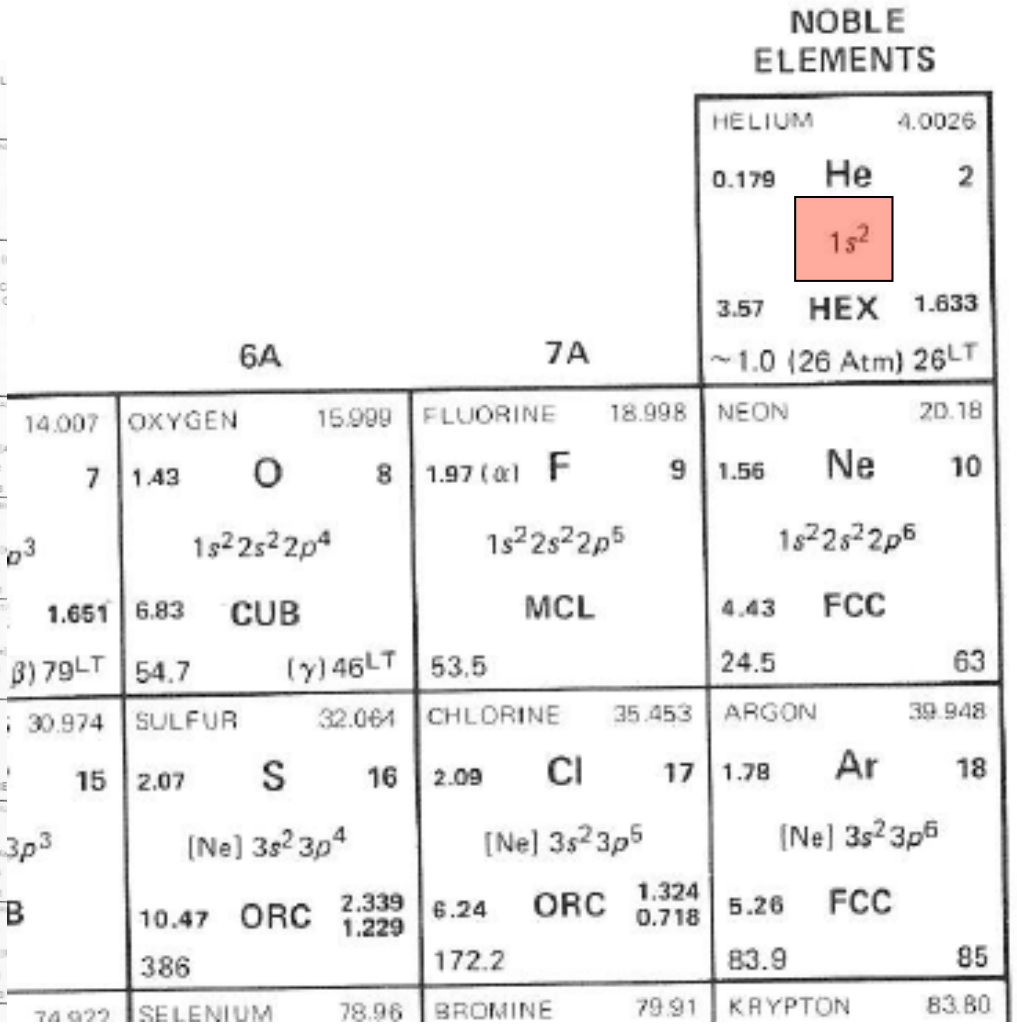

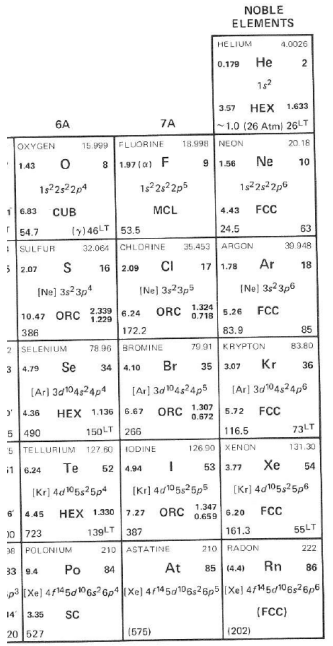

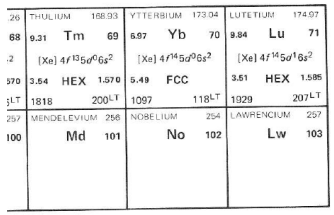

But the real 2-electron wave function is given by

$$|\psi\rangle = a_1|1s\ 1s\rangle + a_2|1s\ 2s\rangle + a_3|1s\ 3s\rangle + a_4|2s\ 2s\rangle + a_5|2p\ 2p\rangle + \ldots$$

IOP PUBLISHING EUROPEAN JOURNAL OF PHYSICS
Eur. J. Phys. 34 (2013) 111–128 doi:10.1088/0143-0807/34/1/111

The spectral decomposition of the helium atom two-electron configuration in terms of hydrogenic orbitals

Joel Hutchinson[1], Marc Baker[1] and Frank Marsiglio[1,2,3]

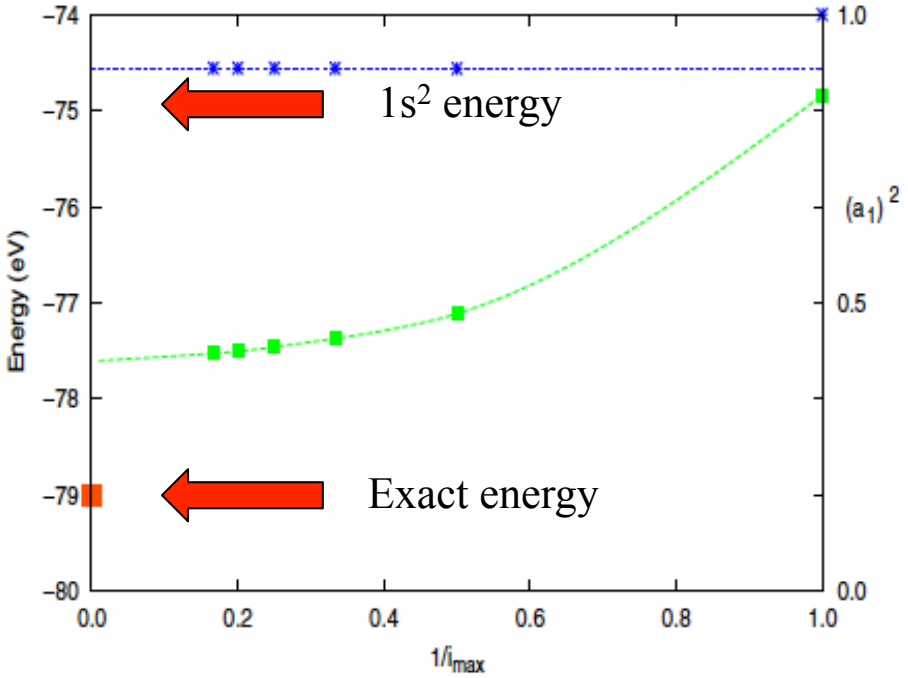

Table 1. Results for some overlaps, a_i.

i	Basis state	a_i	$\lvert a_i\rvert^2$	Total Probability
1	100 100	0.9624	0.9263	0.9263
2	100 200	−0.2148	0.0461	0.9725
3	100 300	−0.0752	0.0057	0.9781
4	100 400	−0.0427	0.0018	0.9799
5	100 500	−0.0289	0.0008	0.9807
6	100 600	−0.0213	0.0005	0.9812
7	100 700	−0.0166	0.0003	0.9815
8	21–1 211	0.0260	0.0007	0.9822
9	210 210	−0.0184	0.0003	0.9825
10	200 200	−0.0146	0.0002	0.9827
11	200 300	−0.0090	0.0001	0.9828
12	100 320	0	0	0.9828

Why is this important?

$$U(Z) = \int d^3r\, d^3r'\, |\varphi_{1s}(r)|^2 \frac{e^2}{|r - r'|} |\varphi_{1s}(r')|^2$$

$$= \frac{5}{4} Z \times 13.606 \text{ eV},$$

$$\varphi_{1s}(r) = \left(\frac{Z^3}{\pi a_0^3}\right)^{1/2} e^{-Zr/a_0}$$

Experimental values:

$$U_{\text{eff}}(1) = I - A = 12.86 \text{ eV} = U(1) - 4.15 \text{ eV}, \quad \text{(2a)}$$

$$U_{\text{eff}}(2) = I_{II} - I_I = 29.92 \text{ eV} = U(2) - 4.10 \text{ eV}. \quad \text{(2b)}$$

J.E. Hirsch, PRL 87, 206402 (2001)

In essentially **all** the lattice models used to understand electron correlations in solids, the "playing field" is static (phonons are a different matter).

In He, when one electron is present, it occupies the 1s orbital:

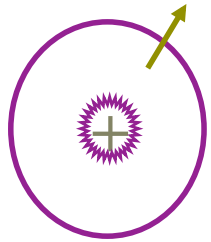

When two electrons are present, in Hubbard-like models they (doubly) occupy the 1s orbital:

- For Hubbard model:

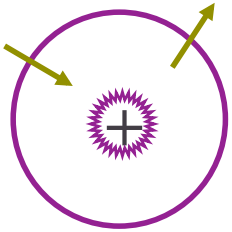

$$\psi(\vec{r}_1,\vec{r}_2) = \Phi_{1s}(\vec{r}_1)\Phi_{1s}(\vec{r}_2)$$

- For real atom

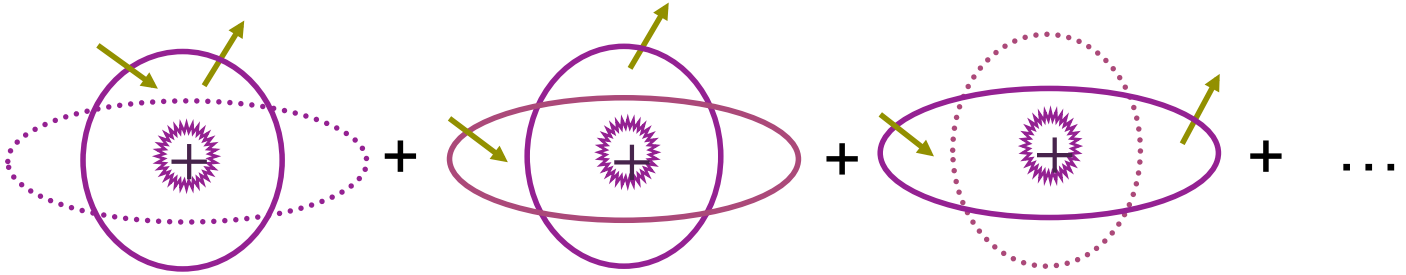

$$\psi(\vec{r}_1,\vec{r}_2) = \sum_{mn} c_{mn}\Phi_m(\vec{r}_1)\Phi_n(\vec{r}_2)$$

This is like what happens in general relativity; the presence of mass alters the underlying space-time structure.

This is like what happens in general relativity; the presence of mass alters the underlying space-time structure.

Here, the presence of a second electron alters the nature of the orbitals that model the conduction band.

A simple way to model this:

hopping term

$$H_{DHB} = -\sum_{<i,j>\sigma} t_{ij}\left(c^{+}_{i\sigma}c_{j\sigma} + c^{+}_{j\sigma}c_{i\sigma}\right) - \mu\sum_{i\sigma} n_{i\sigma} +$$

$$\sum_{i}\left(\omega_o\sigma_i^x + g\omega_o\sigma_i^z\right) + \sum_{i}\left(U - 2g\omega_o\sigma_i^z\right)n_{i\uparrow}n_{i\downarrow}$$

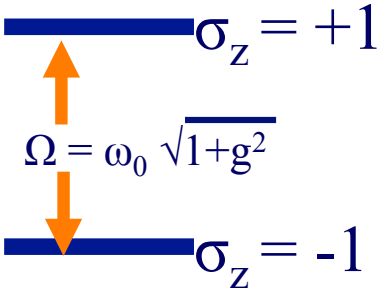

Pseudospin degree of freedom

On-site interaction

The pseudospin degree of freedom represents an adjustment of the orbitals to the number of electrons that happens to be present.

$U_{max} = U + 2g\omega_o$

$U_{min} = U - 2g\omega_o$

Dynamic Hubbard Model

J.E. Hirsch, PRB 65, 184502 (2002)

$$H_{\mathrm{DHM}} = \sum_{<i,j>\sigma} t_{ij}(c^{\dagger}_{i\sigma}c_{j\sigma} + c^{\dagger}_{j\sigma}c_{i\sigma}) - \mu\sum_{i,\sigma} n_{i\sigma}$$

$$+\sum_{i}(\omega_0\sigma^x_i + g\omega_0\sigma^z_i) + \sum_{i}(U - 2g\omega_0\sigma^z_i)n_{i\uparrow}n_{i\downarrow}$$

Parameter

t	electron hopping
U	`bare' electron-electron repulsion
g	electron-pseudospin coupling strength
ω_0	energy (time) scale associated with pseudospin

How do we check this out? (i) effective model
(ii) exact diagonalizations
(iii) Dynamical Mean Field Theory

PHYSICAL REVIEW B 82, 155122 (2010)

Two-site dynamical mean field theory for the dynamic Hubbard model

G. H. Bach
Department of Physics, University of Alberta, Edmonton, Alberta, Canada T6G 2G7

J. E. Hirsch
Department of Physics, University of California–San Diego, La Jolla, California 92093-0319, USA

F. Marsiglio
Department of Physics, University of Alberta, Edmonton, Alberta, Canada T6G 2G7
(Received 4 August 2010; published 15 October 2010)

Giang Bach

Dynamical Mean Field Theory (DMFT)

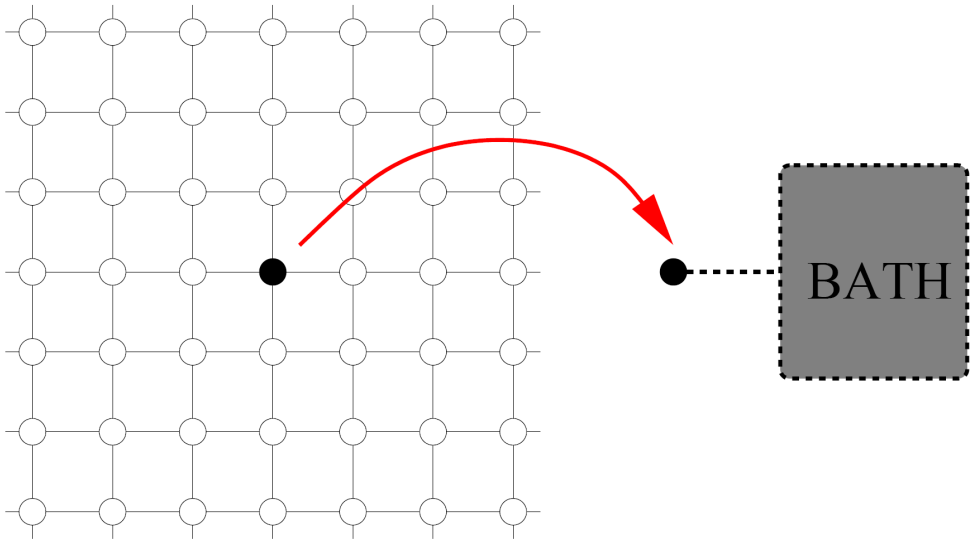

FIGURE 4. Mean-field theory replaces a lattice model by a single site coupled to a self-consistent bath.

Antoine Georges, arXiv:cond-mat/0403123

Dynamical Mean Field Theory (DMFT)

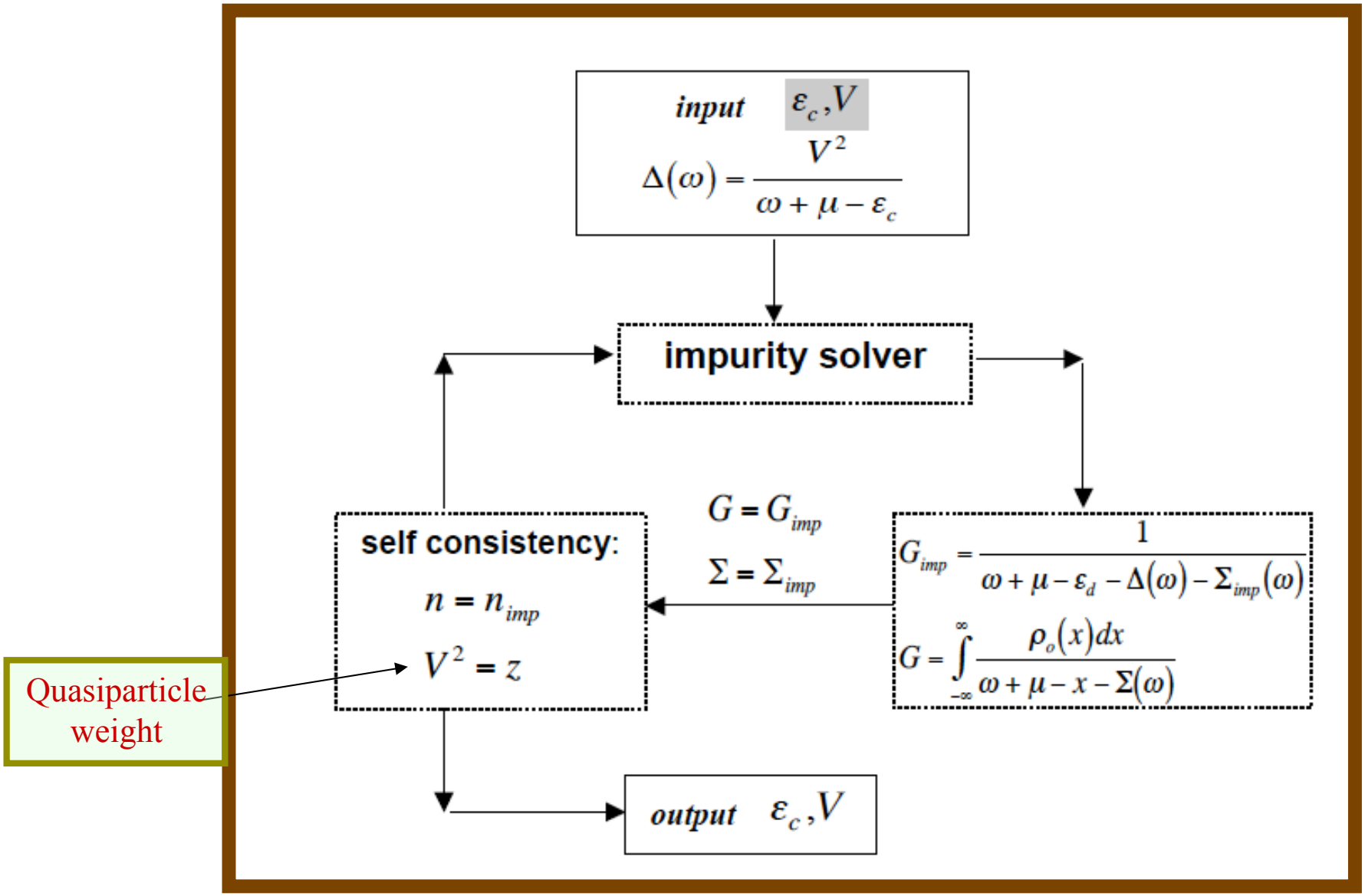

Solver: 2-site exact diagonalization --- G. Kotliar et al. and M. Potthoff, PRB64, 165114 (2001)

For 2-site DMFT, we need to determine the (2) parameters E_c and V (rather than an Infinite set, E_k and V_k). Here are some results:

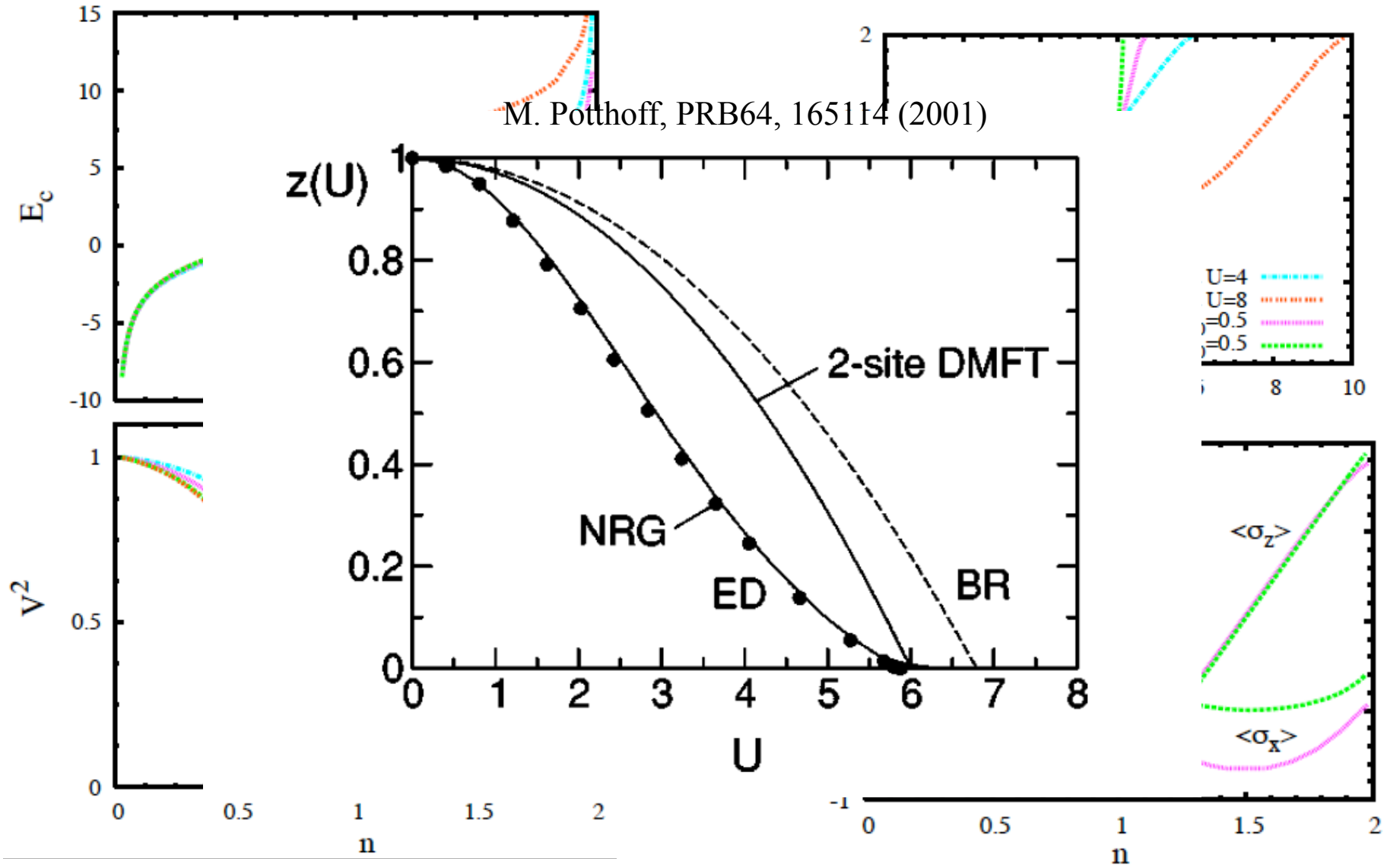

Mott physics vs. orbital relaxation

G.H. Bach et al., PRB 82, 155122 (2010)

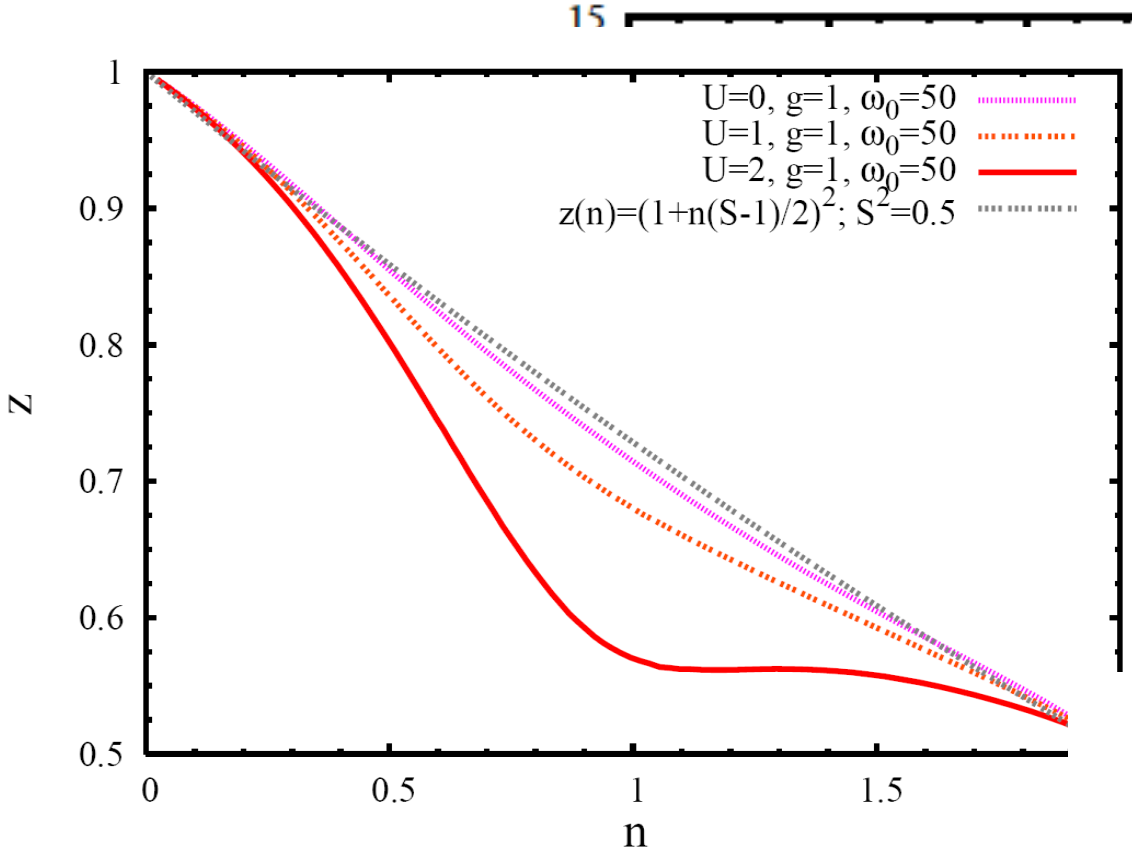

$z = V^2$

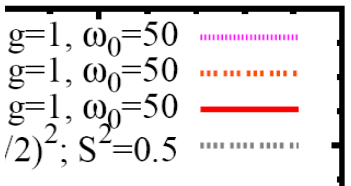

Pseudspin expectation values

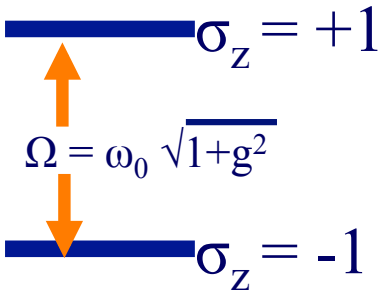

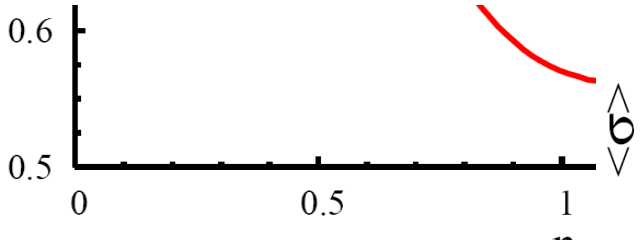

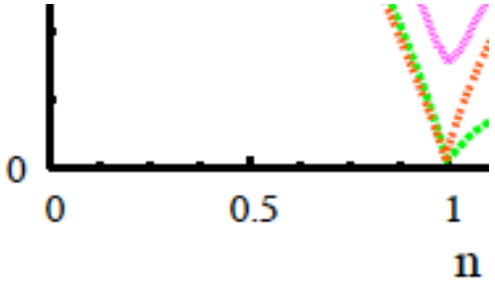

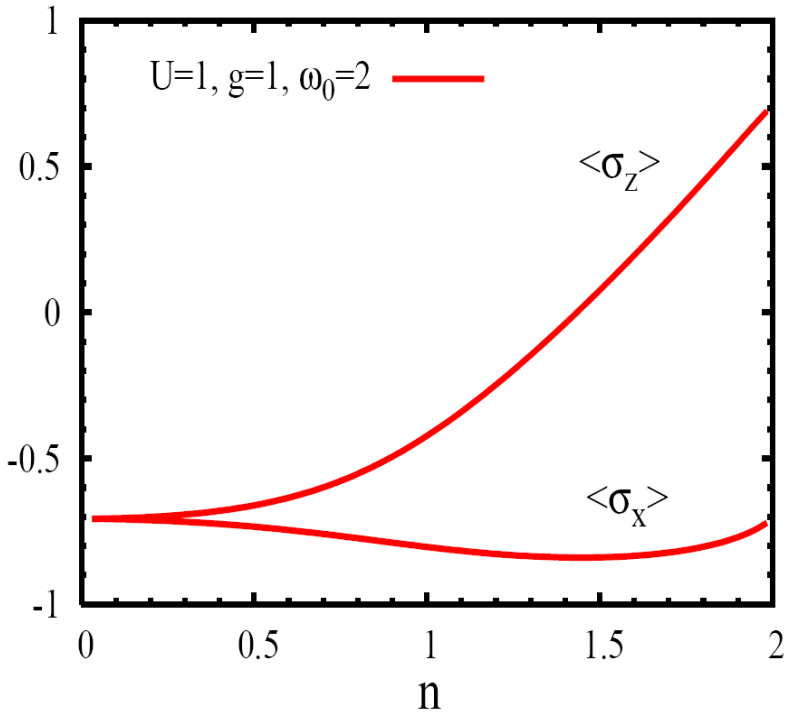

Spectral function

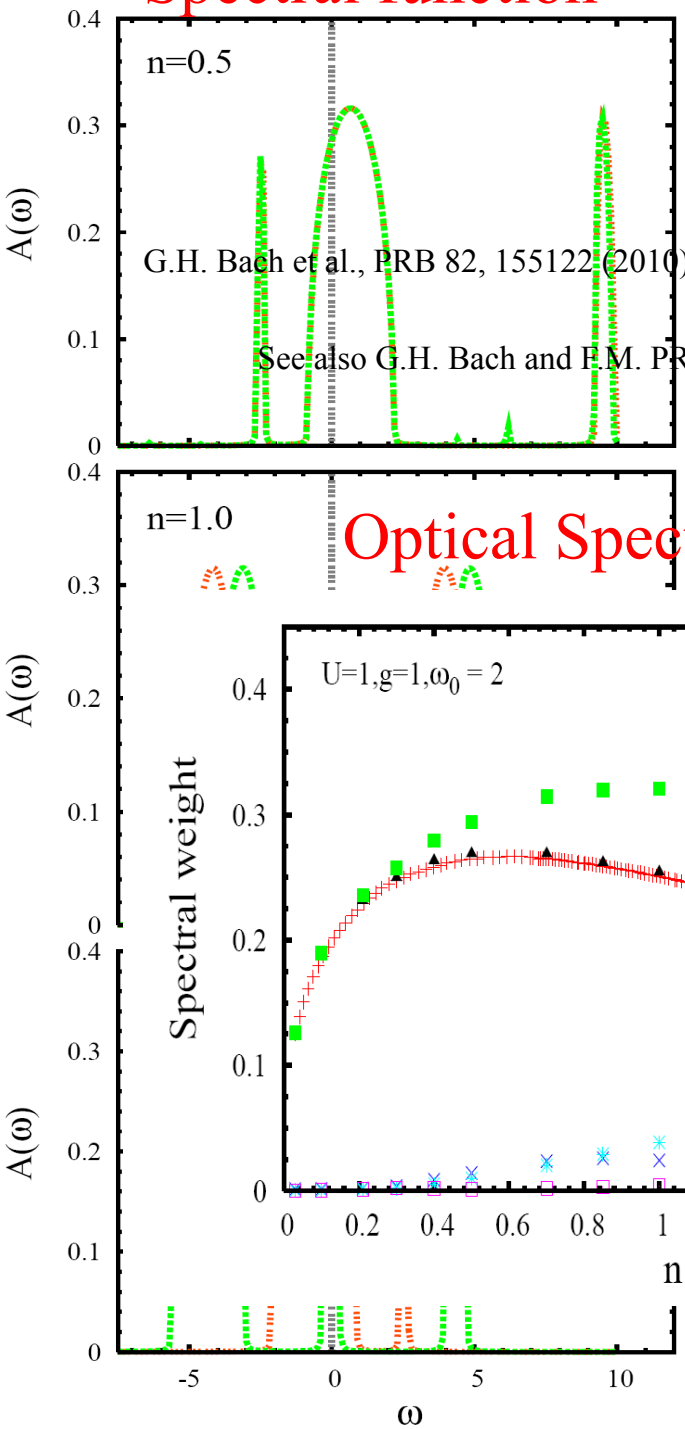

G.H. Bach et al., PRB 82, 155122 (2010)

See also G.H. Bach and F.M. PRB 85, 155134 (2012)

Optical Spectral weight

Optical conductivity

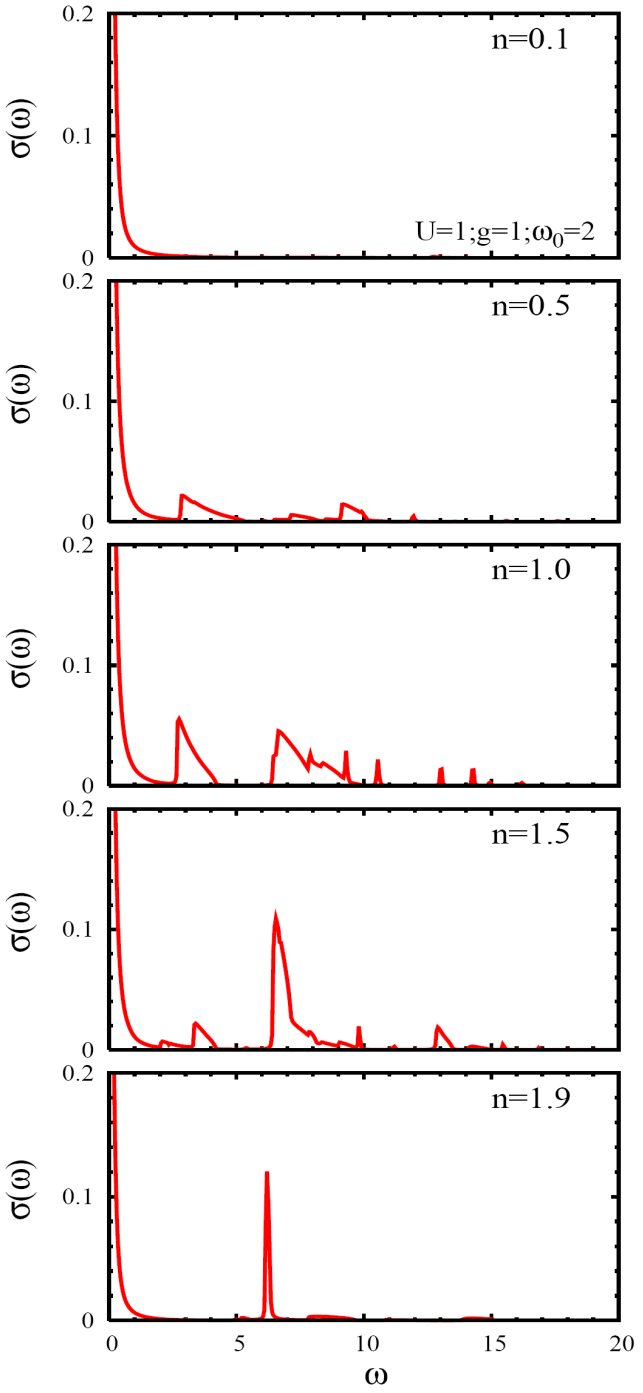

G.H. Bach et al., PRB 82, 155122 (2010)

$z = V^2$

Mott physics vs. orbital relaxation

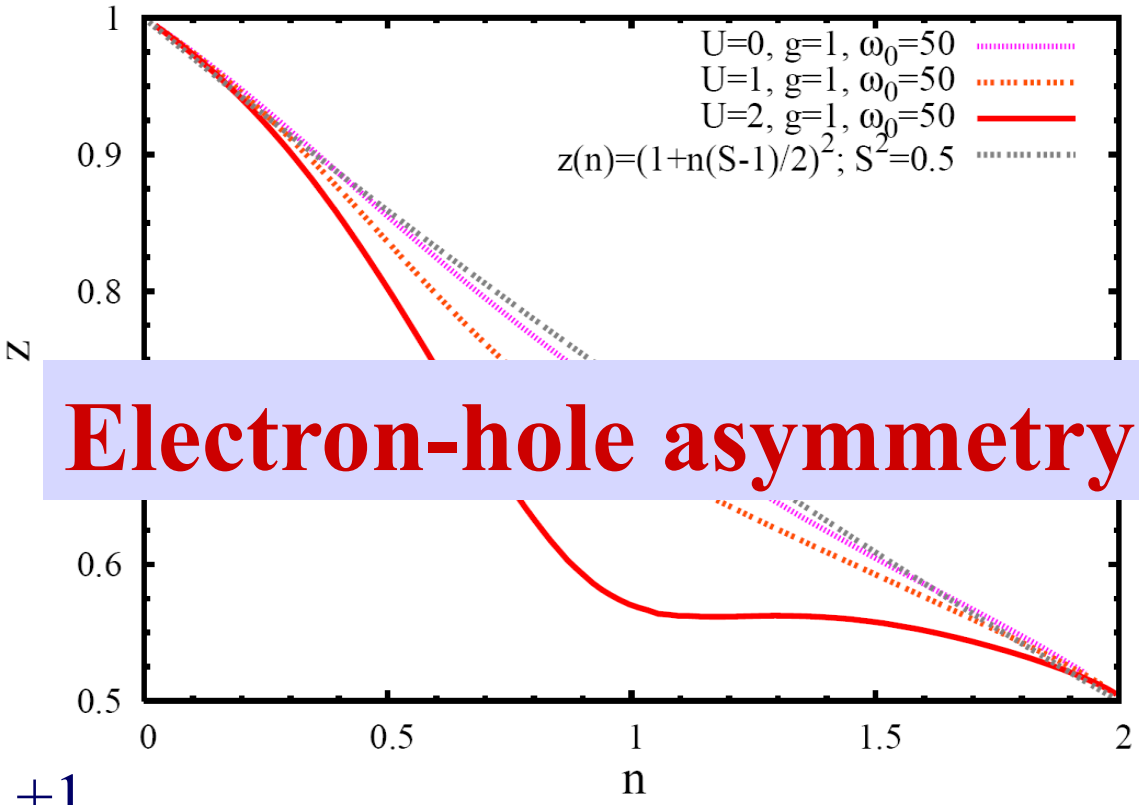

Electron-hole asymmetry!!!

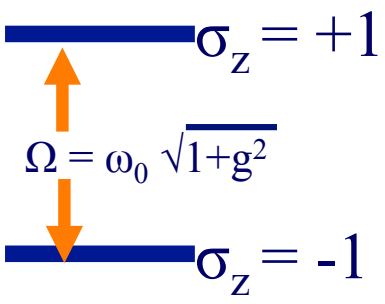

$$\sigma_1^{(3)}(\omega) = \frac{\pi e^2 t}{2\hbar^2}\left[S^2\delta\left(\omega - \frac{2tS^2}{\hbar}\right) + 4S^2\bar{S}^2\frac{t}{\Omega_0}\delta\left(\omega - \frac{\Omega_0}{\hbar}\right) + \bar{S}^4\frac{t}{\Omega_0}\delta\left(\omega - \frac{2\Omega_0}{\hbar}\right)\right]. \quad (29)$$

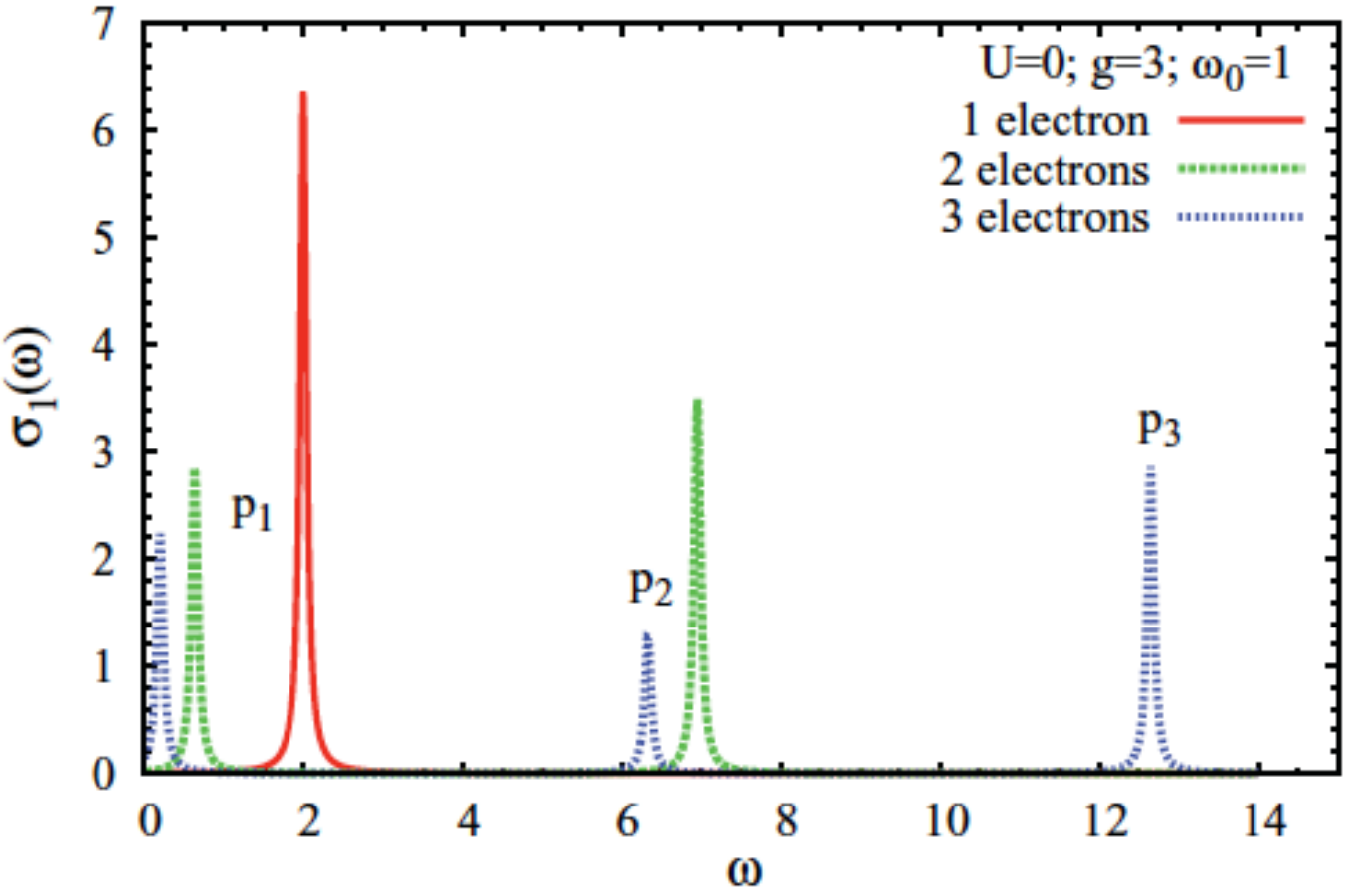

$$\sigma_1^{(1)}(\omega) = \frac{\pi e^2 t}{2\hbar^2}\delta(\omega - 2t/\hbar),$$

Dimer calculations

G.H. Bach and F.M. PRB 85, 155134 (2012)

How do we measure this ?

Optical Sum Rule (Kubo)

$$\int_0^\infty d\nu\ \sigma_1(\nu) = \frac{\pi e^2}{\hbar^2}\frac{1}{N}\sum_k (\frac{\partial^2 \epsilon_k}{\partial k^2}) n_k$$

for all bands (or quadratic dispersion): $= \frac{\pi e^2 n}{2m} = \omega_P^2/8$

for tight-binding band (with nearest neighbour hopping): $\frac{\partial^2 \epsilon_k}{\partial k^2} = -a^2 \epsilon_k$

$$\int_0^\infty d\nu\ \sigma_1(\nu) = \frac{\pi e^2 a^2}{2\hbar^2} < -E_k >$$

PHYSICAL REVIEW B VOLUME 17, NUMBER 12 15 JUNE 1978

Finite-energy f-sum rules for valence electrons

D. Y. Smith
Argonne National Laboratory, Argonne, Illinois 60439

E. Shiles
Argonne National Laboratory, Argonne, Illinois 60439
and Virginia Commonwealth University, Richmond, Virginia 23284

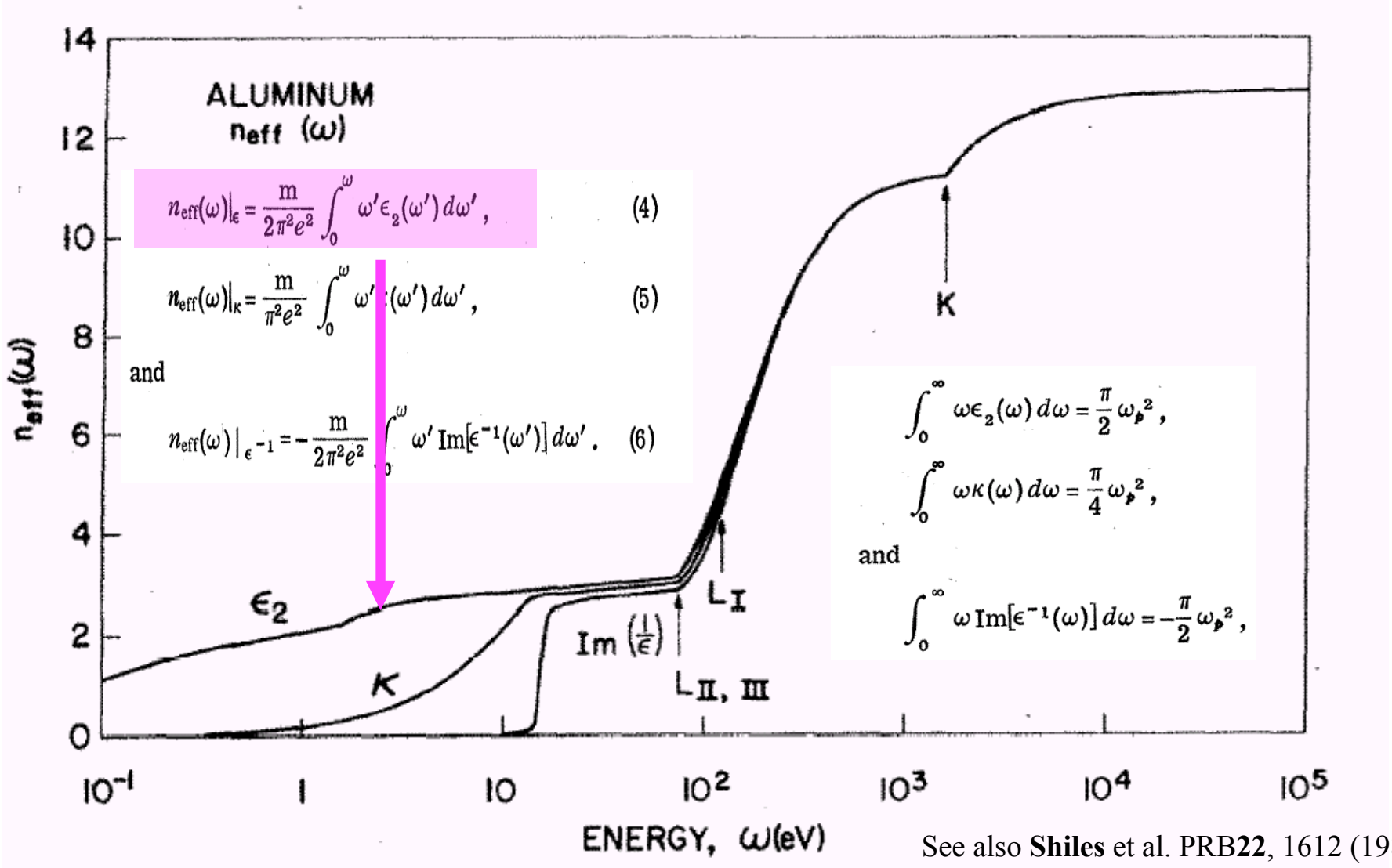

See also **Shiles** et al. PRB**22**, 1612 (1980)

REPORTS

Sum Rules and Interlayer Conductivity of High-T_c Cuprates

D. N. Basov, S. I. Woods, A. S. Katz, E. J. Singley, R. C. Dynes, M. Xu,* D. G. Hinks, C. C. Homes, M. Strongin

Analysis of the interlayer infrared conductivity of cuprate high–transition temperature superconductors reveals an anomalously large energy scale extending up to midinfrared frequencies that can be attributed to formation of the superconducting condensate. This unusual effect is observed in a variety of materials, including $Tl_2Ba_2CuO_{6+x}$, $La_{2-x}Sr_xCuO_4$, and $YBa_2Cu_3O_{6.6}$, which show an incoherent interlayer response in the normal state. Midinfrared range condensation was examined in the context of sum rules that can be formulated for the complex conductivity. One possible interpretation of these experiments is in terms of a kinetic energy change associated with the superconducting transition.

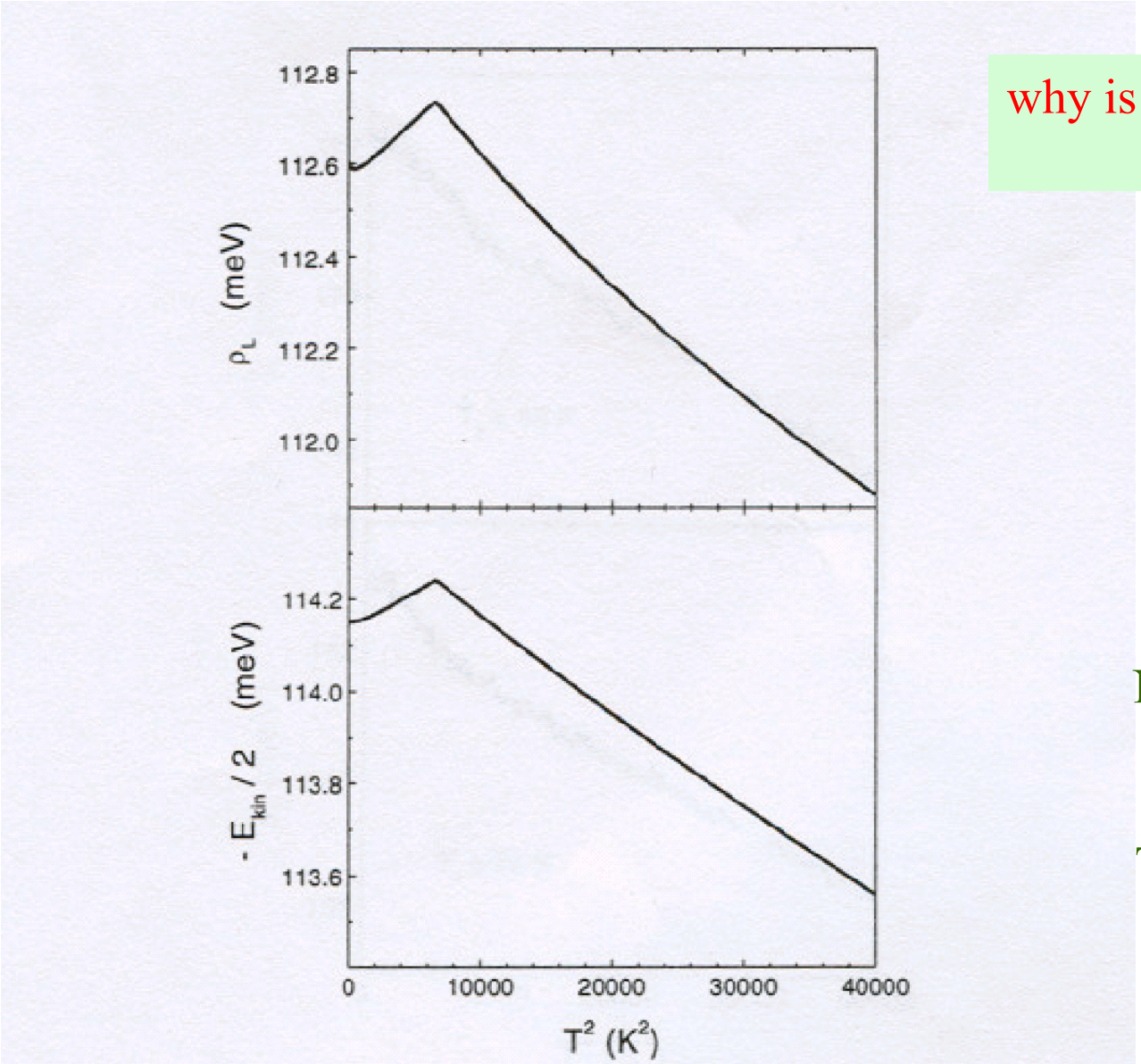

FIG. 6: BCS prediction of the spectral weight function.

van der Marel et al. cond-mat/0302169

why is there temperature dependence in the normal state ?

Answer:
1) n_k ---> f_k (Fermi-Dirac)
2) interactions

$$E_{kin} = 2 \Sigma \varepsilon_k n_k$$

Note: Absolute value of kinetic energy **decreases** in the superconducting state.
This is **conventional** behaviour

Superconductivity-Induced Transfer of In-Plane Spectral Weight in $Bi_2Sr_2CaCu_2O_{8+\delta}$

H. J. A. Molegraaf,[1] C. Presura,[1] D. van der Marel,[1]*
P. H. Kes,[2] M. Li[2]

Science 22 March 2002 295: 2239-2241

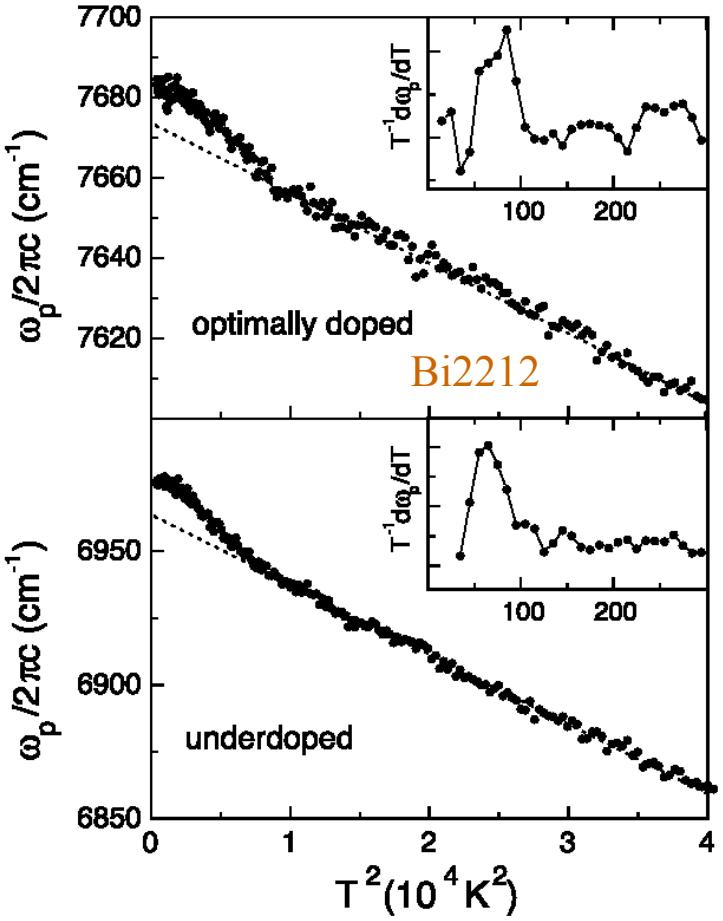

In-plane optical spectral weight transfer in optimally doped $Bi_2Sr_2Ca_2Cu_3O_{10}$

F. Carbone, A. B. Kuzmenko, H. J. A. Molegraaf, E. van Heumen, E. Giannini and D. van der Marel
DPMC, University of Geneva, 24, Quai Ernest-Ansermet, Geneva 4, Switzerland

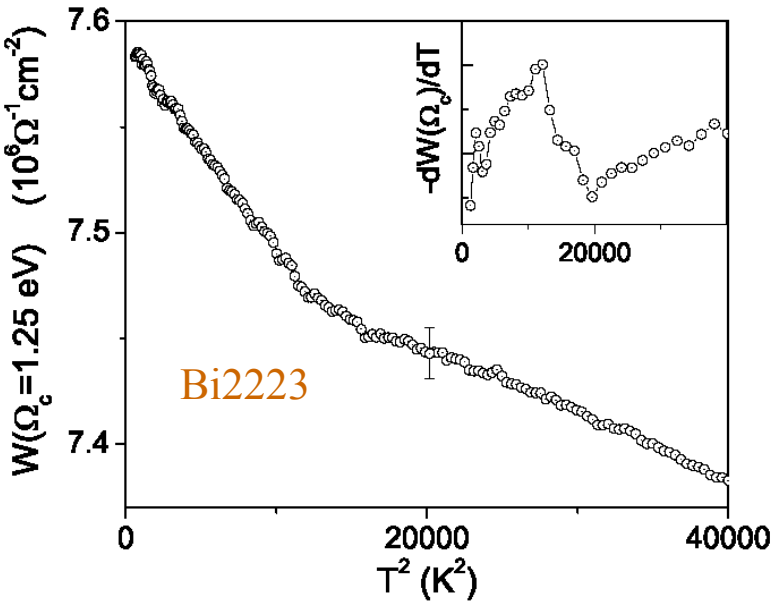

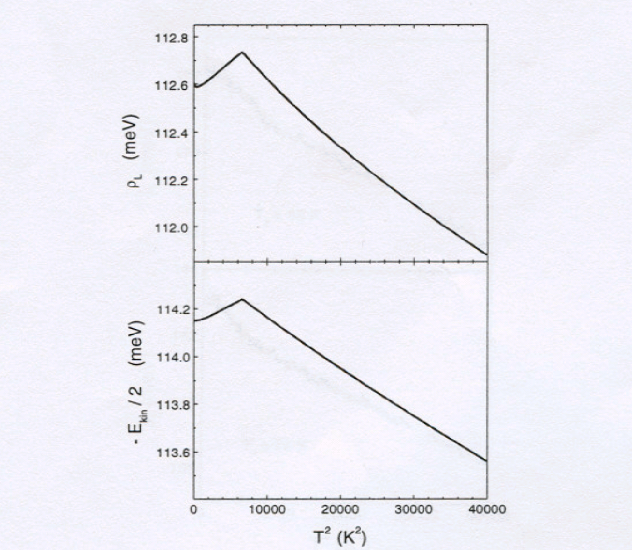

FIG. 6: BCS prediction of the spectral weight function.

M.V. Klein and G. Blumberg,
Science **283**, 42 (1999)

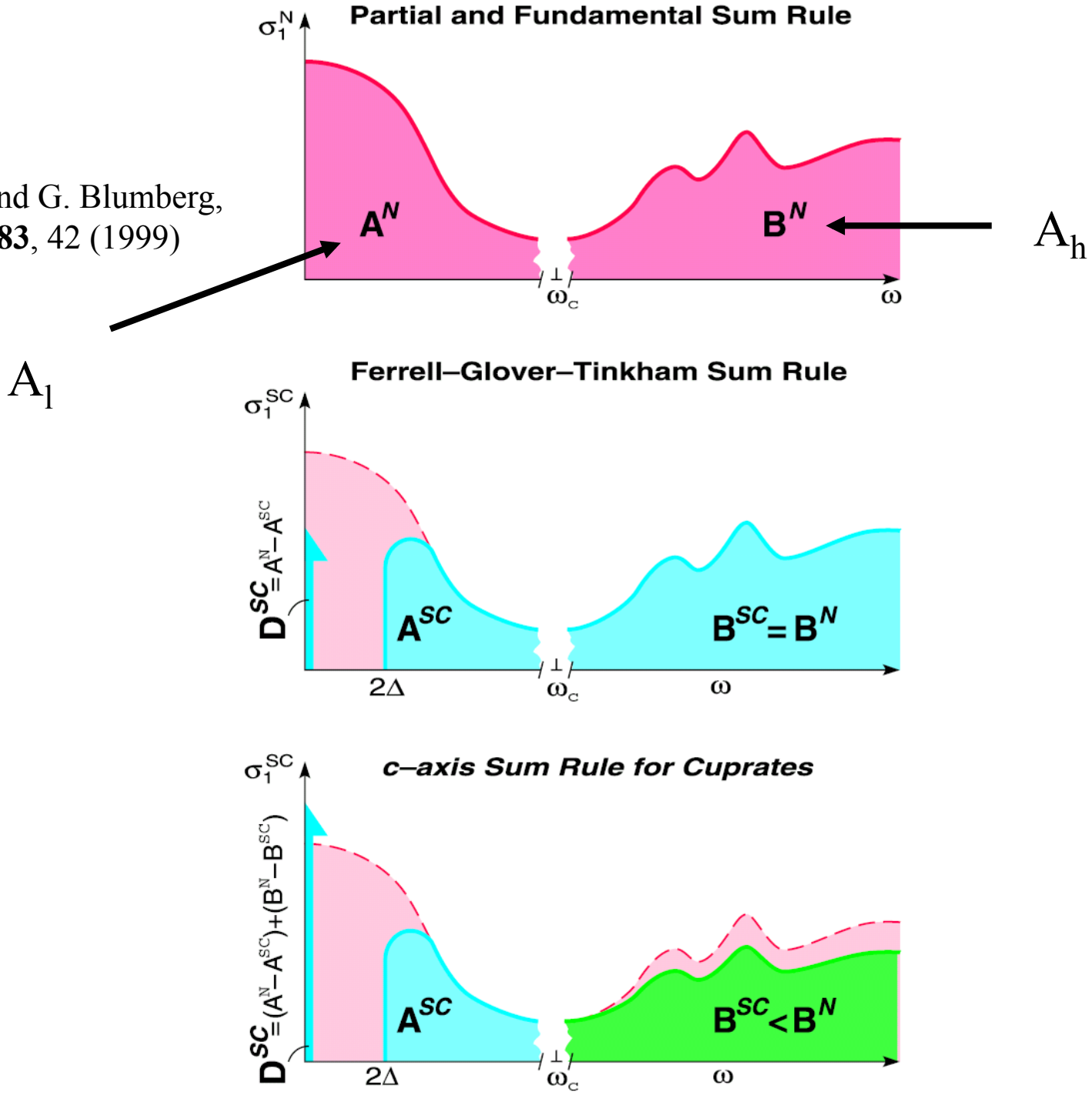

Anomalous sum rule change at Tc

Using a phenomenology of scattering rate collapse:

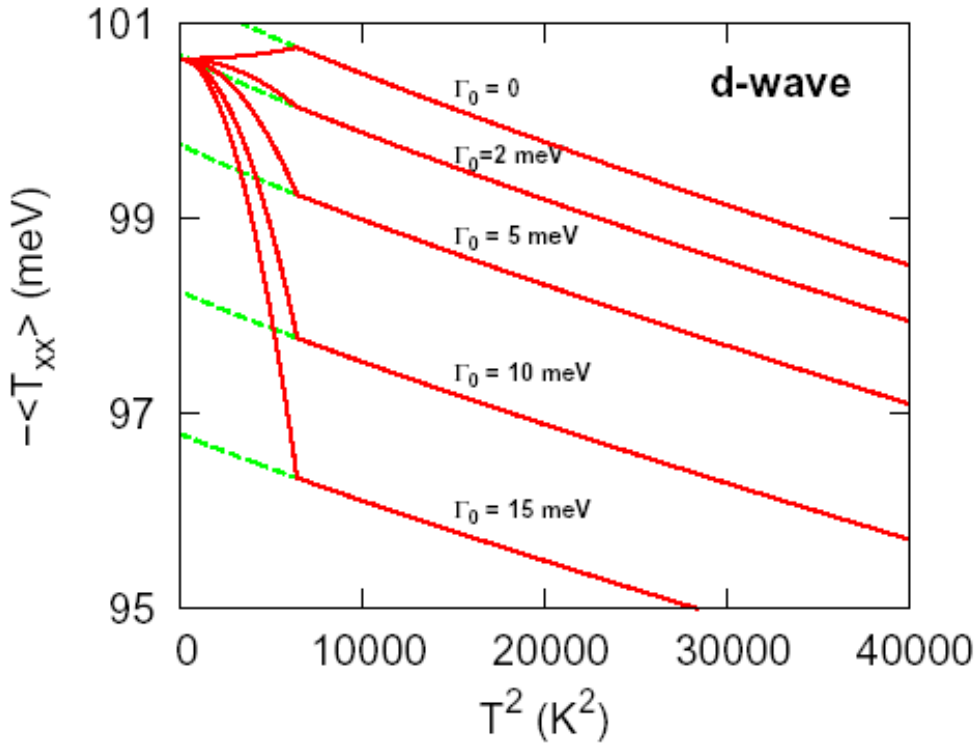

FM, Phys. Rev. B73, 064507

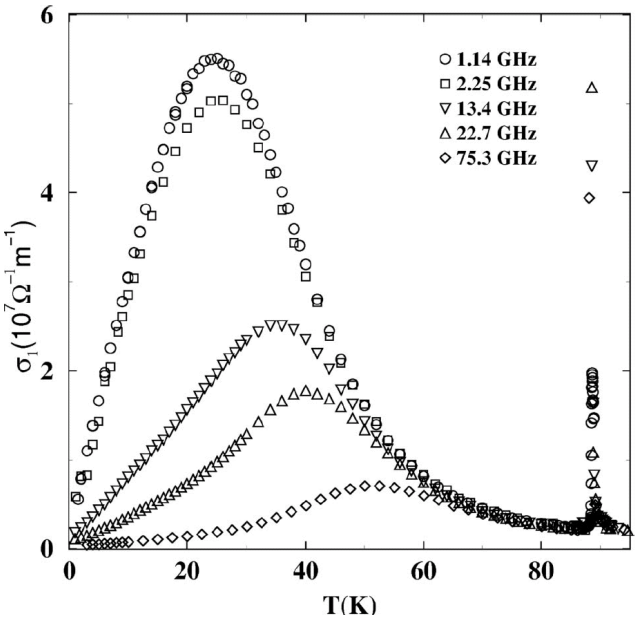

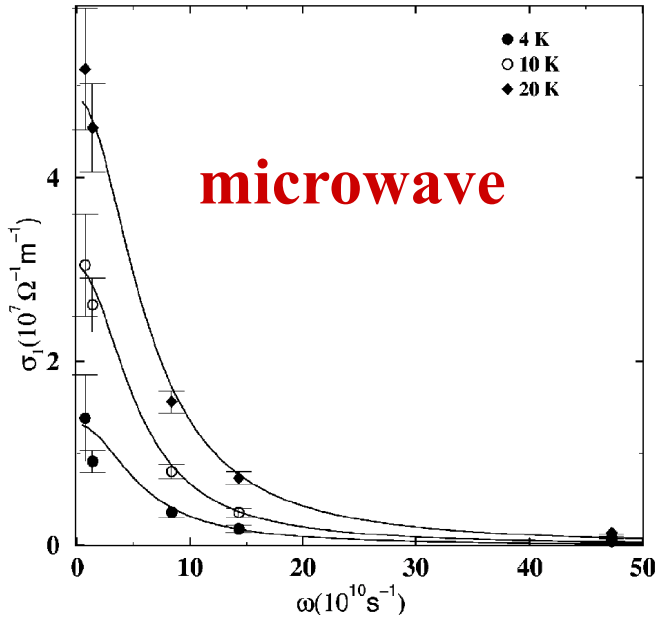

PHYSICAL REVIEW B VOLUME 60, NUMBER 2 1 JULY 1999-II

Microwave spectroscopy of thermally excited quasiparticles in $YBa_2Cu_3O_{6.99}$

A. Hosseini, R. Harris, Saeid Kamal, P. Dosanjh, J. Preston,* Ruixing Liang, W. N. Hardy, and D. A. Bonn

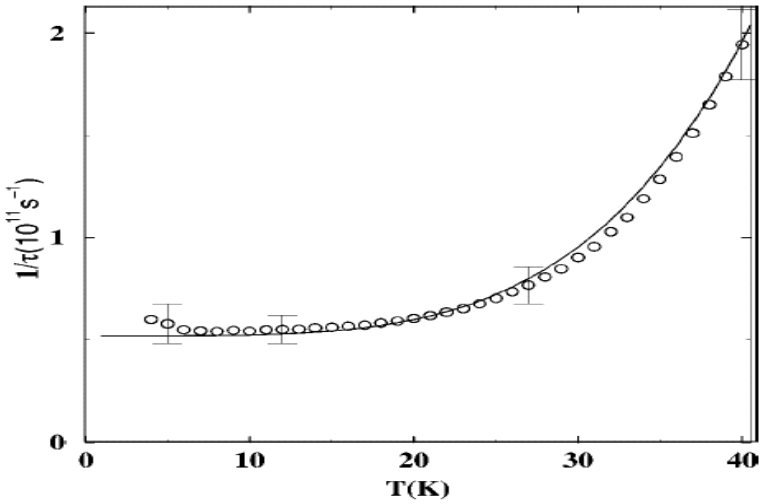

use $1/\tau = 1/\tau_0\,(T/T_c)^4$ below T_c

Summary

I've tried to make the case that the BCS pairing formalism gives an excellent description of the superconducting state

but…

The actual **mechanism** is an active subject of current interest…for

all

superconductors

Key Points

- If one focuses on the 'building block' for conventional superconductivity, i.e. an electron interacting with phonons, one obtains a very polaronic quasi particle, with a huge effective mass. What 'undoes' this effect when one assembles a Fermi sea of such quasi particles (Since we are supposed to recover the so-called Migdal Theorem)?

- What are the essential ingredients buried in the parameter μ^* ?

  (i) even as modelled by a Hubbard U, how effective is retardation for reducing the effective pair repulsion?

  (ii) Maybe the Hubbard and Hubbard-like models don't really capture the essence of electron correlations in metals.

  (iii) The Dynamic Hubbard model tries to incorporate orbital relaxation --- the fact that orbitals expand, etc. when doubly occupied. Do these processes play an important role for superconductivity?

Concerning the Dynamic Hubbard Model

- We find a fundamental electron-hole asymmetry. This asymmetry is apparent in tunneling, and more indirectly through other probes.

- Pairing (requiring further study) results in energy lowering through kinetic energy (not potential energy), as seen in several optical conductivity studies (Basov, van der Marel, Bontemps, Timusk, etc.)

Many thanks to my collaborators: Benfatto, Carbotte, Knigavko,
Schachinger, Timusk, van der Marel,
Kuzmenko, Carbone, van Heumen,
Chandler, Bach, Hirsch, Baillie, Blois, and Zhou

Funding: NSERC, CIAR, ICORE

Many thanks to my collaborators: Benfatto, Carbotte, Knigavko, Schachinger, Timusk, van der Marel, Kuzmenko, Carbone, van Heumen, Chandler, Bach, Hirsch, Baillie, Blois, and Zhou


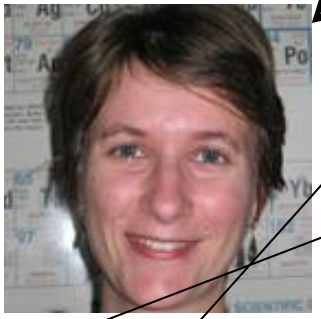

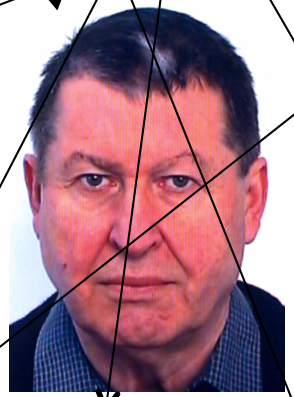






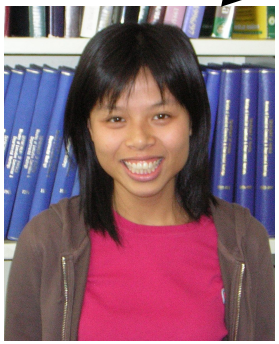


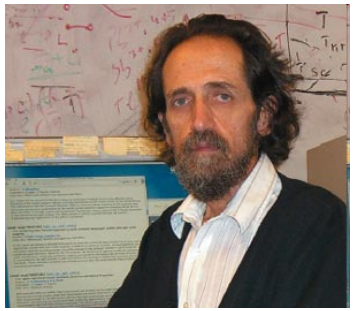
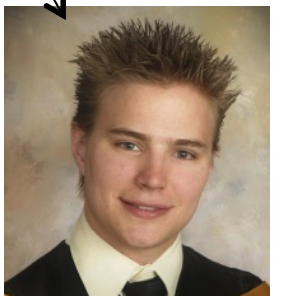

Funding: NSERC, CIAR, ICORE

Also in photoemission, M.R. Norman et al.

Phys. Rev. Lett. 79, 3506–3509 (1997)

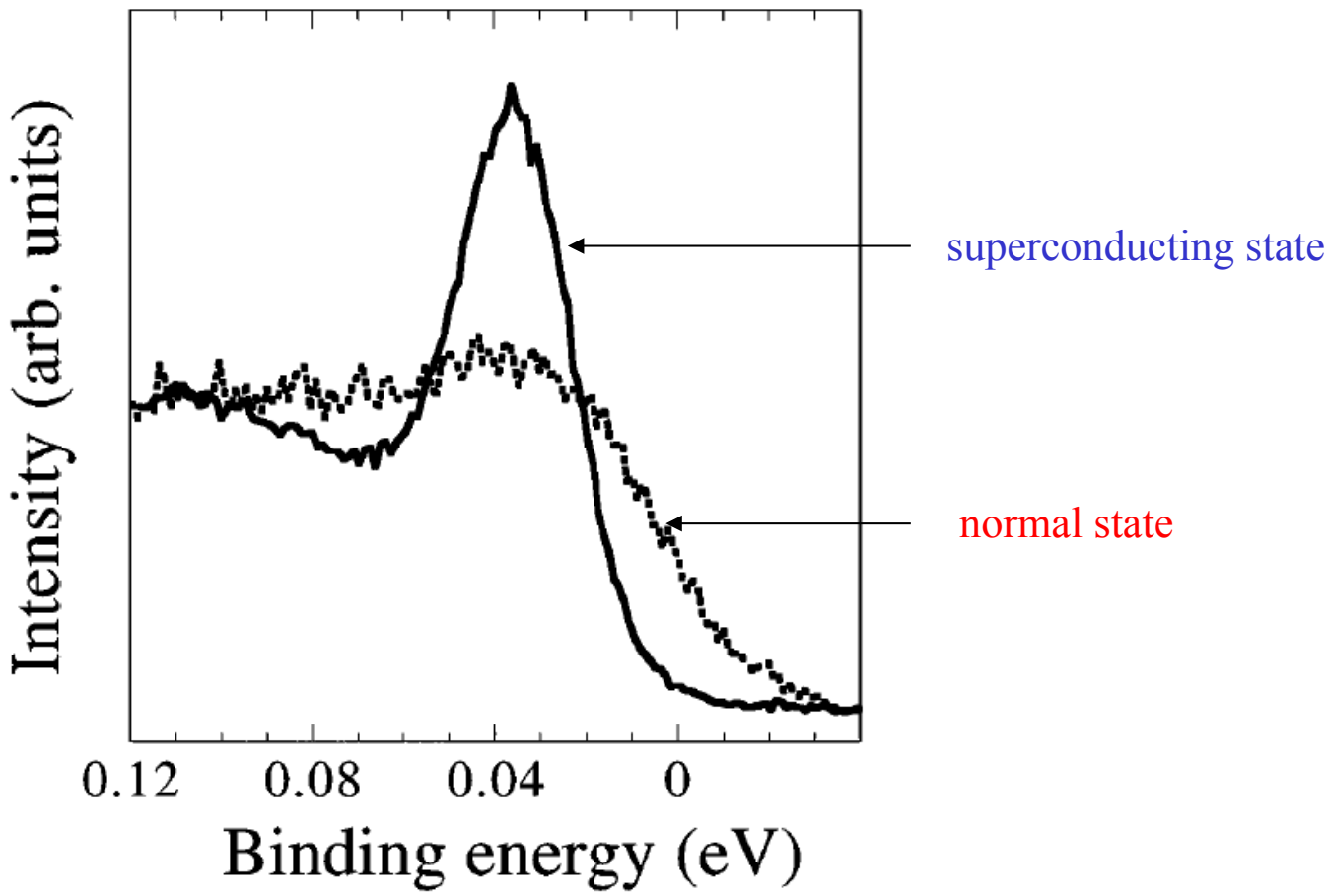

FIG. 1. Comparison of data at $\bar{M}$ in the normal state (105 K, dashed line) and the superconducting state (13 K, solid line) for a slightly overdoped ($T_c = 87$ K) Bi2212 sample with photon polarization $\Gamma - \bar{M}$.

Eliashberg Theory

- Extension of BCS formalism to include dynamical electron-phonon interaction
- builds on Migdal theory in the normal state
- loosely modeled in BCS theory

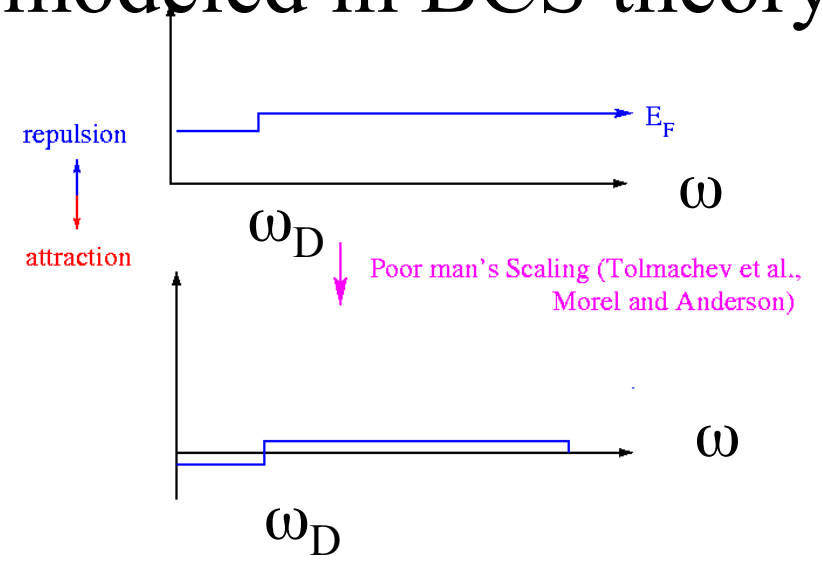

Measurement of $\alpha^2F(\omega)$

1) measure structure in dI/dV accurately

2) "guess" $\alpha^2F(\omega)$

3) compute, using Eliashberg theory, $\frac{dI(\omega)}{dV}$

4) correct trial $\alpha^2F(\omega)$, using functional derivatives

5) iterate until calculated dI/dV agrees with experimental one

- structure beyond phonon region
- agrees fairly well with phonon density of states
- gap ratio comes out right
- mass enhancement comes out right
- agrees with thermodynamics

BUT, complexity of Coulomb repulsion is buried in one number, μ^*

So what's wrong?

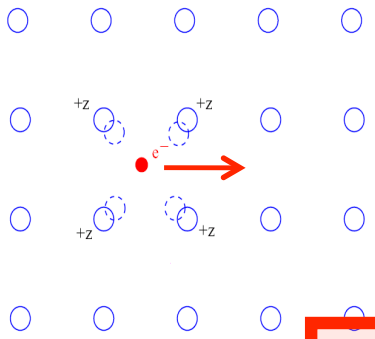

1) How did $\mu = UN(E_F)$ get reduced to μ^*?

2) The building block is the polaron !
How do 'polaron' effects become 'undone'?

Can't seem to couple without very strong polaron effects!

See Zhou Li, D. Baillie, C. Blois, FM, **PRB 81, 115114 2010**
Zhou Li, C. Chandler, FM, **PRB 83, 045104 2011**

Zhou Li

Devin Baillie

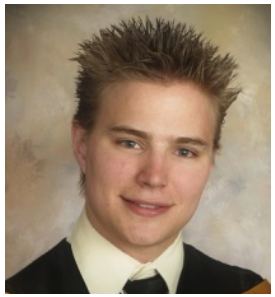

Cindy Blois

Carl Chandler

3) Are we content with a 'zoo' of superconducting materials?